



**HAL**  
open science

# On extremal properties of hyperbolic Coxeter polytopes and their reflection groups

Alexander Kolpakov

► **To cite this version:**

Alexander Kolpakov. On extremal properties of hyperbolic Coxeter polytopes and their reflection groups. Metric Geometry [math.MG]. Université de Fribourg, 2012. English. NNT: . tel-00762315

**HAL Id: tel-00762315**

**<https://theses.hal.science/tel-00762315>**

Submitted on 6 Dec 2012

**HAL** is a multi-disciplinary open access archive for the deposit and dissemination of scientific research documents, whether they are published or not. The documents may come from teaching and research institutions in France or abroad, or from public or private research centers.

L'archive ouverte pluridisciplinaire **HAL**, est destinée au dépôt et à la diffusion de documents scientifiques de niveau recherche, publiés ou non, émanant des établissements d'enseignement et de recherche français ou étrangers, des laboratoires publics ou privés.

Department of Mathematics  
University of Fribourg (Switzerland)

On extremal properties of hyperbolic Coxeter polytopes  
and their reflection groups

THESIS

presented to the Faculty of Science of the University of Fribourg (Switzerland)  
in consideration for the award of the academic grade of *Doctor scientiarum mathematicarum*

by

Aleksandr Kolpakov

from

Novosibirsk (Russia)

Thesis No: 1766  
e-publi.de  
2012

Accepted by the Faculty of Science of the University of Fribourg (Switzerland) upon the recommendation of the jury:

Prof. Dr. Anand Dessai, President of the jury  
University of Fribourg

Prof. Dr. Ruth Kellerhals, Thesis supervisor  
University of Fribourg

Prof. Dr. Michelle Bucher, Referee  
University of Geneva

Prof. Dr. John R. Parker, Referee  
University of Durham (UK)

Prof. Dr. John G. Ratcliffe, Referee  
Vanderbilt University (USA)

Fribourg, 19 November 2012

Thesis supervisor



Prof. Dr. Ruth Kellerhals

Dean



Prof. Dr. Rolf Ingold

# Abstract

This thesis concerns hyperbolic Coxeter polytopes, their reflection groups and associated combinatorial and geometric invariants. Given a Coxeter group  $G$  realisable as a discrete subgroup of  $\text{Isom } \mathbb{H}^n$ , there is a fundamental domain  $\mathcal{P} \subset \mathbb{H}^n$  naturally associated to it. The domain  $\mathcal{P}$  is a Coxeter polytope. Vice versa, given a Coxeter polytope  $\mathcal{P}$ , the set of reflections in its facets generates a Coxeter group acting on  $\mathbb{H}^n$ .

The reflections give a natural set  $S$  of generators for the group  $G$ . Then we can express the growth series  $f_{(G,S)}(t)$  of the group  $G$  with respect to the generating set  $S$ . By a result of R. Steinberg, the corresponding growth series is the power series of a rational function. The growth rate  $\tau$  of  $G$  is the reciprocal to the radius of convergence of such a series. The growth rate is an algebraic integer and, by a result of J. Milnor,  $\tau > 1$ . By a result of W. Parry, if  $G$  acts on  $\mathbb{H}^n$ ,  $n = 2, 3$ , cocompactly, then its growth rate is a Salem number. By a result of W. Floyd, there is a geometric correspondence between the growth rates of cocompact and finite co-volume Coxeter groups acting on  $\mathbb{H}^2$ . This correspondence gives a geometric picture for the convergence of Salem numbers to Pisot numbers. There, Pisot numbers correspond to the growth rates of finite-volume polygons with ideal vertices. We reveal an analogous phenomenon in dimension 3 by considering degenerations of compact Coxeter polytopes to finite-volume Coxeter polytopes with four-valent ideal vertices. In dimension  $n \geq 4$ , the growth rate of a Coxeter group  $G$  acting cocompactly on  $\mathbb{H}^n$  is known to be neither a Salem, nor a Pisot number.

A particularly interesting class of Coxeter groups are right-angled Coxeter groups. In the case of a right-angled Coxeter group acting on  $\mathbb{H}^n$ , its fundamental domain  $\mathcal{P} \subset \mathbb{H}^n$  is a right-angled polytope. Concerning the class of right-angled polytopes in  $\mathbb{H}^4$  (compact, finite volume or ideal, as subclasses), the following questions emerge:

- what are minimal volume polytopes in these families?
- what are polytopes with minimal number of combinatorial compounds (facets, faces, edges, vertices) in these families?

Various results concerning the above questions in the case of finite-volume right-angled polytopes were obtained by È. Vinberg, L. Potyagaïlo and recently by B. Everitt, J. Ratcliffe, S. Tschantz. In the case of compact right-angled polytopes the answer is conjectured by È. Vinberg and L. Potyagaïlo. In this thesis, the above questions in the case of ideal right-angled polytopes are considered and completely answered. We conclude with some partial results concerning the case of compact right-angled polytopes.

# Zusammenfassung

Diese Dissertation behandelt hyperbolische Coxeterpolytope, deren Spiegelungsgruppen und die damit verbundenen kombinatorischen und geometrischen Invarianten. Für eine Coxetergruppe  $G$ , die als diskrete Gruppe in  $\text{Isom } \mathbb{H}^n$  realisierbar ist, gibt es einen Fundamentalbereich  $\mathcal{P} \subset \mathbb{H}^n$ . Der Fundamentalbereich  $\mathcal{P}$  ist ein Coxeterpolytop. Umgekehrt erzeugt ein Coxeter Polytop  $\mathcal{P}$  durch die Menge der Spiegelungen an seinen Fazetten eine Coxetergruppe, die auf  $\mathbb{H}^n$  operiert.

Diese Spiegelungen liefern ein natürliches Erzeugendensystem  $S$  für die Gruppe  $G$ . Damit können wir die Wachstumreihe  $f_{(G,S)}(t)$  der Gruppe  $G$  in Bezug auf die Menge  $S$  betrachten. Nach einem Resultat von R. Steinberg ist diese Wachstumreihe die Potenzreihe einer rationalen Funktion. Die Wachstumsrate  $\tau$  der Gruppe  $G$  ist der Kehrwert des Konvergenzradius ihrer Wachstumreihe. Somit ist die Grösse  $\tau$  eine ganze algebraische Zahl, und nach einem Resultat von J. Milnor gilt  $\tau > 1$ . Falls  $G$  auf  $\mathbb{H}^n$ ,  $n = 2, 3$ , mit kompaktem Fundamentalbereich operiert, gilt nach einem Satz von W. Parry, dass die Wachstumsrate von  $G$  eine Salemzahl ist. Nach einem Resultat von W. Floyd gibt es einen geometrischen Zusammenhang zwischen den Wachstumsraten von Coxetergruppen, welche auf  $\mathbb{H}^2$  kokompakt und mit endlichem Kovolumen operieren. Dieser Zusammenhang erklärt auf geometrische Weise die Konvergenz der Salemzahlen gegen Pisotzahlen. Wir leiten ein entsprechendes Phänomen in Dimension 3 her, indem wir die Entartung von Coxeterpolyedern mit mindestens einer 4-valenten idealen Ecke untersuchen. Es sei hinzugefügt, dass die Wachstumsrate  $\tau$  einer Coxetergruppe  $G \subset \text{Isom } \mathbb{H}^n$  für  $n \geq 4$  im allgemeinen weder eine Salem- noch eine Pisotzahl ist.

Eine besonders interessante Klasse von Coxetergruppen bilden die rechtwinkligen Coxetergruppen. Im Falle einer rechtwinkligen Coxetergruppe, die auf  $\mathbb{H}^n$  operiert, ist ein Fundamentalbereich  $\mathcal{P} \subset \mathbb{H}^n$  ein rechtwinkliges Polytop. Für rechtwinklige Polytope in  $\mathbb{H}^4$ , die in die Teilmengen der kompakten Polytope, Polytope von endlichem Volumen beziehungsweise idealen Polytope eingeteilt werden können, untersuchen wir folgende Fragen:

- welche sind die Polytope von minimalem Volumen in den entsprechenden Teilmengen?
- welche sind die Polytope mit der minimalen Anzahl der kombinatorischen Elemente (Fazetten, Flächen, Kanten, Ecken) in diesen Teilmengen?

Im Falle von rechtwinkligen Polytopen von endlichem Volumen wurde die Antwort von È. Vinberg, L. Potyagaïlo und auch von B. Everitt, J. Ratcliffe, S. Tschantz geliefert. Für kompakte rechtwinklige Polytope stellen È. Vinberg und L. Potyagaïlo eine entsprechende Vermutung auf. In dieser Dissertation geben wir eine vollständige Antwort für die Familie der idealen rechtwinkligen Polytope und beschliessen sie mit einigen Teilresultaten im kompakten Fall.

## Résumé

Cette thèse est centrée sur l'étude des polytopes hyperboliques, des groupes de réflexions et invariants associés. Soit  $G$  un groupe de Coxeter, sous-groupe de  $\text{Isom } \mathbb{H}^n$ . Alors, il existe un domaine fondamental  $\mathcal{P} \subset \mathbb{H}^n$  qui est naturellement associé à ce groupe  $G$ . Le domaine  $\mathcal{P}$  est un polytope de Coxeter. Réciproquement, chaque polytope de Coxeter  $\mathcal{P}$  engendre un groupe de Coxeter agissant sur  $\mathbb{H}^n$ : le groupe engendré par les réflexions par rapport à ses facettes.

Ces réflexions forment un ensemble naturel de générateurs pour le groupe  $G$ . On peut donc exprimer la série de d'accroissement  $f_S(t)$  du groupe  $G$  par rapport à l'ensemble  $S$ . Par un résultat de R. Steinberg, la série d'accroissement associée correspond à la série de Taylor d'une fonction rationnelle. Le taux d'accroissement  $\tau$  de  $G$  est l'inverse du rayon de convergence de cette dernière. Le taux de convergence est un entier algébrique et, par un résultat de J. Milnor,  $\tau > 1$ . Par un résultat de W. Parry, si  $G$  agit sur  $\mathbb{H}^2$  de façon co-compacte, son taux d'accroissement est un nombre de Salem. Par un résultat de W. Floyd, il existe un lien géométrique entre les taux d'accroissement des groupes de Coxeter cocompacts et ceux des groupes à co-volume fini agissant sur  $\mathbb{H}^2$ . Ce lien correspond à une image géométrique de la convergence d'une suite de nombres de Salem vers un nombre de Pisot. Dans cette thèse, on verra un phénomène analogue en dimension 3. En dimension  $n \geq 4$ , le taux d'accroissement d'un groupe de Coxeter agissant de façon cocompacte sur  $\mathbb{H}^n$  n'est plus un nombre de Salem, ni un nombre de Pisot.

Nous nous intéressons à une classe particulière de groupes de Coxeter est celle des groupes de Coxeter rectangulaires. Dans ce cas, les domaines fondamentaux sont des polytopes aux angles dièdres droits. Concernant la classe de polytopes rectangulaires compacts (respectivement, à volume fini, idéaux) dans  $\mathbb{H}^4$ , on pose les problèmes suivants:

- déterminer le volume minimal dans ces familles,
- déterminer le nombre minimal de composante combinatoire (facettes, faces, arêtes, sommets) dans ces familles.

Dans le cas des polytopes rectangulaires à volume fini, la solution a été donnée par È. Vinberg, L. Potyagailo et par B. Everitt, J. Ratcliffe, S. Tschantz. Pour les polytopes rectangulaires compacts, il existe seulement une conjecture. Dans cette thèse, nous répondons à ces questions dans le cas des polytopes rectangulaires idéaux.

## Acknowledgements

First of all, I would like to thank my supervisor, Ruth Kellerhals, for her constant attention to my work. Her encouragement and advice are invaluable for me, since these are the main compound without which the present thesis would have never been written.

I would also like to thank the referees, Michelle Bucher, John R. Parker and John G. Ratcliffe for their interest in my work.

I'm very grateful to the organisers of the Thematic Program on Discrete Geometry and Applications, in particular Marston Conder and Egon Schulte, who invited me to the Fields Institute, Toronto in October, 2011. I express my best gratitude to Jun Murakami for his hospitality during my stay at the Waseda University, Tokyo in December, 2011.

I thank the organisers of the trimester “Geometry and analysis of surface group representations” held at the Henri Poincaré Institute in February-March, 2012, especially Jean-Marc Schlenker and William Goldman for the excellent opportunity to be there.

For many interesting discussions concerning my studies, advice and kind attitude, I would like to thank Ernest Vinberg, Gregory Soifer, Michel Deza, Sarah Rees and Laura Ciobanu. I thank Patrick Ghanaat for many interesting and useful references he has provided me with.

I thank my co-authors, Ruth Kellerhals, Jun Murakami, Sasha Mednykh and Marina Pashkevich for the great experience of working together.

I express my gratitude to the organisers and maintainers of the activities of the Swiss Doctoral Program and Réseau de Recherche Platon.

Financial support during my studies has been mainly acquired from the Swiss National Science Foundation\* and the Department of Mathematics at the University of Fribourg.

Also I would like to thank all my colleagues, who are present and who have accompanied me for some time during my three-years-long stay in Fribourg, for their friendly attitude and collaboration.

Last but not least, I thank my family and friends, those from whom I'm detached and those who are around, for their empathy, understanding and loving at all times.

---

\* projects no. 200021-131967 and no. 200020-121506

# Preface

This thesis is written by the author at the University of Fribourg, Switzerland under supervision of Prof. Dr. Ruth Kellerhals. The manuscript contains 98 pages, 38 figures and 4 tables. It is partitioned into four substantial chapters, an appendix and a list of references.

Throughout Chapter 4, there are two types of theorems, propositions and lemmas: with and without a reference. If the reference is omitted, then the corresponding claim is due to the author. The content of Chapter 4 mainly reproduces the papers [36, 37].



# Contents

<b>1</b>	<b>Polytopes in spaces of constant curvature</b>	<b>1</b>
1.1	The three main geometries . . . . .	1
1.1.1	Models for $\mathbb{X}^n$ . . . . .	1
1.1.2	Hyperplanes in $\mathbb{X}^n$ . . . . .	3
1.1.3	Isometries of $\mathbb{X}^n$ . . . . .	4
1.1.3.1	Isometries of $\mathbb{E}^n$ . . . . .	4
1.1.3.2	Isometries of $\mathbb{S}^n$ . . . . .	5
1.1.3.3	Isometries of $\mathbb{H}^n$ . . . . .	5
1.2	Polytopes in $\mathbb{X}^n$ . . . . .	5
1.2.1	Hyperplanes and half-spaces . . . . .	5
1.2.2	Polytopes . . . . .	6
1.2.3	Gram matrix of a polytope . . . . .	7
1.2.3.1	Acute-angled and Coxeter polytopes . . . . .	8
1.2.4	Examples . . . . .	9
1.2.4.1	A spherical simplex . . . . .	9
1.2.4.2	A Euclidean simplex . . . . .	10
1.2.4.3	A hyperbolic simplex . . . . .	10
1.2.5	Andreev's theorem . . . . .	10
1.2.6	Rivin's theorem . . . . .	12
1.2.7	Examples . . . . .	12
1.2.7.1	Löbell polyhedra . . . . .	12
1.2.7.2	An obtuse-angled icosahedron . . . . .	13
1.2.7.3	Numerical algorithm to construct polyhedra . . . . .	14
<b>2</b>	<b>Growth of Coxeter groups</b>	<b>15</b>
2.1	The growth series, growth function and growth rate . . . . .	15
2.1.1	Basic notions and facts . . . . .	15
2.1.2	Examples . . . . .	17

2.1.2.1	Free groups . . . . .	17
2.1.2.2	Surface groups . . . . .	17
2.2	Coxeter groups . . . . .	18
2.2.1	Basic notions and facts . . . . .	18
2.2.2	Examples . . . . .	18
2.2.2.1	Finite Coxeter groups . . . . .	18
2.2.2.2	Affine Coxeter groups . . . . .	19
2.2.3	Growth of Coxeter groups . . . . .	21
2.2.4	Examples . . . . .	21
2.2.4.1	Spherical triangle groups . . . . .	21
2.2.4.2	Euclidean triangle groups . . . . .	22
2.2.4.3	Hyperbolic triangle groups . . . . .	22
2.2.4.4	Growth rate and co-volume in dimensions two and three	23
<b>3</b>	<b>Reflection groups</b>	<b>26</b>
3.1	Coxeter polytopes and reflection groups . . . . .	26
3.1.1	Basic notions and facts . . . . .	26
3.1.2	Examples . . . . .	28
3.1.2.1	Coxeter simplices in $\mathbb{S}^3$ . . . . .	28
3.1.2.2	Coxeter polyhedra in $\mathbb{E}^3$ . . . . .	29
3.2	Coxeter groups acting on $\mathbb{X}^n$ . . . . .	29
3.2.1	Example . . . . .	31
3.3	Growth of hyperbolic reflection groups . . . . .	31
3.3.1	Coxeter groups acting on $\mathbb{H}^2$ . . . . .	31
3.3.2	Coxeter groups acting on $\mathbb{H}^3$ . . . . .	32
3.3.3	Coxeter groups acting on $\mathbb{H}^n$ , $n \geq 4$ . . . . .	33
<b>4</b>	<b>Main results</b>	<b>36</b>
4.1	Deformation of hyperbolic Coxeter polyhedra, growth rates and Pisot numbers . . . . .	36
4.1.1	Growth rates and algebraic integers . . . . .	36
4.1.1.1	Example . . . . .	38
4.1.2	Coxeter groups acting on hyperbolic three-space . . . . .	39
4.1.2.1	Deformation of finite volume Coxeter polyhedra . . . . .	39
4.1.3	Limiting growth rates of Coxeter groups acting on $\mathbb{H}^3$ . . . . .	45
4.1.4	Examples . . . . .	50
4.1.4.1	Deforming Löbell polyhedra . . . . .	50

4.1.4.2	Deforming a Lambert cube . . . . .	51
4.1.4.3	Finite volume Coxeter polyhedra with an ideal three-valent vertex . . . . .	51
4.2	A note about Wang's theorem . . . . .	52
4.3	The optimality of the hyperbolic 24-cell . . . . .	55
4.3.1	Hyperbolic right-angled polytopes . . . . .	55
4.3.2	The 24-cell and volume minimality . . . . .	56
4.3.3	The 24-cell and facet number minimality . . . . .	58
4.3.3.1	Three-dimensional ideal right-angled hyperbolic polyhedra with few faces . . . . .	58
4.3.3.2	Combinatorial constraints on facet adjacency . . . . .	61
4.3.3.3	Proof of Theorem 27 . . . . .	62
4.3.3.4	A dimension bound for ideal right-angled hyperbolic polytopes . . . . .	72
4.4	Towards the optimality of the hyperbolic 120-cell . . . . .	73
	<b>Bibliography</b>	<b>80</b>

# List of Figures

1.1	The Löbell polyhedron $\mathcal{L}_6$ . . . . .	13
1.2	The icosahedron $\mathcal{I}$ . . . . .	13
4.1	The dodecahedron $\mathcal{D}_n \subset \mathbb{H}^3$ , $n \geq 0$ , with all but one right dihedral angles. The specified angle equals $\frac{\pi}{n+2}$ . . . . .	38
4.2	A ridge of type $\langle k_1, k_2, n, l_1, l_2 \rangle$ . . . . .	39
4.3	Two possible positions of the contracted edge $e$ . The forbidden 3-circuit is dotted and forbidden prism bases are encircled by dotted lines . . . . .	41
4.4	The first possible position of the contracted edge $e$ . The forbidden 4-circuit is dotted. Face $IV$ is at the back of the picture . . . . .	41
4.5	The second possible position of the contracted edge $e$ . The forbidden 3-circuit is dotted. Face $III$ is at the back of the picture . . . . .	42
4.6	Two possible ridges resulting in a four-valent vertex under contraction	42
4.7	Pushing together and pulling apart the supporting planes of polyhedron's faces results in an "edge contraction"- "edge insertion" process	43
4.8	Forbidden 3-circuit: the first case . . . . .	43
4.9	Forbidden 3-circuit: the second case. The forbidden circuit going through the ideal vertex is dotted. Face $III$ is at the back of the picture . . . . .	44
4.10	Forbidden 4-circuit. The forbidden circuit going through the ideal vertex is dotted. Face $II$ is at the back of the picture . . . . .	44
4.11	Simple polyhedra with eight vertices . . . . .	48
4.12	Löbell polyhedron $\mathcal{L}_n$ , $n \geq 5$ with one of its perfect matchings marked with thickened edges. Left- and right-hand side edges are identified. All the dihedral angles are right . . . . .	50
4.13	The dodecahedron $\mathcal{D}$ with one ideal three-valent vertex. All the unspecified dihedral angles are right . . . . .	51
4.14	Vertex figure for a vertex of a compact face subject to contraction . . . . .	53

4.15	Antiprism $\mathcal{A}_k$ , $k \geq 3$ . . . . .	59
4.16	Circuits deprecated by Andreev's theorem . . . . .	60
4.17	The vertex figure $\mathcal{P}_v$ . . . . .	62
4.18	Three facets of $\mathcal{P}$ isometric to $\mathcal{A}_5$ and their neighbours . . . . .	64
4.19	Hyperbolic octahedrites with 8 (left) and 9 (right) vertices . . . . .	65
4.20	Hyperbolic octahedrite with 10 vertices . . . . .	65
4.21	Hyperbolic octahedrite with 10 vertices as a facet of $\mathcal{P}$ and its neighbours	66
4.22	Hyperbolic octahedrite with 9 vertices as a facet of $\mathcal{P}$ and its neighbours (omitted edges are dotted) . . . . .	67
4.23	Sub-graphs $\tau$ (on the left) and $\sigma$ (on the right) . . . . .	68
4.24	Sub-graph $\sigma$ in an octahedron (on the left) and in the facet $P(i)$ (on the right) . . . . .	68
4.25	The segment $v_i v_j$ belongs to a quadrilateral face . . . . .	69
4.26	Sub-graphs $\nu$ (on the left) and $\omega$ (on the right) . . . . .	69
4.27	Embeddings of the graph $\nu$ into octahedrite facets with 8 (left) and 9 (right) vertices . . . . .	70
4.28	Embeddings of the graph $\omega$ into the octahedrite facet with 10 vertices	70
4.29	Embeddings of the graph $\omega$ into the octahedrite facet with 10 vertices	70
4.30	Embeddings of the graph $\omega$ into the octahedrite facet with 10 vertices	71
4.31	Hyperbolic octahedrite with 8 vertices as a facet of $\mathcal{P}$ and its neighbours	72
4.32	The polyhedra $R5$ , $R6$ and $R7$ (from left to right) . . . . .	74
4.33	The polyhedra $R6_1^1$ , $R6_1^2$ and $R6_2^2$ (from left to right) . . . . .	75
34	Prisms that admit contraction of an edge: the first picture . . . . .	76
35	Prisms that admit contraction of an edge: the second picture . . . . .	77
36	Prisms that admit contraction of an edge: the third picture . . . . .	77

# Chapter 1

## Polytopes in spaces of constant curvature

### 1.1 The three main geometries

It is known [59, Theorem 2.1], that there exist only three complete simply-connected Riemannian manifolds of constant sectional curvature in every dimension  $n \geq 2$ : the sphere  $\mathbb{S}^n$ , the Euclidean space  $\mathbb{E}^n$  and the hyperbolic space  $\mathbb{H}^n$ . The corresponding curvatures are  $+1$ ,  $0$  and  $-1$ . We shall discuss of the projective model for these geometries first, in order to give a uniform picture of them and their isometry groups. By the end, we will consider particular cases of dimension two and three hyperbolic geometries and indicate several ways to represent these spaces and their isometries.

The main references for this chapter are [59, Chapters 1-2], [45, Chapters 1-3] and [54, Chapter 4].

#### 1.1.1 Models for $\mathbb{X}^n$

Let  $k \in \{-1, 0, +1\}$  and let us consider the vector space  $\mathbb{R}^{n+1}$  equipped with the following bilinear form on it:

$$\langle x, y \rangle_k = x_1 y_1 + \cdots + x_n y_n + k x_{n+1} y_{n+1}, \quad (1.1)$$

where  $x = (x_1, \dots, x_{n+1})$ ,  $y = (y_1, \dots, y_{n+1})$ .

The form  $\langle \cdot, \cdot \rangle_0$  is positive definite if  $k = +1$ , semi-definite if  $k = 0$ , and has Lorentzian signature  $(n, 1)$  if  $k = -1$ .

Two well-known quadric surfaces arise due to (1.1):

- 1) The sphere  $\mathbb{S}^n = \{x \in \mathbb{R}^{n+1} \mid \langle x, x \rangle_1 = 1\}$ ,
- 2) The two-sheeted hyperboloid  $H^n = \{x \in \mathbb{R}^{n+1} \mid \langle x, x \rangle_{-1} = -1\}$ .

Taking the hyperplane  $\mathbb{E}^n = \{x \in \mathbb{R}^{n+1} | x_{n+1} = 0\}$  equipped with the metric

$$d_E(x, y) = \sqrt{\langle x - y, x - y \rangle}, \quad (1.2)$$

we obtain the unique  $n$ -dimensional complete simply-connected Riemannian space of constant sectional curvature 0.

The bilinear form  $\langle \cdot, \cdot \rangle_1$  defines the angular distance on  $\mathbb{S}^n$ , by means of the formula

$$\cos d_S(x, y) = \langle x, y \rangle_1. \quad (1.3)$$

for every pair of points  $x, y \in \mathbb{S}^n$ . We get the distance in the interval  $[0, \pi]$ .

The space  $\mathbb{S}^n$  endowed with the distance given by (1.3) is known to be the unique  $n$ -dimensional compact complete simply-connected Riemannian space of constant sectional curvature +1.

Now we pass to the case  $k = -1$ . The bilinear form  $\langle \cdot, \cdot \rangle_{-1}$  is not positive definite on the whole  $\mathbb{R}^{n+1}$ . However, we still may define a Riemannian metric on  $H^n$ . The tangent space to a point  $x \in H^n$  is defined by

$$T_x(H^n) = \{y \in \mathbb{R}^{n+1} | \langle x, y \rangle_{-1} = 0\}.$$

The form  $\langle \cdot, \cdot \rangle_{-1}$  is positive definite on  $T_x(H^n)$  for every  $x \in H^n$ , since  $\langle x, x \rangle_{-1} = -1$  on  $H^n$  and the signature of the bilinear form in question is  $(n, 1)$ .

Since the hyper-surface  $H^n$  is not connected, we choose one of its connected components,

$$H_+^n = \{x \in \mathbb{R}^{n+1} | \langle x, x \rangle_{-1} = -1, x_{n+1} > 0\}.$$

Then endow it with the Riemannian structure defined by the restriction of the form  $\langle \cdot, \cdot \rangle_{-1}$  to each  $T_x H_+^n$  in the tangent bundle  $TH_+^n$ . We obtain the resulting Riemannian space  $\mathbb{H}^n$ . The metric on  $\mathbb{H}^n$  is

$$\cosh d_H(x, y) = \langle x, y \rangle_{-1}. \quad (1.4)$$

The space  $\mathbb{H}^n$  with the metric  $d_H$  is *the hyperboloid* or *vector space model* for the unique  $n$ -dimensional complete simply-connected Riemannian space of constant sectional curvature  $-1$ , called the hyperbolic space  $\mathbb{H}^n$ .

We now describe briefly several other models for  $\mathbb{H}^n$ , that we shall use later on. Each of them has its own advantages, which will be of use to provide explanation of various geometric facts in a less sophisticated way.

There are two conformal models of  $\mathbb{H}^n$ , which are due to H. Poincaré, *the ball model*  $\mathbb{B}^n$  (see [45, Section 4.5]) and *the upper half-space model*  $\mathbb{U}^n$  (see [45, Section 4.6]).

The conformal property means that the angles between hyperplanes seen in these models correspond to the real angles measured by means of Riemannian geometry.

The ball model is the most symmetric one and an equidistant set with respect to its center  $\mathbf{o} = (0, 0, \dots, 0)$  is a usual Euclidean sphere. More precisely, the equidistant sphere  $S_{\mathbf{o},r} = \{x | d_H(x, \mathbf{o}) = r\}$  is the Euclidean sphere of radius  $\tanh(r/2)$  around  $\mathbf{o}$ . Each sphere  $S_{\mathbf{o},r}$  carries a natural metric of constant positive sectional curvature.

In the upper half-space model one may easily observe horospheres. Namely, the horosphere  $S_{\infty,a} = \{x \in \mathbb{U}^n | x_n = a\}$ ,  $a > 0$ , centred at the point  $\infty$  is a plane parallel to  $\partial\mathbb{U}^n$ . It carries a natural metric of zero sectional curvature.

Also, the upper half-space model is suitable for computations, since the Poincaré extension allows us to reduce the dimension of the isometry group [45, Section 4.4].

Of particular interest is *the projective ball model*  $\mathbb{D}^n$  (see [45, Section 6.1]), where the geodesics are straight line segments, and hyperplanes are parts of Euclidean hyperplanes inside the unit ball. This property is particularly good for drawing pictures (see Section 1.1.2).

### 1.1.2 Hyperplanes in $\mathbb{X}^n$

In case of  $\mathbb{E}^n$ , an  $(n - 1)$ -dimensional hyperplane  $H_{e,t}$  is given by

$$\langle x, e \rangle_1 + t = 0, \tag{1.5}$$

where  $e \in \mathbb{R}^n$ ,  $\langle e, e \rangle_1 = 1$  and  $t \in \mathbb{R}$ .

Let us define a *reflection*  $\rho_{e,t}$  in the hyperplane  $H_{e,t}$  defined by (1.5) as

$$\rho_{e,t}(x) = x - 2(\langle x, e \rangle_1 + t)e. \tag{1.6}$$

By analogy, an  $(n - 1)$ -dimensional hyperplane  $H_e$  in  $\mathbb{S}^n$  is the intersection

$$H_e = \{x \in \mathbb{R}^{n+1} | \langle x, e \rangle_1 = 0\} \cap \mathbb{S}^n. \tag{1.7}$$

A reflection in the spherical hyperplane  $H_e$  given by (1.7) is the restriction of the corresponding Euclidean reflection in the hyperplane  $H_{e,0}$  to the sphere  $\mathbb{S}^n$ .

An  $(n - 1)$ -dimensional Lorentzian hyperplane  $H_{e,t}$  is given by the equation

$$H_e = \{x \in \mathbb{R}^{n+1} | \langle x, e \rangle_{-1} = 0\}. \tag{1.8}$$

The vector  $e$  is called *time-like* if  $\|e\|_{-1}^2 = -1$ , *space-like* if  $\|e\|_{-1}^2 = 1$  and *light-like* if  $\|e\|_{-1}^2 = 0$ . Depending on the squared Lorentzian norm of the vector  $e$ , the



hyperplane  $H_e$  is either *space-like*, if every vector  $x \in H_e$  is space-like, or *time-like*, if a vector  $x \in H_e$  is time-like, or *light-like* otherwise.

An  $(n - 1)$ -dimensional hyperplane  $H_e$  in the hyperboloid model  $\mathbb{H}^n$  of the hyperbolic space is given by

$$H_e = \{x \in \mathbb{R}^{n+1} \mid \langle x, e \rangle_{-1} = 0\} \cap H_+^n \neq \emptyset, \quad (1.9)$$

which means that the vector  $e$  is space-like.

Let us define a *Lorentzian reflection* in the Lorentzian hyperplane (1.8) as

$$\rho_e(x) = x - 2\langle x, e \rangle_{-1} e. \quad (1.10)$$

A reflection in the hyperbolic hyperplane  $H_e$  is the restriction of  $\rho_e(x)$  given by (1.10) to  $H_+^n$ .

Hyperplanes in other models of hyperbolic geometry, the ball  $\mathbb{B}^n$  and the upper half-space model  $\mathbb{U}^n$ , are described in [45, Sections 4.5-6].

### 1.1.3 Isometries of $\mathbb{X}^n$

In the following we shall list and describe the groups of isometries of the spaces  $\mathbb{X}^n$  introduced above. Let us denote the isometry group of  $\mathbb{X}^n$  by  $\text{Isom } \mathbb{X}^n$ . Since the Riemannian space  $\mathbb{X}^n$  has a natural orientation coming from that of the ambient space  $\mathbb{R}^{n+1}$  of its model, there exists the index two subgroup  $\text{Isom}^+ \mathbb{X}^n$  of the orientation-preserving isometries.

The most part of the present subsection will describe different representations for the isometries of the hyperbolic space with respect to its models.

#### 1.1.3.1 Isometries of $\mathbb{E}^n$

Let  $O(n)$  denote the group of orthogonal transformations of  $\mathbb{R}^n$ . Let  $SO(n)$  denote the group of orientation-preserving orthogonal transformations of  $\mathbb{R}^n$ . Recall that  $\mathbb{R}^n$  acts on itself by parallel translations. Then the isometry group of  $\mathbb{E}^n$  is the semi-direct product  $\text{Isom } \mathbb{E}^n \cong \mathbb{R}^n \rtimes O(n)$ .

The following theorem gives a description of a Euclidean isometry in terms of reflections.

**Theorem 1** *Any isometry of  $\mathbb{E}^n$  is a composition of a finite number of reflections. One needs at most  $n + 1$  reflections.*

### 1.1.3.2 Isometries of $\mathbb{S}^n$

Let us note that the group  $O(n+1)$  maps bijectively the sphere  $\mathbb{S}^n$  on itself. Since this group preserves the bilinear form  $\langle \cdot, \cdot \rangle_1$ , it preserves the distance defined by (1.3). Indeed, by restricting the action of  $O(n+1)$  on  $\mathbb{R}^{n+1}$  to the sphere, we obtain its full isometry group. Thus,  $\text{Isom } \mathbb{S}^n \cong O(n+1)$ . Again, any element of  $\text{Isom } \mathbb{S}^n$  is a composition of a finite number of reflections in spherical hyperplanes.

### 1.1.3.3 Isometries of $\mathbb{H}^n$

The hyperbolic space  $\mathbb{H}^n$  has several models as mentioned above. Since they are all equivalent, we may translate the notion of isometry from one model to another.

Let us describe the isometry group  $\text{Isom } \mathbb{H}^n$  by using the hyperboloid model. Let  $O(n, 1)$  be the group of all linear automorphisms of  $\mathbb{R}^{n+1}$  that preserves the bilinear form  $\langle \cdot, \cdot \rangle_{-1}$ .

Concerning the hyperboloid  $H^n$ , the action of this group could be one of the following type:

- Preserving the sheet  $H_+^n$  and its counterpart  $H_-^n = H^n \setminus H_+^n$ .
- Reversing the sheets  $H_+^n$  and  $H_-^n$ .

Let  $O^\circ(n, 1)$  denote the index two subgroup of  $O(n, 1)$  that preserves the sheets of  $H^n$ . The action of  $O^\circ(n, 1)$  now restricts to  $H_+^n$ , so that the group acts on  $H_+^n$  by isometries. Hence  $\text{Isom } \mathbb{H}^n \cong O^\circ(n, 1)$ . As before, any isometry of  $\mathbb{H}^n$  is a composition of a finite number of hyperbolic reflections [5, Theorem A.2.4].

## 1.2 Polytopes in $\mathbb{X}^n$

### 1.2.1 Hyperplanes and half-spaces

With every hyperplane  $H_e = \{x \in \mathbb{R}^{n+1} \mid \langle x, e \rangle_k = 0\}$  in  $\mathbb{X}^n$ , as described in Section 1.1.2, we associate the positive half-space  $H_e^+ = \{x \in \mathbb{R}^{n+1} \mid \langle x, e \rangle_k \geq 0\}$ . The negative half-space  $H_e^-$  is defined correspondingly by the condition  $\langle x, e \rangle_k \leq 0$ .

An  $(n-k)$ -dimensional hyperplane  $H^{(n-k)}$  in  $\mathbb{X}^n$  is an intersection of  $k$  distinct  $(n-1)$ -dimensional hyperplanes  $H_i^{(n-1)}$ ,  $i = 1, \dots, k$ , given by (1.9) with linearly independent normals  $e_i$ ,  $i = 1, \dots, k$ .

Now we draw our attention mainly to the case  $\mathbb{X}^n = \mathbb{H}^n$ . Two  $(n-1)$ -dimensional hyperplanes  $H_1 := H_{e_1}$  and  $H_2 := H_{e_2}$  in  $\mathbb{H}^n$  intersect if  $|\langle e_1, e_2 \rangle_{-1}| < 1$ . The angle between  $H_1$  and  $H_2$  is then defined by  $\cos \alpha_{12} = \langle e_1, e_2 \rangle_{-1}$ . In case  $|\langle e_1, e_2 \rangle_{-1}| = 1$

the hyperplanes  $H_1$  and  $H_2$  are said to be *parallel*. They do not intersect inside  $\mathbb{H}^n$ . If  $|\langle e_1, e_2 \rangle_{-1}| > 1$ , the hyperplanes  $H_1$  and  $H_2$  are said to be *ultra-parallel* and have a common perpendicular of length  $h_{12}$ . The perpendicular is unique and its length is defined by  $\cosh h_{12} = |\langle e_1, e_2 \rangle_{-1}|$ . A detailed explanation is provided by [45, Sections 3.1-2].

## 1.2.2 Polytopes

A polytope  $\mathcal{P}$  in  $\mathbb{X}^n$  is the intersection of a finite number of half-spaces  $H_i^-$ ,  $i = 1, \dots, m$ , that is  $\mathcal{P} = \bigcap_{i=1}^m H_i^-$ , satisfying the following conditions:

- If  $\mathbb{X}^n = \mathbb{S}^n$ , then  $\mathcal{P}$  fits in an open hemisphere. This means that for every two points  $x, y \in \mathcal{P}$  we have  $d_S(x, y) < \pi$ .
- If  $\mathbb{X}^n = \mathbb{E}^n$  or  $\mathbb{H}^n$ , then  $\mathcal{P}$  has finite volume.

Later on, in Section 1.2.3.1 we shall see that for the class of acute-angled polytopes there is a clear criterion for volume finiteness.

One may vary the number of half-spaces in the definition of  $\mathcal{P}$ , so that still  $\mathcal{P} = \bigcap_{i \in I} H_i^-$ ,  $I$  is a finite set. Each hyperplane  $H_i$  corresponding to a half-space  $H_i^-$  is a *supporting hyperplane* of  $\mathcal{P}$  if the condition  $H_i \cap \partial \mathcal{P} \neq \emptyset$  is satisfied. The intersection of a supporting hyperplane  $H_i$  and  $\mathcal{P}$  is a *facet* of  $\mathcal{P}$ . A  $k$ -dimensional face of  $\mathcal{P}$ ,  $0 \leq k \leq n-1$ , is a non-empty intersection of at least  $(n-k)$  hyperplanes  $H_i$ ,  $i \in I$ , containing a  $k$ -dimensional ball of the respective ambient space. An  $(n-1)$ -dimensional face of  $\mathcal{P}$  is a *facet* of  $\mathcal{P}$ , while a 0-dimensional face of  $\mathcal{P}$  is a *vertex*.

If  $\mathcal{P}$  is a compact polytope in  $\mathbb{X}^n = \mathbb{S}^n$  or  $\mathbb{E}^n$ , then  $\mathcal{P}$  is the geodesic convex hull of its vertices (see [45, Theorems 6.3.17-18]).

Let us now consider a convex hyperbolic polytope  $\mathcal{P}$  in the projective ball model  $\mathbb{D}^n$ . Its closure  $\text{cl } \mathcal{P}$  could be viewed as a polytope in  $\mathbb{E}^n$ , and then two types of vertices will arise: a vertex of  $\text{cl } \mathcal{P}$  inside  $\mathbb{D}^n$  is a *proper* (or *finite*) vertex of  $\mathcal{P}$ , while a vertex of  $\text{cl } \mathcal{P}$  on  $\partial \mathbb{D}^n$  is an *ideal* vertex of  $\mathcal{P}$ . In what follows, we shall call a vertex of  $\mathcal{P}$  either its proper or ideal vertex, indicating it, if necessary. According to [45, Theorem 6.4.7], a convex polytope  $\mathcal{P} \subset \mathbb{H}^n$  is the geodesic convex hull of its vertices (proper and ideal, if any).

If  $v$  is a proper vertex of  $\mathcal{P}$  viewed in the ball model  $\mathbb{B}^n$ , then by means of a suitable isometry we may arrange it to be the centre  $\mathbf{o}$  of the unit ball. Then the sphere  $S_{\mathbf{o}, \varepsilon}$  of a sufficiently small radius  $\varepsilon$  intersects the faces of  $\mathcal{P}$  containing  $v$  in an

$(n-1)$ -dimensional polytope  $\mathcal{P}_v$ , called *the vertex figure* of  $v$ . This polytope inherits a constant positive curvature metric from the sphere  $S_{\mathbf{o},\varepsilon}$  (see Section 1.1.1).

If  $v$  is an ideal vertex of  $\mathcal{P}$  viewed in the upper half-space model  $\mathbb{U}^n$ , then we may arrange it to be the point  $\infty$ . Then the vertex figure  $\mathcal{P}_v$  is the intersection of the horosphere  $S_{\infty,a}$  with a sufficiently large  $a$  and the faces of  $\mathcal{P}$  containing  $v$  in their closure. The polytope  $\mathcal{P}_v$  inherits a zero sectional curvature metric from  $S_{\infty,a}$  (see Section 1.1.1).

Let  $\Omega_k(\mathcal{P})$  denote the set of  $k$ -dimensional faces of  $\text{cl } \mathcal{P}$ ,  $0 \leq k \leq n-1$ . We set  $\Omega_n(\mathcal{P}) := \mathcal{P}$ . Then  $\Omega_*(\mathcal{P}) = \bigcup_{k=0}^n \Omega_k(\mathcal{P}) \cup \emptyset$  ordered with respect to the face inclusion relation is a lattice called *the face lattice* of  $\mathcal{P}$ . Let  $f_k = \text{card } \Omega_k(\mathcal{P})$  be the number of  $k$ -dimensional faces of  $\mathcal{P}$ ,  $0 \leq k \leq n-1$ . The vector  $\mathbf{f}(\mathcal{P}) = (f_0, f_1, \dots, f_{n-1})$  is *the face vector* of  $\mathcal{P}$ . Two polytopes  $\mathcal{P}_1$  and  $\mathcal{P}_2$  in  $\mathbb{X}^n$  are *combinatorially isomorphic* if their face lattices are isomorphic. The polytopes  $\mathcal{P}_1$  and  $\mathcal{P}_2$  are *isometric* if there exists an element  $\phi \in \text{Isom } \mathbb{X}^n$  such that  $\phi(\mathcal{P}_1) = \mathcal{P}_2$ .

### 1.2.3 Gram matrix of a polytope

Let  $\mathcal{P}$  be a polytope in  $\mathbb{X}^n$ , defined by  $\mathcal{P} = \bigcap_{i=1}^m H_i^-$ , where  $H_i := H_{e_i}$  and the normals are outward with respect to  $H_i^-$ . Then *the Gram matrix* of  $\mathcal{P}$  is defined by

$$G(\mathcal{P}) = (\langle e_i, e_j \rangle_k)_{i,j=1}^m. \quad (1.11)$$

The matrix  $G(\mathcal{P})$  is symmetric and has unit diagonal.

If  $\mathbb{X}^n = \mathbb{S}^n$ , the polytope  $\mathcal{P}$  is compact, the matrix  $G(\mathcal{P})$  is positive semi-definite of rank  $n+1$  and defines  $\mathcal{P}$  up to an isometry. Given two supporting hyperplanes  $H_i$  and  $H_j$  for the respective facets of  $\mathcal{P}$ , we have that *the dihedral angle*  $\alpha_{ij}$  between them is defined by  $\cos \alpha_{ij} = -\langle e_i, e_j \rangle_1$ .

If  $\mathbb{X}^n = \mathbb{E}^n$ , the polytope  $\mathcal{P}$  is compact and the matrix  $G(\mathcal{P})$  is positive semi-definite of rank  $n$ . The entries of  $G(\mathcal{P})$  have the following meaning:

$$\langle e_i, e_j \rangle_0 = \begin{cases} -\cos \alpha_{ij} & \text{if } H_i \cap H_j \neq \emptyset, \\ -1 & \text{if } H_i \text{ and } H_j \text{ are parallel.} \end{cases}$$

If  $\mathbb{X}^n = \mathbb{H}^n$ , then the polytope  $\mathcal{P}$  may not be compact, however it has finite volume. The matrix  $G(\mathcal{P})$  is indefinite of rank  $n+1$  and has Lorentzian signature  $(n, 1)$ . Its entries enjoy the following relations (see [45, Sections 3.1-2]):

$$\langle e_i, e_j \rangle_{-1} = \begin{cases} -\cos \alpha_{ij} & \text{if } H_i \text{ and } H_j \text{ intersect,} \\ -1 & \text{if } H_i \text{ and } H_j \text{ are parallel,} \\ -\cosh h_{ij} & \text{if } H_i \text{ and } H_j \text{ are ultra-parallel.} \end{cases}$$

### 1.2.3.1 Acute-angled and Coxeter polytopes

A polytope  $\mathcal{P}$  in  $\mathbb{X}^n$  is called *acute-angled* if all its dihedral angles are less than or equal to  $\pi/2$ . A polytope  $\mathcal{P}$  is a *Coxeter polytope* if all its dihedral angles are sub-multiples of  $\pi$ , that means, of the form  $\pi/m$ , where  $m \geq 2$  is an integer.

Consider acute-angled polytopes in  $\mathbb{X}^n \neq \mathbb{H}^n$ . It turns out, that there is a short and convenient description of them.

**Theorem 2 (Theorem 1.5, [59])** *Let  $\mathcal{P}$  be an acute-angled polytope in  $\mathbb{X}^n$ . Then*

- *if  $\mathbb{X}^n = \mathbb{S}^n$  then  $\mathcal{P}$  is a simplex;*
- *if  $\mathbb{X}^n = \mathbb{E}^n$  then  $\mathcal{P}$  is either a simplex or a direct product of lower-dimensional simplices.*

Furthermore, the following theorem describes acute-angled simplices in  $\mathbb{X}^n = \mathbb{S}^n$ ,  $\mathbb{E}^n$  in terms of their Gram matrices.

**Theorem 3 (Theorem 1.7, [59])** *Any positive definite (degenerate indecomposable positive semi-definite) real symmetric matrix with unit diagonal and non-positive entries off it is the Gram matrix of an acute-angled spherical (resp., Euclidean) simplex which is defined uniquely up to an isometry of  $\mathbb{S}^n$  (resp.,  $\mathbb{E}^n$ ).*

If we drop the condition “to be indecomposable” for the matrix above, then after a certain permutation of its rows and columns the corresponding block-diagonal matrix should be checked block by block in accordance with Theorem 3. If each block corresponds to a Euclidean simplex, then we have a direct product structure as mentioned in Theorem 2.

Let us turn to polytopes in the hyperbolic space  $\mathbb{H}^n$ . The following theorem describes their Gram matrices.

**Theorem 4 (Theorem 2.2, [59])** *Any indecomposable real symmetric matrix of Lorentzian signature  $(n, 1)$  with unit diagonal and non-positive entries off it is the Gram matrix of an acute-angled polytope in  $\mathbb{H}^n$ . This polytope is unique up to an isometry.*

Moreover, by looking at the principal sub-matrices of a given Gram matrix  $G := G(\mathcal{P})$  of a polytope  $\mathcal{P} \subset \mathbb{H}^n$ , we may describe its combinatorial structure directly from the matrix  $G$ .

A positive definite principle sub-matrix of the Gram matrix  $G := G(\mathcal{P})$  of a polytope  $\mathcal{P}$  is said to be *elliptic* if it is positive definite.

**Theorem 5 (Theorem 2.3, [59])** *Let  $\mathcal{P} \subset \mathbb{H}^n$  be an acute-angled polytope. Let  $G := G(\mathcal{P})$  denote its Gram matrix. With each lower-dimensional face  $F$  we associate a principal sub-matrix  $G^F$  formed by the rows and columns corresponding to the facets of  $\mathcal{P}$  that contain  $F$ . Then the mapping  $F \rightarrow G^F$  is a one-to-one correspondence between the set of all faces of the polyhedron  $\mathcal{P}$  and the set of all elliptic principal sub-matrices of the matrix  $G$ .*

The theorem above helps to detect *all* lower-dimensional faces of the polytope  $\mathcal{P} \subset \mathbb{H}^n$ , including its proper (or finite) vertices. However,  $\mathcal{P}$  may have an ideal vertex which is not described by Theorem 5. Given the Gram matrix  $G := G(\mathcal{P})$  and an ideal vertex  $v \in \Omega_0(\mathcal{P})$ , let  $G^v$  be the sub-matrix of  $G$  that consists of the rows and columns corresponding to the facets of  $\text{cl } \mathcal{P}$  containing  $v$ .

A real symmetric matrix with non-positive elements off the diagonal is said to be *parabolic* if a certain permutation of its rows and columns brings it to the block-diagonal form, where each block is a degenerate indecomposable positive semi-definite matrix.

**Theorem 6 (Theorem 2.5, [59])** *Let  $\mathcal{P} \subset \mathbb{H}^n$  be an acute-angled polytope with the Gram matrix  $G := G(\mathcal{P})$ . Then the mapping  $v \rightarrow G^v$  is a one-to-one correspondence between the set of all ideal vertices of  $\mathcal{P}$  and the set of all parabolic principal rank  $(n - 1)$  sub-matrices of the matrix  $G$ .*

Given a vertex  $v \in \Omega_0(\mathcal{P})$ , proper or ideal, the matrix  $G^v$  is the matrix of its vertex figure  $\mathcal{P}_v$ , that enjoys respectively the properties of either the Gram matrix of an acute-angled polytope in  $\mathbb{S}^n$ , or those of an acute-angled polytope in  $\mathbb{E}^n$ .

If every vertex  $v$  of an acute-angled polytope  $\mathcal{P} \subset \mathbb{H}^n$  with Gram matrix  $G$  has either elliptic or parabolic  $G^v$ , then  $\mathcal{P}$  has finite volume (see [58, Theorem 4.1]).

## 1.2.4 Examples

### 1.2.4.1 A spherical simplex

According to Theorem 3, the identity  $4 \times 4$  matrix is the Gram matrix of a totally right-angled simplex in  $\mathbb{S}^3$ .

### 1.2.4.2 A Euclidean simplex

The following matrix is the Gram matrix of a Euclidean simplex, corresponding to the affine Coxeter group  $\tilde{A}_3$  (see Section 2.2.2.2):

$$G = \begin{pmatrix} 1 & -\cos \frac{\pi}{3} & 0 & -\cos \frac{\pi}{3} \\ -\cos \frac{\pi}{3} & 1 & -\cos \frac{\pi}{3} & 0 \\ 0 & -\cos \frac{\pi}{3} & 1 & -\cos \frac{\pi}{3} \\ -\cos \frac{\pi}{3} & 0 & -\cos \frac{\pi}{3} & 1 \end{pmatrix}.$$

The fact that it determines a Euclidean simplex follows from Theorem 3. We have that  $\det G = 0$  and the other principal minors are positive.

### 1.2.4.3 A hyperbolic simplex

Let us consider the orthoscheme  $(3, 3, 6)$  (see, e.g. [59, Section 3.2, p. 124] for the definition), that is a hyperbolic simplex with the Gram matrix

$$G = \begin{pmatrix} 1 & -\cos \frac{\pi}{3} & 0 & 0 \\ -\cos \frac{\pi}{3} & 1 & -\cos \frac{\pi}{3} & 0 \\ 0 & -\cos \frac{\pi}{3} & 1 & -\cos \frac{\pi}{6} \\ 0 & 0 & -\cos \frac{\pi}{6} & 1 \end{pmatrix}.$$

The fact that it determines a hyperbolic simplex follows from Theorem 4. Moreover, by Theorem 5 applied to the order three principal sub-matrices, the corresponding simplex has three proper vertices. By Theorem 6, it has a single ideal vertex.

## 1.2.5 Andreev's theorem

The Gram matrix approach to the existence of an acute-angled polytope in  $\mathbb{H}^n$  suggested by Theorem 4 could always be applied, however the Gram matrix may have an arbitrarily large order, what makes an actual computation difficult. In lower dimensions, there exist a number of theorems that allow us to decide about the existence of a given polytope in terms of its dihedral angles only.

**Theorem 7** *A convex  $k$ -gon with dihedral angles  $0 \leq \alpha_i < \pi$ ,  $i = 1, \dots, k$ , exists in  $\mathbb{H}^2$  if and only if*

$$\alpha_1 + \alpha_2 + \dots + \alpha_k < (k - 2)\pi.$$

The following results concerning acute-angled polyhedra in  $\mathbb{H}^3$  are helpful in the study of Coxeter groups acting on the hyperbolic space.

**Theorem 8 (E.M. Andreev, [2, 59])** *A compact acute-angled polyhedron in  $\mathbb{H}^n$ ,  $n \geq 3$ , is determined by its face lattice and dihedral angles up to an isometry.*

In order to state the next theorem, let us define a  $k$ -circuit,  $k \geq 3$ , to be an ordered sequence of faces  $F_1, \dots, F_k$  of a given polyhedron  $\mathcal{P}$  such that each face is adjacent only to the previous and the following ones, while the last one is adjacent only to the first one and to the penultimate one, and no three of them share a common vertex.

**Theorem 9 (E.M. Andreev, [3, 59])** *Let  $\mathcal{P}$  be a combinatorial polyhedron, not a simplex, such that three or four faces meet at every vertex. Enumerate all the faces of  $\mathcal{P}$  by  $1, \dots, |\Omega_2(\mathcal{P})|$ . Let  $F_i$  be a face,  $E_{ij} = F_i \cap F_j$  an edge, and  $V_{ijk} = \bigcap_{s \in \{i,j,k\}} F_s$  or  $V_{ijkl} = \bigcap_{s \in \{i,j,k,l\}} F_s$  a vertex of  $\mathcal{P}$ . Let  $\alpha_{ij} \geq 0$  be the weight of the edge  $E_{ij}$ . The following conditions are necessary and sufficient for the polyhedron  $\mathcal{P}$  to exist in  $\mathbb{H}^3$  having the dihedral angles  $\alpha_{ij}$ :*

- (m<sub>0</sub>)  $0 < \alpha_{ij} \leq \pi/2$ .
- (m<sub>1</sub>) *If  $V_{ijk}$  is a vertex of  $\mathcal{P}$ , then  $\alpha_{ij} + \alpha_{jk} + \alpha_{ki} \geq \pi$ , and if  $V_{ijkl}$  is a vertex of  $\mathcal{P}$ , then  $\alpha_{ij} + \alpha_{jk} + \alpha_{kl} + \alpha_{li} = 2\pi$ .*
- (m<sub>2</sub>) *If  $F_i, F_j, F_k$  form a 3-circuit, then  $\alpha_{ij} + \alpha_{jk} + \alpha_{ki} < \pi$ .*
- (m<sub>3</sub>) *If  $F_i, F_j, F_k, F_l$  form a 4-circuit, then  $\alpha_{ij} + \alpha_{jk} + \alpha_{kl} + \alpha_{li} < 2\pi$ .*
- (m<sub>4</sub>) *If  $\mathcal{P}$  is a triangular prism with bases  $F_1$  and  $F_2$ , then  $\alpha_{13} + \alpha_{14} + \alpha_{15} + \alpha_{23} + \alpha_{24} + \alpha_{25} < 3\pi$ .*
- (m<sub>5</sub>) *If among the faces  $F_i, F_j, F_k$ , the faces  $F_i$  and  $F_j$ ,  $F_j$  and  $F_k$  are adjacent,  $F_i$  and  $F_k$  are not adjacent, but concurrent in a vertex  $v_\infty$ , and all three  $F_i, F_j, F_k$  do not meet at  $v_\infty$ , then  $\alpha_{ij} + \alpha_{jk} < \pi$ .*

For a triangular prism one more condition is needed. Namely, that at least one of the dihedral angles between its lateral faces and bases is strictly less than  $\pi/2$ . For a tetrahedron the extra condition is that the signature of its Gram matrix has to be Lorentzian.



## 1.2.6 Rivin's theorem

Let us consider an ideal convex polyhedron  $\mathcal{P}$  in  $\mathbb{H}^3$ , that is a polyhedron with all vertices on  $\partial\mathbb{H}^3$ . Such a polyhedron is said to be *ideal* for brevity's sake. We may view it as a convex Euclidean polyhedron in the projective model  $\mathbb{D}^3$ . Then  $\mathcal{P}$  turns out to be a polyhedron inscribed in the sphere  $\partial\mathbb{D}^3$  representing the ideal boundary. Let  $\mathcal{P}^*$  denote its dual, i.e. the polytope such that each facet  $F \in \Omega_{n-1}(\mathcal{P})$  corresponds to a vertex  $v \in \Omega_0(\mathcal{P}^*)$ . If  $e$  is an edge of  $\mathcal{P}$ , let  $\alpha(e)$  be the dihedral angle along it. For the corresponding edge  $e^*$  of the dual, let us set  $\alpha(e^*) = \pi - \alpha(e)$ . The following theorem holds.

**Theorem 10 (I. Rivin, [46])** *The dual polyhedron  $\mathcal{P}^*$  of a convex ideal polyhedron  $\mathcal{P} \subset \mathbb{H}^3$  satisfies the following conditions:*

- $0 < \alpha(e^*) < \pi$  for all edges of  $\mathcal{P}^*$ ,
- if the edges  $e_1^*, \dots, e_k^*$  form the boundary of a face of  $\mathcal{P}^*$ , then

$$\sum_{i=1}^k \alpha(e_i^*) = 2\pi,$$

- if the edges  $e_1^*, \dots, e_k^*$  form a closed circuit but do not bound a face, then

$$\sum_{i=1}^k \alpha(e_i^*) > 2\pi.$$

*Conversely, any polyhedron  $\mathcal{P}^*$  with a given face lattice and dihedral angles satisfying the above conditions is the dual of a convex ideal polyhedron  $\mathcal{P} \subset \mathbb{H}^3$ . The polyhedron  $\mathcal{P}$  is unique up to an isometry.*

Observe that the theorem above does **not** require the polyhedron  $\mathcal{P}$  to be acute-angled, and so we have more freedom.

## 1.2.7 Examples

### 1.2.7.1 Löbell polyhedra

Let us consider the family of polyhedra  $\mathcal{L}_n$ ,  $n \geq 5$  (see also Section 4.1.4.1). Combinatorially, each one is presented by bottom and top  $n$ -gons with two stripes of pentagons in between, going around the border of both  $n$ -gonal faces. In Fig. 1.1 the polyhedron  $\mathcal{L}_6$  is given drawn in the ball model  $\mathbb{B}^3$  by means of a computer script

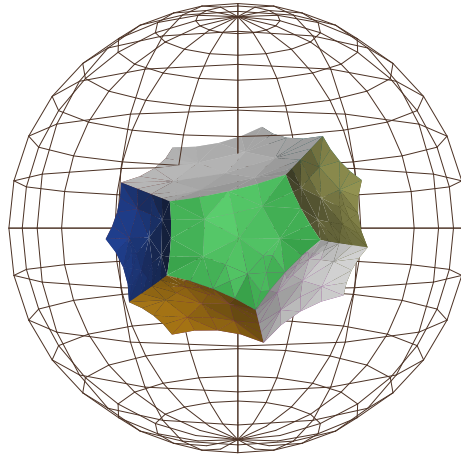


Figure 1.1: The Löbell polyhedron  $\mathcal{L}_6$

from [16]. Let us point out, that  $\mathcal{L}_5$  is combinatorially a dodecahedron. By Andreev's theorem (Theorem 9), all  $\mathcal{L}_n$  are realisable as compact right-angled polyhedra in  $\mathbb{H}^3$ .

The polyhedra  $\mathcal{L}_n$ ,  $n \geq 6$ , provide fundamental domains for a family of discrete and torsion-free groups of isometries  $\Gamma_n$  and of pairwise non-isometric compact hyperbolic manifolds  $\mathbb{H}^3/\Gamma_n$ , while the dodecahedron  $\mathcal{L}_5$  cannot be such a fundamental domain [56].

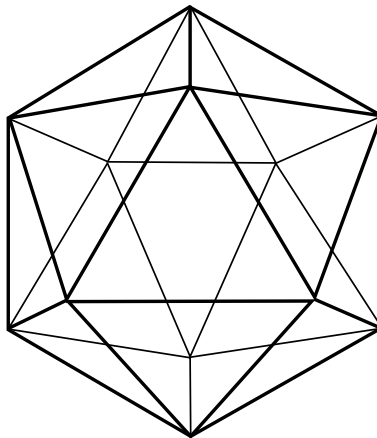


Figure 1.2: The icosahedron  $\mathcal{I}$

### 1.2.7.2 An obtuse-angled icosahedron

Let us consider a regular icosahedron  $\mathcal{I}$  in Fig. 1.2. We want to realise it as an ideal hyperbolic polyhedron with all dihedral angles  $3\pi/5$ . In the notation of Rivin's theorem (Theorem 10), one has  $\alpha(e) = 3\pi/5$  and  $\alpha(e^*) = 2\pi/5$ .

The dual polyhedron  $\mathcal{I}^*$  of the icosahedron is a dodecahedron. Thus, if a circuit of edges  $\{e_i^*\}_{i=1}^5$  bounds a face, we obtain for the angle sum  $\sum_{i=1}^5 \alpha(e_i^*) = 5 \cdot 2\pi/5 = 2\pi$ . If a closed circuit of edges  $\{e_i^*\}_{i=1}^n$  does not bound a face, then it circumferences at least two adjacent pentagons in  $\mathcal{I}^*$ . Hence  $n \geq 8$  and the corresponding sum is  $\sum_{i=1}^n \alpha(e_i^*) \geq 8 \cdot 2\pi/5 > 2\pi$ . Thus,  $\mathcal{I}$  is realisable as an ideal hyperbolic polyhedron. Finally, let us note that in this case all the dihedral angles are equal to  $3\pi/5 > \pi/2$ , so Andreev's theorem is not applicable.

### 1.2.7.3 Numerical algorithm to construct polyhedra

There exists a number of MATLAB scripts running an algorithm producing acute-angled polyhedra with given combinatorics and dihedral angles. This algorithm has first been described in the original paper of Andreev [2]. However, it contains a significant combinatorial flaw corrected in [16]. The scripts are created by R. Roeder [16], who discovered the flaw in the original algorithm while coding the first version of his scripts. Many examples of acute-angled polyhedra studied numerically with help of Roeder's scripts are given in [47].

# Chapter 2

## Growth of Coxeter groups

### 2.1 The growth series, growth function and growth rate

The main reference for next section is [25, Chapters VI-VII].

#### 2.1.1 Basic notions and facts

Let  $G$  denote a multiplicative group. A subset  $S \subset G \setminus \{1\}$  is a *generating set* for the group if every element  $g \in G$  can be written as a product of elements in  $S$ . The elements of  $S$  are called *generators* of  $G$ . If the set  $S$  may be chosen to be finite, we say that the group  $G$  is *finitely generated*. For the rest of this work we suppose all groups to be finitely generated. Also we suppose that the generating set  $S$  is *symmetric*, that is, for each  $s \in S$  its inverse  $s^{-1} \in S$  as well.

Let us denote by  $F(S)$  the free group of rank  $\text{card } S$  generated by  $S$ . Let  $R$  be a finite collection of words in  $F(S)$ . Then we say a group  $G$  to have the presentation  $\langle S | R \rangle$  with generators  $S$  and relations  $R$  if  $G \cong F(S) / \langle\langle R \rangle\rangle$ , where  $\langle\langle \cdot \rangle\rangle$  means the normaliser of a set of words in  $G$ . Let us also denote by  $\langle T \rangle$  a subgroup of  $G$  generated by a subset  $T \subset S$ .

Let us choose a generating set  $S = \{s_1, \dots, s_m\}$  for a group  $G$ . The *length function*  $\|\cdot\|_S : G \rightarrow \mathbb{Z}_{\geq 0}$  is defined as the minimal number of elements from  $S$  needed to write an element  $g \in G$  up. In the case  $g = 1$ , we set  $\|1\|_S = 0$ .

Let  $a_k, k \geq 0$ , denote the number of elements  $g \in G$  such that  $\|g\|_S = k$ . E.g., we have  $a_0 = 1$  and  $a_1 = \text{card } S$ . Let  $f_{(G,S)}(t)$  denote the respective *growth series* of the group  $G$ , defined by

$$f_{(G,S)}(t) = \sum_{k=0}^{\infty} a_k t^k. \quad (2.1)$$

If the group  $G$  is finite, then its growth series is just a polynomial with the property that  $f(1) = \text{card } G$ . In general, the function  $f(t) := f_{(G,S)}(t)$  is holomorphic in  $t$  inside the disc of convergence  $\{t \in \mathbb{C} \mid |t| < R\}$  with  $R = 1/(\text{card } S - 1)$ , at least [18].

If the group  $G$  happens to be reducible, i.e.  $G \cong G_1 \times G_2$  such that  $G_i$ ,  $i = 1, 2$  are generated by  $S_i$ ,  $i = 1, 2$  then its growth function splits into factors as follows.

**Proposition 1** *With  $G$ ,  $G_i$  and  $S_i$ ,  $i = 1, 2$ , as above we have*

$$f_{(G,S)}(t) = f_{(G_1,S_1)}(t) f_{(G_2,S_2)}(t), \quad (2.2)$$

where  $S = (S_1 \times \{1\}) \cup (\{1\} \times S_2)$

Let us define the *growth rate*  $\tau$  of  $G$  by  $\tau = \limsup_{n \rightarrow \infty} \sqrt[n]{a_n}$ . Then,  $\tau$  is related to the radius of convergence of the series (2.1) by  $R = \tau^{-1}$  according to Hadamard's formula.

If the growth rate  $\tau$  of  $G$  with respect to a certain generating set is bigger than 1, then we say  $G$  has (at least) *exponential growth*. Since a finitely generated group  $G$  with generating set  $S$  satisfies  $a_k \leq (\text{card } S)^k$ ,  $k \geq 0$ , its growth could be at most exponential.

**Theorem 11 (Proposition VI.27 [25])** *The exponential growth property does not depend on the generating set.*

In contrast to Theorem 11, the *value* of the growth rate  $\tau$  depends on the chosen generating set. Therefore,  $\tau$  is not a group invariant, but an invariant for the pair  $\langle G, S \rangle$ . As in [25, 24] one may define the following “least” growth rate

$$\tau_G = \inf_S \{ \tau_{G,S} \mid \tau_{G,S} \text{ is a growth rate of } G \text{ with respect to the generating set } S \}. \quad (2.3)$$

The recent references with examples and explicit computations of  $\tau_G$  for various groups are [55, 61].

The following theorem by J. Milnor describes a wide and important class of groups having exponential growth.

**Theorem 12 (J. Milnor, [39])** *If  $M$  is a compact connected Riemannian manifold with negative sectional curvatures, then its fundamental group  $G := \pi_1(M)$  has exponential growth, i.e. there exists  $\gamma > 1$  such that*

$$a_k \geq \gamma^k, \text{ for all } k \geq 0. \quad (2.4)$$

More generally, every Gromov hyperbolic group has exponential growth (refer to [25] for more details).

## 2.1.2 Examples

### 2.1.2.1 Free groups

Let  $F_n$  be the free group on  $n$  generators  $s_1, \dots, s_n$ . The symmetric generating set  $S_n$  for it will be  $\{s_1^{\pm 1}, \dots, s_n^{\pm 1}\}$ . For the growth series coefficients of  $F_n$  we have  $a_0 = 1$  and  $a_k = 2n(2n - 1)^{k-1}$ ,  $k \geq 1$ . Finally, the rational function

$$f_{(F_n, S_n)}(t) = \frac{1 - (2n - 1)t^2}{(1 - t)(1 - (2n - 1)t)} \quad (2.5)$$

corresponds to the analytic extension of the growth series (2.1) beyond the open disc  $|t| < R = 1/(2n - 1)$ . The convergence radius of this series is exactly  $R$ , corresponding in this case to the real pole of  $f_{(F_n, S_n)}(t)$  with the smallest absolute value.

Let us now consider the groups  $F_2$  and  $F_3$ . Their growth functions are given respectively by formula (2.5). Then recall the fact that  $F_3$  is isomorphic to the subgroup  $F_2^{(2)}$  of even length words in  $F_2$ . That is, if  $F_2 = \langle a^{\pm 1}, b^{\pm 1} \rangle$ , then  $F_2^{(2)} = \langle a^{\pm 2}, b^{\pm 2}, ab, b^{-1}a^{-1} \rangle \cong F_3$ . Then we have

$$f_{(F_2^{(2)}, S_2)}(t) = \frac{f_{(F_2, S_2)}(\sqrt{t}) + f_{(F_2, S_2)}(-\sqrt{t})}{2} = \frac{1 - 9t^2}{1 - 10t + 9t^2} \neq f_{(F_3, S_3)}(t). \quad (2.6)$$

Thus, the growth function is defined by both the group and its generating set together.

All free groups are of exponential growth, as could be seen from formula (2.5).

### 2.1.2.2 Surface groups

Let  $\Sigma_g$  be a compact genus  $g \geq 0$  orientable surface. The surfaces  $\Sigma_g$  with  $g \geq 2$  are known to be *hyperbolic*, that is they are realisable as Riemannian two-dimensional manifolds of constant sectional curvature  $-1$ . Thus, by Theorem 12,  $\pi_1(\Sigma_g)$ ,  $g \geq 2$ , has exponential growth. The corresponding growth function with respect to the standard presentation

$$\pi_1(\Sigma_g) = \langle a_1, b_1, \dots, a_g, b_g \mid \prod_{n=1}^g [a_n, b_n] \rangle \quad (2.7)$$

was computed by J.W. Cannon and Ph. Wagreich [8]. From the explicit computation one can also see that the growth rate  $\tau$  with respect to generating set from (2.7) is greater than 1.

However, the growth of  $\pi_1(\Sigma_1) = \langle a, b \mid aba^{-1}b^{-1} \rangle \cong \mathbb{Z} \times \mathbb{Z}$  is linear. The torus  $\Sigma_1$  admits a Euclidean metric, but no hyperbolic one due to the Gauß-Bonnet theorem [45, Theorem 9.3.1]. Indeed, for  $\pi_1(\Sigma_1)$  we have  $a_0 = 1$  and  $a_k = 4k$ ,  $k \geq 1$ . Since

the growth function for  $\mathbb{Z} \cong \langle a \rangle \cong \langle b \rangle$  is  $\frac{1+t}{1-t}$ , by Proposition 1, the growth function of  $\pi_1(\Sigma_1)$  is  $(\frac{1+t}{1-t})^2$ . Thus, the corresponding growth rate  $\tau$  is equal to 1 and, due to Theorem 11, can not be greater for any generating set.

## 2.2 Coxeter groups

The main references for this section are [29] and [12].

### 2.2.1 Basic notions and facts

A Coxeter group  $G$  can be defined in several different ways, all equivalent, that we shall consider below. The first description is given in terms of generators and relations. A group  $G$  is a Coxeter group, if it has a presentation of the form

$$G = \langle s_1, s_2, \dots, s_n | (s_i s_j)^{m_{ij}} \rangle, \quad (2.8)$$

where  $m_{ii} = 1$  for all  $i = 1, \dots, n$ ,  $m_{ij} = m_{ji} \in \{2, 3, \dots, \infty\}$  for all  $i, j = 1, \dots, n$ ,  $i \neq j$ . The property  $m_{ij} = \infty$  leaves us with no relation of the form  $(s_i s_j)^{m_{ij}}$ .

The symmetric matrix  $M = (m_{ij})_{i,j=1}^n$  is called the Coxeter matrix for the group  $G$ . The pair  $(G, S)$ , where  $G$  is a Coxeter group with generating set  $S = \{s_1, s_2, \dots, s_n\}$  is called a Coxeter system.

The Coxeter matrix can also be given by means of a labelled graph called the Coxeter diagram of  $(G, S)$ . To produce such a graph out of the Coxeter matrix or the group presentation [6, 12] we will use the following rules:

- (1) The vertices of the graph are labelled by generator subscripts  $i$  for  $s_i \in S$ .
- (2) Vertices  $i$  and  $j$  are connected if and only if  $m_{ij} \geq 3$ .
- (3) An edge is labelled with the value of  $m_{ij}$  whenever  $m_{ij} \geq 4$ .

Sometimes, concerning rule (3), we use a multiple edge of multiplicity  $m_{ij} - 2$  to indicate the value of  $m_{ij}$ . However, this way of depicting a Coxeter diagram becomes inconvenient if  $m_{ij}$  is large.

### 2.2.2 Examples

#### 2.2.2.1 Finite Coxeter groups

The list of finite Coxeter groups is given below in Table 2.1. It contains three infinite families  $A_n$ ,  $n \geq 1$ ,  $B_n = C_n$ ,  $n \geq 2$ , and  $D_n$ ,  $n \geq 4$ , of increasing rank  $n$  and a

one-parameter family of rank two  $G_2^{(n)}$ ,  $n \geq 3$ . Furthermore, there are the singletons  $E_6, E_7, E_8, F_4$  and  $H_3, H_4$ .

Group	Coxeter diagram
$A_n$	
$B_n = C_n$	
$D_n$	
$E_6$	
$E_7$	
$E_8$	
$F_4$	
$G_2^{(n)}$	
$H_3$	
$H_4$	

Table 2.1: Finite Coxeter groups

The groups  $A_3, B_3$  and  $H_3$  are known to be the symmetry groups of the Platonic solids. Namely,  $A_3$  corresponds to the symmetries of a regular tetrahedron,  $B_3$  to a regular cube/octahedron,  $H_3$  to a regular dodecahedron/icosahedron.

### 2.2.2.2 Affine Coxeter groups

The list of affine Coxeter groups is given below in Table 2.2 (see Section 3 for the geometric terminology). It contains four infinite families  $\tilde{A}_n$ ,  $n \geq 2$ ,  $\tilde{B}_n, \tilde{C}_n$ ,  $n \geq 3$ , and  $\tilde{D}_n$ ,  $n \geq 4$ , of increasing  $n$  rank. Besides, there are five singleton groups  $\tilde{E}_6, \tilde{E}_7, \tilde{E}_8, \tilde{F}_4$  and  $\tilde{G}_2$ .

The affine Coxeter groups are infinite, but each contains a normal abelian subgroup such that the respective quotient is a finite Coxeter group. An obvious correspondence between the diagrams in Table 2.1 and Table 2.2 is the addition of one extra node and one or two extra edges.



Group	Coxeter diagram
$\tilde{A}_n$	
$\tilde{B}_n$	
$\tilde{C}_n$	
$\tilde{D}_n$	
$\tilde{E}_6$	
$\tilde{E}_7$	
$\tilde{E}_8$	
$\tilde{F}_4$	
$\tilde{G}_2$	

Table 2.2: Affine Coxeter groups

As an example, let us consider the group  $\tilde{A}_3$  having the following presentation:

$$\tilde{A}_3 \cong \langle a, b, c | a^2, b^2, c^2, (ab)^3, (bc)^3, (ac)^3 \rangle.$$

Then consider its abelian normal subgroup  $N = \langle abcb, baca, cbab \rangle$ . We easily see that the quotient group is  $\tilde{A}_3/N \cong A_2$ .

REMARK. Given a Coxeter diagram, the corresponding Coxeter system is completely defined. That is, each Coxeter diagram corresponds to a unique pair  $(G, S)$ . However, speaking about the group  $G$  we don't have a 1-to-1 correspondence between Coxeter groups and diagrams. As an example, one may consider the dihedral group  $D_6$  of order 12. Observe that it corresponds to two different Coxeter systems,  $G_2^{(6)}$  and  $A_1 \times A_2$ .

### 2.2.3 Growth of Coxeter groups

We have introduced the notion of growth in Section 2.1. Now we shall restrict ourselves to the particular case of Coxeter groups.

By the result of Steinberg [53] the growth function of a Coxeter group is known to be rational. The key result concerning its computation [53, Theorem 1.28] tells us that there exists a correspondence between the growth function of the whole group and the growth functions of its finite subgroups. Namely, the following theorem holds:

**Theorem 13 (R. Steinberg, [53])** *Let  $G$  be a Coxeter group with generating set  $S$ . Then*

$$\frac{1}{f_{(G,S)}(t^{-1})} = \sum_{T \in \mathcal{F}} \frac{(-1)^{\text{card } T}}{f_{(T,T)}(t)}, \quad (2.9)$$

where  $\mathcal{F} = \{T \subseteq S \mid \text{the subgroup of } G \text{ generated by } T \text{ is finite}\}$ .

Since a finite subgroup of  $G$  generated by a subset  $T \subset S$  is a Coxeter group itself, then Table 2.1 contains all possible subgroups from  $\mathcal{F}$  in (2.9).

The rational function  $f_{(G,S)}(t) = P(t)/Q(t)$  obtained from the Steinberg formula (2.9) is an analytic continuation of the growth series (2.1). Let  $R$  be its convergence radius and  $\tau = R^{-1}$  be the growth rate of  $(G, S)$ . Then  $R$  is a pole of  $f_{(G,S)}(t)$ . Moreover,  $R$  is the least positive real zero of the denominator  $Q(t)$ .

### 2.2.4 Examples

#### 2.2.4.1 Spherical triangle groups

The finite Coxeter groups have polynomial growth functions. The maximal degree of the growth polynomial  $f(t)$  of a finite Coxeter group  $G$  equals  $\text{card } G$ . Consider three generator finite Coxeter groups, also known as sphere tilings, in order to give an example. These belong to the more general class of triangle groups, having the presentation

$$\Delta_{k,l,m} = \langle a, b, c \mid a^2, b^2, c^2, (ab)^k, (bc)^l, (ac)^m \rangle. \quad (2.10)$$

The group Euler characteristic of  $\Delta_{k,l,m}$  equals  $\chi := \chi(\Delta_{k,l,m}) = 1/k + 1/l + 1/m - 1$ . If  $\chi$  is positive, then  $\Delta_{k,l,m}$  is called *spherical*, if  $\chi$  is zero  $\Delta_{k,l,m}$  is *Euclidean*, otherwise *hyperbolic*. Indeed, depending on  $\chi$ , the group  $\Delta_{k,l,m}$  is respectively either a sphere, or a Euclidean, or a hyperbolic plane tiling group.

The finite ones have the triple  $(k, l, m)$  equal to  $(2, 2, n)$ ,  $n \geq 2$ ,  $(2, 3, 3)$ ,  $(2, 3, 4)$  and  $(2, 3, 5)$  only. These groups are called *spherical triangle groups* and correspond to regular tilings of the sphere  $\mathbb{S}^2$  by triangles. The corresponding growth functions

were computed in [52] and are given below in Table 2.3. The notation  $[n]$ ,  $n \geq 1$  an integer, stands for the sum  $1 + t + \dots + t^{n-1}$ . Also, we put  $[n, m] := [n] \cdot [m]$ , and so on.

Group	Coxeter system	Growth function
$\Delta_{22n}$	$A_1 \times G_2^{(n)}$	$[2, 2, n]$
$\Delta_{233}$	$A_3$	$[2, 3, 4]$
$\Delta_{234}$	$B_3$	$[2, 4, 6]$
$\Delta_{235}$	$H_3$	$[2, 6, 10]$

Table 2.3: Finite triangle groups

#### 2.2.4.2 Euclidean triangle groups

Here the groups  $\Delta_{k,l,m}$  of Euclidean plane tilings are given by triplets  $(k, l, m)$  equal  $(2, 4, 4)$ ,  $(3, 3, 3)$  and  $(2, 3, 6)$ . These are exactly the three generator affine Coxeter groups. We can find the corresponding growth functions  $f_{klm}(t)$  by means of the Steinberg formula (2.9). Since the group itself is infinite in case of a Euclidean triangle group, we have

$$\frac{1}{f_{klm}(t^{-1})} = 1 - \frac{3}{[2]} + \frac{1}{[2, k]} + \frac{1}{[2, l]} + \frac{1}{[2, m]}. \quad (2.11)$$

Here we substitute the above mentioned values of the parameters  $k, l, m$  and finally obtain

$$f_{244}(t) = \frac{[2, 4]}{(1-t)^2[3]}, \quad f_{333}(t) = \frac{[3]}{(1-t)^2}, \quad f_{236}(t) = \frac{[2, 6]}{(1-t)^2[5]}. \quad (2.12)$$

#### 2.2.4.3 Hyperbolic triangle groups

These are triangle groups  $\Delta_{k,l,m}$  with  $\chi(\Delta_{k,l,m}) < 0$ . As an example we give the triangle group  $\Delta_{2,3,7}$ . This group has a faithful representation into the group of isometries  $\text{Isom } \mathbb{H}^2$  of the hyperbolic plane  $\mathbb{H}^2$  [45, Section 7.2]. In this way one can make visible that the finite subgroups in formula (2.9) are generated by one or a pair of the generators. We deduce the expression

$$f_{237}(t) = \frac{[2]^2[3, 7]}{1 + t - t^3 - t^4 - t^5 - t^6 - t^7 + t^9 + t^{10}} \quad (2.13)$$

The growth rate of  $\Delta_{2,3,7}$  is  $\tau \approx 1.17628$  and equals the least known Salem number [28]. This is an algebraic integer of a special type, whose minimal polynomial over  $\mathbb{Z}$  is given by the denominator of  $f_{237}(t)$ . Later on, a more profound connection between growth rates of Coxeter groups and Salem numbers will come in sight (see Chapter 4, Section 4.1).

#### 2.2.4.4 Growth rate and co-volume in dimensions two and three

In the paper [28] (see also [33]) by E. Hironaka the minimal growth rate of cocompact Coxeter groups acting on  $\mathbb{H}^2$  is computed. This is the growth rate of  $\Delta_{2,3,7}$  triangle group. Moreover, the group  $\Delta_{2,3,7}$  is uniquely determined by its growth minimality property. On the other hand, the result [51] of C. Siegel, implies that the minimal co-volume cocompact reflection group acting on  $\mathbb{H}^2$  is exactly  $\Delta_{2,3,7}$ .

The following question is posed in [23, Problem 16].

QUESTION. Is there a direct connection between the area of hyperbolic polygon and the asymptotic growth rate of the underlying Coxeter reflection group?

In general the answer is “no” according to the following propositions [33].

Let  $\mathcal{P} \subset \mathbb{H}^n$  be a Coxeter polytope. Then we denote by  $G := G(\mathcal{P})$  the group generated by the set  $S$  of reflections in its facets. We denote the growth rate of  $G$  with respect to  $S$  by  $\tau_{\mathcal{P}} := \tau(G(\mathcal{P}))$ .

**Proposition 2** *There exist two infinite families  $\mathcal{P}_k$  and  $\mathcal{Q}_k$ ,  $k \geq 4$ , of compact hyperbolic Coxeter polygons, such that  $\tau_{\mathcal{P}_k} = \tau_{\mathcal{Q}_k}$ , but  $|\text{Area } \mathcal{P}_k - \text{Area } \mathcal{Q}_k|$  is unbounded for  $k \rightarrow \infty$ .*

PROOF. Let  $\mathcal{P}_k$ ,  $k \geq 4$ , be a hyperbolic  $k$ -gon with all angles equal  $\pi/3$ . Let  $\mathcal{Q}_k$ ,  $k \geq 4$ , be a hyperbolic  $(k+1)$ -gon with right angles. The polygons  $\mathcal{P}_k$  and  $\mathcal{Q}_k$ ,  $k \geq 4$ , exist by Theorem 7. The corresponding growth functions of  $G(\mathcal{P}_k)$  and  $G(\mathcal{Q}_k)$  are

$$f_{\mathcal{P}_k}(t) = \frac{[3]}{t^2 - (k-1)t + 1}, \quad f_{\mathcal{Q}_k}(t) = \frac{[2]^2}{t^2 - (k-1)t + 1}.$$

Observe that the growth rate of  $G(\mathcal{P}_k)$  equals that of  $G(\mathcal{Q}_k)$ ,  $k \geq 4$ , since the denominator polynomials of  $f_{\mathcal{P}_k}(t)$  and  $f_{\mathcal{Q}_k}(t)$  coincide.

According to Serre’s formula [49],  $\text{Area } \mathcal{P}_k = -2\pi/f_{\mathcal{P}_k}(1)$  and  $\text{Area } \mathcal{Q}_k = -2\pi/f_{\mathcal{Q}_k}(1)$ . We compute  $\text{Area } \mathcal{P}_k = 2\pi/3 \cdot (k-3)$ ,  $\text{Area } \mathcal{Q}_k = 2\pi/4 \cdot (k-3)$  and  $|\text{Area } \mathcal{P}_k - \text{Area } \mathcal{Q}_k| = \pi/6 \cdot (k-3)$ . Thus  $|\text{Area } \mathcal{P}_k - \text{Area } \mathcal{Q}_k| \rightarrow \infty$  as  $k \rightarrow \infty$ . Q.E.D.

**Proposition 3** *There exist two infinite families  $\mathcal{R}_k$  and  $\mathcal{S}_k$ ,  $k \geq 2$ , of compact hyperbolic Coxeter polygons, such that  $\text{Area } \mathcal{R}_k = \text{Area } \mathcal{S}_k$ , but  $|\tau_{\mathcal{R}_k} - \tau_{\mathcal{S}_k}|$  is unbounded for  $k \rightarrow \infty$ .*

PROOF. Let  $\mathcal{R}_k$  be a hyperbolic  $(4k)$ -gon with right angles and let  $\mathcal{S}_k$  be a hyperbolic  $(3k)$ -gon with all angles equal  $\pi/3$ . Both families of polygons exist for  $k \geq 2$  by Theorem 7. The corresponding growth functions are

$$f_{\mathcal{R}_k}(t) = \frac{[2]^2}{1 - (4k-2)t + t^2}, \quad f_{\mathcal{S}_k}(t) = \frac{[3]}{1 - (3k-1)t + t^2}.$$

Then Serre's formula [49] gives  $\text{Area } \mathcal{R}_k = -2\pi/f_{\mathcal{R}_k}(1)$  and  $\text{Area } \mathcal{S}_k = -2\pi/f_{\mathcal{S}_k}(1)$ , that implies  $\text{Area } \mathcal{R}_k = \text{Area } \mathcal{S}_k = 2\pi(k-1)$ . A straightforward computation of the roots of the denominator polynomials provides  $|\tau_{\mathcal{R}_k} - \tau_{\mathcal{S}_k}| \rightarrow \infty$  as  $k \rightarrow \infty$ . One can even deduce that  $\tau_{\mathcal{R}_k}/\tau_{\mathcal{S}_k} \rightarrow 4/3$  for  $k \rightarrow \infty$ . Q.E.D.

We may address an analogous question in the three-dimensional case. According to [33], the minimal growth rate  $\tau_{(3,5,3)} \approx 1.35098$  belongs to the reflection group of the hyperbolic orthoscheme  $(3, 5, 3)$ . However, the minimal volume among the Coxeter simplices belongs to  $(4, 3, 5)$ , as computed in [31, Appendix]. We illustrate the discrepancy between the growth rate and the covolumes of Coxeter groups acting on  $\mathbb{H}^3$  as follows [33].

**Proposition 4** *There exist two infinite families  $\mathcal{N}_k$  and  $\mathcal{M}_k$ ,  $k \geq 5$ , of compact hyperbolic Coxeter polyhedra, such that  $\tau_{\mathcal{N}_k} = \tau_{\mathcal{M}_k}$ , but  $|\text{Vol } \mathcal{N}_k - \text{Vol } \mathcal{M}_k|$  is unbounded for  $k \rightarrow \infty$ .*

PROOF. Following [56], let  $\mathcal{L}_k$ ,  $k \geq 5$ , be the  $k$ -th Löbell polyhedron (refer to Fig. 4.12 in Section 4). The dihedral angles of  $\mathcal{L}_k$  are right. Let  $L_1$  and  $L_2$  be two isometric copies of  $\mathcal{L}_{2k}$ ,  $k \geq 5$ . By matching them together along  $(2k)$ -gonal faces  $F_1$  and  $F_2$ , one obtains *the garland* of  $L_1$  and  $L_2$ . The edges of  $F_i$ ,  $i = 1, 2$ , disappear since the dihedral angles along them double after glueing and become equal to  $\pi$ . By analogy, we construct a garland of several polyhedra by matching  $l \geq 2$  isometric copies of  $\mathcal{L}_k$  along  $(2k)$ -gonal faces. Denote such a garland by  $\mathcal{L}_k^{(l)}$  for  $k \geq 5$ ,  $l \geq 2$ .

Using Löbell polyhedra and their garlands, we construct two desired families  $\mathcal{N}_k$  and  $\mathcal{M}_k$ . Let  $\mathcal{N}_k$ ,  $k \geq 5$ , be the Löbell polyhedron  $\mathcal{L}_{2k}$ . Let  $\mathbf{f} = (f_0, f_1, f_2)$  be its  $\mathbf{f}$ -vector that consists of the number of vertices  $f_0$ , the number of edges  $f_1$  and the number of faces  $f_2$ . For the polyhedron  $\mathcal{N}_k$  we have  $\mathbf{f}(\mathcal{N}_k) = (8k, 12k, 4k + 2)$ . Let  $\mathcal{M}_k$ ,  $k \geq 5$ , be the garland  $\mathcal{L}_k^{(3)}$  defined above. In this case  $\mathbf{f}(\mathcal{M}_k) = (8k, 12k, 4k + 2)$ , since the edges of glued faces disappear together with their vertices.

Observe that  $\mathcal{N}_k$  and  $\mathcal{M}_k$  are right-angled and so formula (3.5) of [34, Remark 5] applies. For the corresponding growth functions  $f_{\mathcal{N}_k}$  and  $f_{\mathcal{M}_k}$  of  $G(\mathcal{N}_k)$  and  $G(\mathcal{M}_k)$  we have

$$f_{\mathcal{N}_k}(t) = f_{\mathcal{M}_k}(t) = \frac{[2]^3}{1 - (4k-1)t + (4k-1)t^2 - t^3}.$$

Thus, the growth rates of  $G(\mathcal{N}_k)$  and  $G(\mathcal{M}_k)$  are equal for every  $k \geq 5$ .

Consider the volumes of  $\mathcal{N}_k$  and  $\mathcal{M}_k$ ,  $k \geq 5$ . By formula (7) of [56, Corollary 2], we have the following asymptotic behaviour for  $k$  large enough:

$$\text{Vol } \mathcal{N}_k \sim 20 k \mathbf{v}_3, \quad \text{Vol } \mathcal{M}_k \sim 30 k \mathbf{v}_3,$$

where the constant  $\mathbf{v}_3$  is the volume of a regular ideal tetrahedron, which equals  $2\Lambda(\pi/6) \approx 1.014$  in terms of the Lobachevsky function. Now it is seen that  $|\text{Vol}\mathcal{N}_k - \text{Vol}\mathcal{M}_k| \sim 10k\mathbf{v}_3$  is unbounded for  $k \rightarrow \infty$ . Q.E.D.

**Proposition 5** *There exist two infinite families  $\mathcal{U}_k$  and  $\mathcal{V}_k$ ,  $k \geq 6$ , of compact hyperbolic Coxeter polyhedra, such that  $\text{Vol}\mathcal{U}_k = \text{Vol}\mathcal{V}_k$ , but  $|\tau_{\mathcal{U}_k} - \tau_{\mathcal{V}_k}|$  is unbounded for  $k \rightarrow \infty$ .*

PROOF. Let  $\mathcal{L}^{(l)}(k)$  be a garland obtained from  $l \geq 2$  isometric copies of  $\mathcal{L}_k$ ,  $k \geq 6$ , glued along  $k$ -gonal faces as in the proof of Proposition 4. Let  $\mathcal{L}_k(l)$  be the garland obtained from  $l \geq 2$  isometric copies of  $\mathcal{L}_k$ ,  $k \geq 6$ , glued along pentagonal faces. We set  $\mathcal{U}_k$  to be  $\mathcal{L}_k^{(2)}$  and  $\mathcal{V}_k$  to be  $\mathcal{L}_k(2)$ . The corresponding growth functions are

$$f_{\mathcal{U}_k}(t) = \frac{[2]^3}{1 - (3k - 1)t + (3k - 1)t^2 - t^3}$$

and

$$f_{\mathcal{V}_k}(t) = \frac{[2]^3}{1 - (4k - 6)t + (4k - 6)t^2 - t^3}.$$

An easy computation of the roots of the denominator polynomials of  $f_{\mathcal{U}_k}(t)$  and  $f_{\mathcal{V}_k}(t)$ ,  $k \geq 6$ , yields  $|\tau_{\mathcal{U}_k} - \tau_{\mathcal{V}_k}| \rightarrow \infty$  as  $k \rightarrow \infty$ . More precisely,  $\tau_{\mathcal{U}_k}/\tau_{\mathcal{V}_k} \rightarrow 3/4$  for  $k \rightarrow \infty$ . On the other hand,  $\text{Vol}\mathcal{U}_k = \text{Vol}\mathcal{V}_k = 2 \text{Vol}\mathcal{L}_k$ . Q.E.D.

# Chapter 3

## Reflection groups

### 3.1 Coxeter polytopes and reflection groups

The main references for this chapter are [6, Chapter 5] and [59, Chapter 5].

#### 3.1.1 Basic notions and facts

Let us recall the notion of a reflection in a hyperplane of  $\mathbb{X}^n$ . First, consider the case of  $\mathbb{X}^n = \mathbb{E}^n$ . A reflection in  $\mathbb{E}^n$  in the hyperplane  $H := H_{e,t}$  given by formula (1.5), is

$$s_H(x) = x - 2(\langle x, e \rangle_1 + t)e.$$

Now consider the case  $\mathbb{X}^n = \mathbb{S}^n$ . A spherical hyperplane  $H := H_e$  is defined in Section 1.1.2 by formula (1.7). The corresponding reflection in the hyperplane  $H$  is given by

$$s_H(x) = x - 2\langle x, e \rangle_1 e. \quad (3.1)$$

In case of the hyperbolic space  $\mathbb{X}^n = \mathbb{H}^n$ , let us consider its hyperboloid described in Section 1.1.3.3. Then the reflection in the Lorentzian hyperplane  $H := H_e$  with space-like normal vector  $e$  defined by formula (1.9) is given by

$$s_H(x) = x - 2\langle x, e \rangle_{-1} e. \quad (3.2)$$

A *reflection group* acting on  $\mathbb{X}^n$  is a discrete group generated by a finite number of reflections.

Let us recall that every discrete group  $G$  acting by isometries on  $\mathbb{X}^n$  has a fundamental domain, that tessellates the space  $\mathbb{X}^n$  under the action of  $G$  [45]. There is always a convex fundamental domain for a discrete group, namely a Dirichlet polytope, which is a particular convex polytope in  $\mathbb{X}^n$  [45, Sections 6.7 and 13.5].

A *Coxeter polytope* in  $\mathbb{X}^n$  is a polytope with dihedral angles given by integer submultiples of  $\pi$ , i.e. each having the form  $\pi/m$ , for some integer  $m \geq 2$ .

The following theorem highlights a relation between reflection groups and Coxeter polytopes in  $\mathbb{X}^n$ .

**Theorem 14 (Proposition 1.4, [59])** *Let  $G$  be a reflection group acting on  $\mathbb{X}^n$  and let  $\mathcal{P} \subset \mathbb{X}^n$  be a fundamental domain for  $G$ . Then  $\mathcal{P}$  is a Coxeter polytope, unique up to an isometry, and  $G$  is generated by reflections in the supporting hyperplanes of its facets.*

Group notation	Coxeter diagram
$(k, 2, l), k, l \geq 2$	
$(5, 3, 3)$	
$(3, 4, 3)$	
$(4, 3, 3)$	
$(2, 3, 5)$	
$(3, 3, 3)$	
$(2, 3, 4)$	
$(2, 3, 3)$	
$(3, 3^{1,1})$	

Table 3.1: Coxeter simplices in  $\mathbb{S}^3$

Let us note that Theorem 14 immediately implies that a reflection group  $G$  acting on a constant curvature space  $\mathbb{X}^n$  is a Coxeter group. Given a Coxeter polytope  $\mathcal{P}$ , let us define its Coxeter diagram as follows:

- (1) Each vertex of the diagram  $v_i$  corresponds to a facet  $F_i, i = 1, \dots, \text{card } \Omega_{n-1}(P)$ .
- (2) Two vertices  $v_i$  and  $v_j$  are connected by an edge whenever the corresponding dihedral angle between the facets is of the form  $\pi/m_{ij}, m_{ij} \geq 3$ . If  $m_{ij} \geq 4$ , then the edge is labelled  $m_{ij}$ .



- (3) Two vertices  $v_i$  and  $v_j$  are connected by an edge labelled  $\infty$ , if  $F_i$  and  $F_j$  have parallel supporting hyperplanes in  $\mathbb{X}^n = \mathbb{H}^n$ , i.e. share a point at the ideal boundary  $\partial\mathbb{H}^n$ .
- (4) Two vertices  $v_i$  and  $v_j$  are connected by a dashed edge, if  $F_i$  and  $F_j$  have a common perpendicular in  $\mathbb{X}^n = \mathbb{E}^n$  or  $\mathbb{H}^n$ . The edge may be labelled by the length of the common perpendicular, or the length could be omitted.

As one may observe, the Coxeter diagram of a Coxeter polytope is the Coxeter diagram that determines the corresponding reflection group with some additional indications having a geometric meaning.

### 3.1.2 Examples

#### 3.1.2.1 Coxeter simplices in $\mathbb{S}^3$

In Table 3.1 we collect all Coxeter simplices in  $\mathbb{S}^3$  [11]. The corresponding reflection groups produce a finite tiling of  $\mathbb{S}^3$  and thus are finite themselves. In general, any reflection group acting on  $\mathbb{X}^n = \mathbb{S}^n$  is finite, since  $\mathbb{S}^n$  is compact.

Group notation	Polyhedron	Coxeter diagram
$(\infty, 2, \infty, 2, \infty, 2)$	Cube	
$(\infty, 2, 4, 4)$	Prism	
$(\infty, 2, 3, 6)$	Prism	
$(\infty, 2, (3^3))$	Prism	
$(4, 2, 4)$	Simplex	
$(4, 3^{1,1})$	Simplex	
$((3^4))$	Simplex	

Table 3.2: Coxeter polyhedra in  $\mathbb{E}^3$

### 3.1.2.2 Coxeter polyhedra in $\mathbb{E}^3$

In Table 3.2 we collect all possible Coxeter polyhedra of finite volume in  $\mathbb{E}^3$  [11]. One may observe that their combinatorial type is either a simplex, or a prism (a product of a simplex and an interval), or a cube (a product of three intervals) as implied by Theorem 2.

## 3.2 Coxeter groups acting on $\mathbb{X}^n$

We are interested in Coxeter groups  $G = \langle S|R \rangle$  acting discretely by reflections on a constant sectional curvature space  $\mathbb{X}^n = \mathbb{S}^n, \mathbb{E}^n$  or  $\mathbb{H}^n$ , such that a fundamental domain is a compact or finite-volume polytope  $\mathcal{P} \subset \mathbb{X}^n$ . If  $\mathcal{P}$  is compact then the action of  $G$  on  $\mathbb{X}^n$  is called *co-compact*. If  $\mathcal{P}$  has finite volume then the action of  $G$  on  $\mathbb{X}^n$  is *of finite co-volume*. Sometimes one does not distinguish between a Coxeter group  $G$  and its action by reflection on  $\mathbb{X}^n$ , so  $G$  itself is called respectively co-compact or of finite co-volume.

By Theorem 14, classifying Coxeter groups acting discretely and co-compactly (or finite co-volume actions) on  $\mathbb{X}^n$  means classifying compact (or finite-volume) Coxeter polytopes in  $\mathbb{X}^n$ .

By Theorem 2, if  $\mathbb{X}^n = \mathbb{S}^n$  or  $\mathbb{E}^n$ , such a classification means listing all Coxeter simplices in  $\mathbb{X}^n$  (see Section 2.2.2.1 and Section 2.2.2.2) by means of their Coxeter diagrams. In case  $\mathbb{X}^n = \mathbb{E}^n$  one should take into consideration all possible products of the lower-dimensional simplices, as well.

In case of the hyperbolic space  $\mathbb{X}^n = \mathbb{H}^n$ , the picture is rather different. The following two theorems tell us that the dimension  $n$  of the space cannot be arbitrarily large.

**Theorem 15 (È. Vinberg, [58])** *There is no co-compact Coxeter group acting on  $\mathbb{H}^n$ , if  $n > 30$ .*

**Theorem 16 (M.N. Prokhorov, [44])** *There is no finite co-volume Coxeter group acting on  $\mathbb{H}^n$ , if  $n > 995$ .*

The bounds in the above theorems are apparently far from being exact, since the known examples of compact Coxeter polytopes in  $\mathbb{H}^n$  go up to dimension 8 and those of finite-volume Coxeter polytopes – up to dimension 21.

Let us consider the following class of Coxeter groups, that are of particular interest. A Coxeter group  $G = \langle S|R \rangle$ , with generating set  $S = \{s_1, \dots, s_n\}$  and relations

$R = \{(s_i s_j)^{m_{ij}}\}_{i,j=1}^n$  is called *right-angled* if  $m_{ii} = 1$ ,  $m_{ij} = 2$  or  $\infty$  if  $i \neq j$ , for all  $i, j = 1, \dots, n$ .

If such a group acts discretely on  $\mathbb{X}^n$  by reflections, the corresponding fundamental domains are Coxeter polytopes having only right dihedral angles.

In case  $\mathbb{X}^n = \mathbb{H}^n$ , they could be compact or of finite volume. There are more precise dimension bounds for this class of polytopes given by the following theorems (see also Section 3.2.1).

**Theorem 17 (È. Vinberg, L. Potyagaïlo, [43])** *There is no co-compact right-angled Coxeter group acting on  $\mathbb{H}^n$ , if  $n > 4$ , and the bound is sharp. There is no finite co-volume right-angled Coxeter group acting on  $\mathbb{H}^n$ , if  $n > 14$ .*

In case of a finite co-volume action, the bound has been recently improved.

**Theorem 18 (G. Dufour, [15])** *There is no finite co-volume right-angled Coxeter group acting on  $\mathbb{H}^n$ , if  $n > 12$ .*

The most important technical feature in all Theorems 15-18 is the following inequality.

**Theorem 19 (V. Nikulin, [41])** *Let  $\mathcal{P} \subset \mathbb{H}^n$  be a convex polytope. Let  $f_k^\ell(\mathcal{P}) := \frac{1}{f_k(\mathcal{P})} \sum_{F \in \Omega_k(\mathcal{P})} f_\ell(F)$  be the average number of  $\ell$ -dimensional faces of  $\mathcal{P}$  in each  $k$ -dimensional one. Then for  $1 \leq \ell < k \leq \lfloor \frac{n}{2} \rfloor$ , the following inequality holds:*

$$f_k^\ell(\mathcal{P}) < \binom{n-\ell}{n-k} \frac{\binom{\lfloor \frac{n}{2} \rfloor}{\ell} + \binom{\lfloor \frac{n+1}{2} \rfloor}{\ell}}{\binom{\lfloor \frac{n}{2} \rfloor}{k} + \binom{\lfloor \frac{n+1}{2} \rfloor}{k}}. \quad (3.3)$$

The right-hand side of the inequality above depends on the combinatorial parameters  $k$ ,  $\ell$  and  $n$  only and is a decreasing function in  $n$  if  $k$  and  $\ell$  are fixed, while the left-hand side depends on the geometry of the polytopes of a given type. Thus, estimating the quantity  $f_k^\ell(\mathcal{P})$  from below, one gets an upper bound on  $n$ . Different geometric and combinatorial techniques to obtain a lower bound for  $f_k^\ell(\mathcal{P})$  are described in [58, 43, 15].

There are many examples of co-compact Coxeter groups acting on  $\mathbb{X}^n = \mathbb{H}^n$  and several combinatorial families of Coxeter polyhedra are classified in [20, 21]. There are even infinitely many non-isometric Coxeter polyhedra in dimensions  $2 \leq n \leq 19$  [1].

### 3.2.1 Example

Let  $\mathcal{P}_2$  be a regular right-angled pentagon in  $\mathbb{H}^2$ , which exists by Theorem 7. Let  $\mathcal{P}_3$  be a regular dodecahedron with regular pentagonal faces, which exists by Andreev's theorem (Theorem 9). Let  $\mathcal{P}_4 \subset \mathbb{H}^4$  be a polytope with all angles right and combinatorially isomorphic to the 120-cell, that means,  $\mathcal{P}_4$  is the regular four-dimensional polytope having 120 dodecahedral facets, 720 pentagonal faces, 1200 edges and 600 vertices. Such a polytope can be obtained by means of *the Wythoff construction* [11] applied to the hyperbolic simplex given by the Coxeter scheme  $\circ \text{---} \overset{5}{\bullet} \text{---} \bullet \text{---} \bullet \text{---} \overset{4}{\bullet} \text{---} \bullet$ . Thus, there are examples of compact right-angled hyperbolic polytopes  $\mathcal{P}_n$  in dimensions  $n = 2, 3, 4$ .

Now let us note that the minimal number of sides of a right-angled polygon is five, according to Theorem 7. As well, each vertex figure of a right-angled compact polytope is a right-angled spherical simplex. Thus, all low-dimensional faces are also right-angled. This implies that for a compact right-angled polytope  $\mathcal{P} \subset \mathbb{H}^n$  we have  $f_3^2(\mathcal{P}) \geq 5$ , since each two-dimensional face is a right-angled polygon and has at least five edges. By plugging this estimate into equation (3.3), we obtain  $n \leq 4$ . Thus, the first assertion of Theorem 17 follows.

## 3.3 Growth of hyperbolic reflection groups

### 3.3.1 Coxeter groups acting on $\mathbb{H}^2$

By means of Steinberg's formula 2.9 from Section 2.2.3 we may compute the growth function of a given Coxeter group  $G = \langle S|R \rangle$ , as soon as we determine its *finite principal* subgroups. If such a group acts on the hyperbolic plane  $\mathbb{H}^2$  by reflections, this task is fairly easy. The fundamental polytope  $\mathcal{P}$  for the group  $G$  acting on  $\mathbb{H}^2$  is a hyperbolic  $k$ -gon with plane angles satisfying the conditions of Theorem 7. If  $s_i$  and  $s_j$  are reflections in two adjacent sides intersecting in  $\mathbb{H}^2$ , then the subgroup  $\langle s_i, s_j | s_i^2, s_j^2, (s_i s_j)^{m_{ij}} \rangle$  is a dihedral group  $D_{m_{ij}}$  of order  $2m_{ij}$ . If  $s_i$  and  $s_j$  are parallel and meet in a vertex at  $\partial\mathbb{H}^2$  or admit a common perpendicular, then the group  $\langle s_i, s_j \rangle \cong \mathbb{Z}_2 * \mathbb{Z}_2$  is infinite. There is a simple expression for the growth function  $f_{(G,S)}(t)$  of  $G$  if the polygon  $\mathcal{P}$  is compact. Let  $v$  be a vertex of  $\mathcal{P}$  with the corresponding plane angle  $\frac{\pi}{m_{ij}}$ . Let  $g_v(t)$  be a function associated to  $v$  of the form

$$g_v(t) = -\frac{t}{[2]} \frac{[m_{ij}]}{[m_{ij} + 1]}. \quad (3.4)$$

Then, according to formulas (0.2)-(0.3) in [42], we have

$$\frac{1}{f_{(G,S)}(t^{-1})} = 1 + \sum_{v \in \Omega_0(\mathcal{P})} g_v(t). \quad (3.5)$$

### 3.3.2 Coxeter groups acting on $\mathbb{H}^3$

Let us now consider the case of a Coxeter group  $G = \langle S|R \rangle$  acting by reflections on  $\mathbb{H}^3$ . According to Andreev's theorem (Theorem 9) a fundamental polytope  $\mathcal{P}$  for the group  $G$  is either a Coxeter tetrahedron (a Lanner or a quasi-Lanner tetrahedron, as classified in [29, Section 6.9] or [45, Sections 7.2 and 7.3]), a Coxeter triangular prism (as classified in [32, 58]) or, if it has a different combinatorial type, a polyhedron with the following properties:

- (1) The polyhedron  $\mathcal{P}$  satisfies conditions  $(\mathbf{m}_0)$ - $(\mathbf{m}_5)$  of Andreev's theorem.
- (2) If  $v \in \Omega_0(\text{cl } \mathcal{P})$  is a *proper vertex* of  $\mathcal{P}$ , then  $v$  is necessarily trivalent and its stabiliser  $Stab(v)$ , generated by reflections in the adjacent faces, is a finite triangle group from Table 3.3.

Vertex group $Stab(v)$	Coxeter exponents		
	$m_1$	$m_2$	$m_3$
$\Delta_{22n}, n \geq 2$	1	1	$n - 1$
$\Delta_{233}$	1	2	3
$\Delta_{234}$	1	3	5
$\Delta_{235}$	1	5	9

Table 3.3: Coxeter exponents

The following theorem holds if the fundamental polyhedron  $\mathcal{P}$  for the group  $G$  is compact.

**Theorem 20 (W. Parry, [42])** *Let  $G = \langle S|R \rangle$  be a co-compact reflection group acting on  $\mathbb{H}^3$  with fundamental Coxeter polyhedron  $\mathcal{P}$ . Then the growth function  $f_{(S,R)}(t)$  satisfies the identity*

$$\frac{1}{f_{(S,R)}(t^{-1})} = \frac{t-1}{t+1} + \sum_{v \in \Omega_0(\mathcal{P})} g_v(t), \quad (3.6)$$

where

$$g_v(t) = \frac{t(1-t)}{2} \frac{[m_1, m_2, m_3]}{[m_1 + 1, m_2 + 1, m_3 + 1]} \quad (3.7)$$

is a function associated with each vertex  $v \in \Omega_0(\mathcal{P})$ ; the integers  $m_1, m_2, m_3$  are the Coxeter exponents (as defined in [29, Section 3.16, p. 75]) of the finite Coxeter group  $\text{Stab}(v)$  given in Table 3.3.

### 3.3.3 Coxeter groups acting on $\mathbb{H}^n$ , $n \geq 4$

Let us introduce several notions concerning the form of the growth function for a given Coxeter group  $G = \langle S|R \rangle$ . According to Steinberg's formula (Theorem 13), such a growth function has the form

$$f_{(G,S)}(t) = \frac{p(t)}{q(t)}, \quad (3.8)$$

with relatively prime polynomials  $p(t)$  and  $q(t)$  over the integers. We shall change its form for the purpose of technical convenience. First of all, the right-hand side of Steinberg's formula (2.9) comprises some of the growth functions of finite Coxeter groups given in Table 3.4. Namely, it has the form

$$\sum_{T \in \mathcal{F}} \frac{(-1)^{\text{card } T}}{f_{((T),T)}(t)},$$

with  $\mathcal{F} = \{T \subseteq S \mid \text{the subgroup generated by } T \text{ is finite}\}$ .

Group	Coxeter exponents	Growth function
$A_n$	$1, 2, \dots, n-1, n$	$[1, 2, \dots, n, n+1]$
$B_n$	$1, 3, \dots, 2n-3, 2n-1$	$[2, 4, \dots, 2n-2, 2n]$
$D_n$	$1, 3, \dots, 2n-5, 2n-3, n-1$	$[2, 4, \dots, 2n-1][n]$
$G_2^{(n)}$	$1, n-1$	$[2, n]$
$F_4$	$1, 5, 7, 11$	$[2, 6, 8, 12]$
$E_6$	$1, 4, 5, 7, 8, 11$	$[2, 5, 6, 8, 9, 12]$
$E_7$	$1, 5, 7, 9, 11, 13, 17$	$[2, 6, 8, 10, 12, 14, 18]$
$E_8$	$1, 7, 11, 13, 17, 19, 23, 29$	$[2, 8, 12, 14, 18, 20, 24, 30]$
$H_3$	$1, 5, 9$	$[2, 6, 10]$
$H_4$	$1, 11, 19, 29$	$[2, 12, 20, 30]$

Table 3.4: Irreducible finite Coxeter groups and their growth functions [52]

Each  $f_T(t) := f_{((T),T)}(t)$  is actually a polynomial, so we may define *the virgin form* of the numerator for  $f_{(G,S)}(t)$  as

$$\text{Virg}(S) := \text{LCM} \{f_T(t) \mid T \in \mathcal{F}\}. \quad (3.9)$$

From Steinberg's formula (2.9), it follows that the polynomial  $p(t)$  in expression (3.8) for the growth function divides  $\text{Virg}(S)$ . Thus, we may write  $f_{(G,S)}(t)$  in the form

$$f_{(G,S)}(t) = \frac{\text{Virg}(S)}{q(t)r(t)}, \quad (3.10)$$

with a suitable polynomial  $r(t) \in \mathbb{Z}[t]$  resulting from the ratio of the virgin form of the numerator to  $p(t)$ .

The polynomial  $\text{Virg}(S)$  has factors of the form  $[k]$ ,  $k \geq 2$ , and of the form  $1 + x^k$ ,  $k \geq 2$ . Each factor of the form  $1 + x^k$  could be turned into  $[2k]$  by means of the identity  $[k](1 + x^k) = [2k]$ ,  $k \geq 2$ . By applying this procedure to the factors of  $\text{Virg}(S)$ , we get *the extended form* of the numerator  $\text{Ext}(S)$ . Again, we may write

$$f_{(G,S)}(t) = \frac{P(t)}{Q(t)}, \quad (3.11)$$

with  $P(t)$  in the extended form and  $Q(t)$  a polynomial over the integers.

If the function  $f_{(G,S)}(t)$  has its numerator in the extended form, we say  $f_{(G,S)}(t)$  is in its *complete form*. Later on, in Chapter 4, we shall use both of these forms to represent growth functions in a suitable way.

Now recall several general facts concerning growth functions of reflection groups acting on  $\mathbb{H}^n$  and their relation to the co-volume of the respective group.

Let  $P(t)$  be a polynomial and let  $\tilde{P}(t) := t^{\deg P} P(t^{-1})$  be *the reciprocal polynomial* to  $P(t)$ . If  $\tilde{P}(t)$  equals  $P(t)$ , then  $P(t)$  is *a reciprocal polynomial*. If  $\tilde{P}(t)$  equals  $-P(t)$ , then  $P(t)$  is *an anti-reciprocal one*.

Let  $f(t)$  be a rational function, which is not a polynomial. Then we say  $f(t)$  to be *reciprocal* if  $f(t^{-1})$  equals  $f(t)$  and *anti-reciprocal* if  $f(t^{-1})$  equals  $-f(t)$ .

The following theorem concerns the growth function of a Coxeter group acting co-compactly on  $\mathbb{H}^n$ .

**Theorem 21 (R. Charney, M. Davis, [9])** *Let  $G$  be a Coxeter group generated by a set  $S$  of reflections in the facets of a compact polytope in  $\mathbb{H}^n$ . Then  $f_{(G,S)}(t^{-1}) = (-1)^n f_{(G,S)}(t)$ .*

According to the above theorem, the function given by formula (3.5) is reciprocal, and that given by formula (3.6) is anti-reciprocal.

By representing the growth function of a co-compact Coxeter group  $G$  acting discretely on  $\mathbb{H}^n$  in its complete form,

$$f_{(G,S)}(t) = \frac{P(t)}{Q(t)} = \frac{P(t)}{\sum_{i=0}^N b_i t^i}, \quad (3.12)$$

one has a recursion formula representing the coefficients  $b_k$ ,  $k = 0, \dots, N$ , in combinatorial terms related to choosing finite principal subgroups of  $G$ . The precise formula is due to R. Kellerhals and G. Perren ([34, Theorem 2.5]).

The following theorem relates together the growth function  $f_{(G,S)}(t)$ , the Euler characteristic  $\chi(G)$  and the co-volume of a given Coxeter group  $G$  generated by the set  $S$  of reflections in the facets of a finite-volume polytope in  $\mathbb{H}^n$ , if  $n \geq 2$  is even.

**Theorem 22 (G.J. Heckman, T. Zehrt, [27, 62])** *Let  $G$  be a Coxeter group generated by a set  $S$  of reflections in the facets of a finite-volume polytope in  $\mathbb{H}^n$ . Then*

$$\frac{1}{f_{(G,S)}(1)} = \chi(G) = \chi_{\text{orb}}(\mathbb{H}^n/G) = \begin{cases} (-1)^{\frac{n}{2}} \frac{2\text{Vol}\mathcal{P}}{\text{Vol}\mathbb{S}^n}, & \text{if } n \text{ is even;} \\ 0, & \text{if } n \text{ is odd.} \end{cases} \quad (3.13)$$

where  $\chi(G)$  is the Euler characteristic of  $G$ ,  $\chi_{\text{orb}}(\mathbb{H}^n/G)$  is the orbifold Euler characteristic of the quotient space  $\mathbb{H}^n/G$  and  $\text{Vol}\mathcal{P}$  is the hyperbolic volume of  $\mathcal{P}$ .



# Chapter 4

## Main results

### 4.1 Deformation of hyperbolic Coxeter polyhedra, growth rates and Pisot numbers

Growth series for Coxeter groups are series expansions of certain rational functions according to Steinberg's formula (2.9). By considering the growth function of a hyperbolic Coxeter group, being a discrete group generated by a finite set  $S$  of reflections in hyperplanes of hyperbolic space  $\mathbb{H}^n$ , J.W. Cannon [7, 8], P. Wagreich [60], W. Parry [42] and W. Floyd [22] in the beginning of the 1980's discovered a connection between the real poles of the corresponding growth function and algebraic integers such as Salem numbers and Pisot numbers for  $n = 2, 3$ . In particular, there is a kind of geometric convergence for the fundamental domains of cocompact planar hyperbolic Coxeter groups giving a geometric interpretation of the convergence of Salem numbers to Pisot numbers, the behaviour discovered by R. Salem [48] much earlier in 1944. In the following, we provide a generalisation of the result by W. Floyd [22] to the three-dimensional case (c.f. Theorem 23). These results are published in [36] and are, to a large extent, reproduced here, up to a few exceptions.

#### 4.1.1 Growth rates and algebraic integers

Let  $\mathcal{P} \subset \mathbb{H}^n$ ,  $n \geq 2$ , be a finite-volume hyperbolic Coxeter polyhedron and let  $G = G(\mathcal{P})$  be a discrete subgroup of  $\text{Isom}(\mathbb{H}^n)$  it gives rise to, in accordance with Theorem 14, generated by the set  $S$  of reflections in the finitely many bounding hyperplanes of  $\mathcal{P}$ . We call  $G = G(\mathcal{P})$  a hyperbolic Coxeter group. In the following we will study the growth function of  $G = (G, S) = G(\mathcal{P})$ .

Observe that all finite subgroups of  $G$  are stabilisers of elements  $F \in \Omega_k(\mathcal{P})$  for some  $k \geq 0$ . The growth rate of the reflection group  $G(\mathcal{P})$  is  $\tau > 1$ , if  $\mathcal{P}$  is compact,

by Milnor's theorem (Theorem 12) or, if  $\mathcal{P}$  has finite volume, by the result of de la Harpe [26] and so the growth function  $f_S(t)$  has a pole in  $(0, 1)$ .

In the context of growth rates we shall look at particular classes of algebraic integers.

A *Salem number* is a real algebraic integer  $\alpha > 1$  such that  $\alpha^{-1}$  is an algebraic conjugate of  $\alpha$  and all the other algebraic conjugates lie on the unit circle of the complex plane. Its minimal polynomial over  $\mathbb{Z}$  is called a *Salem polynomial*.

A Pisot-Vijayaraghavan number, or a *Pisot number* for short, is a real algebraic integer  $\beta > 1$  such that all the algebraic conjugates of  $\beta$  are in the open unit disc of the complex plane. The corresponding minimal polynomial over  $\mathbb{Z}$  is called a *Pisot polynomial*.

The following result is very useful in order to detect Pisot polynomials.

**Lemma 1 (W. Floyd, [22])** *Let  $P(t)$  be a monic polynomial with integer coefficients such that  $P(0) \neq 0$ ,  $P(1) < 0$ , and  $P(t)$  is not reciprocal. Let  $\tilde{P}(t)$  be the reciprocal polynomial for  $P(t)$ . Suppose that for every sufficiently large integer  $m$ ,  $\frac{t^m P(t) - \tilde{P}(t)}{t-1}$  is a product of cyclotomic polynomials and a Salem polynomial. Then  $P(t)$  is a product of cyclotomic polynomials and a Pisot polynomial.*

The convergence of Salem numbers to Pisot numbers was first discovered and analysed in [48]. A geometrical relation between these algebraic integers comes into view as follows. Growth functions of planar hyperbolic Coxeter groups were calculated explicitly in [22, Section 2]. The main result of [22] states that the growth rate  $\tau$  of a co-compact hyperbolic Coxeter group – being a Salem number by [42] – converges from below to the growth rate of a finite co-volume hyperbolic Coxeter group under a certain deformation process performed on the corresponding fundamental domains. More precisely, one deforms the given compact Coxeter polygon by decreasing one of its angles  $\pi/m$ . This process results in pushing one of its vertices toward the ideal boundary  $\partial\mathbb{H}^2$  in such a way that every polygon under this process provides a co-compact hyperbolic Coxeter group.

Therefore, a sequence of Salem numbers  $\alpha_m$  given by the respective growth rates  $\tau_m$  arises. The limiting Coxeter polygon is of finite area having exactly one ideal vertex, and the growth rate  $\tau_\infty$  of the corresponding Coxeter group equals the limit of  $\beta = \lim_{m \rightarrow \infty} \alpha_m$  and is a Pisot number. We study analogous phenomena in the case of spatial hyperbolic Coxeter groups.

#### 4.1.1.1 Example

Let  $\mathcal{D}_n \subset \mathbb{H}^3$ ,  $n \in \mathbb{N}$ , be a hyperbolic dodecahedron with all but one right dihedral angles. The remaining angle along the thickened edge of  $\mathcal{D}_n$ , as shown in Fig. 4.1, equals  $\frac{\pi}{n+2}$ ,  $n \geq 0$ . The initial polyhedron  $\mathcal{D}_0$  is known as the Löbell polyhedron  $\mathcal{L}_5$ . As  $n \rightarrow \infty$ , the sequence of polyhedra tends to a right-angled hyperbolic polyhedron  $\mathcal{D}_\infty$  with precisely one vertex at infinity. Let us compute the growth functions and growth rates of  $G(\mathcal{D}_n)$ ,  $n \geq 0$ , and  $G(\mathcal{D}_\infty)$ .

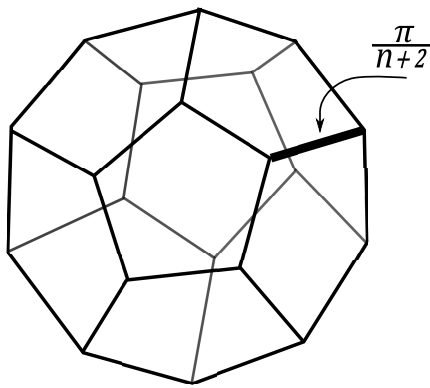


Figure 4.1: The dodecahedron  $\mathcal{D}_n \subset \mathbb{H}^3$ ,  $n \geq 0$ , with all but one right dihedral angles. The specified angle equals  $\frac{\pi}{n+2}$

By Theorem 20, the growth function of  $G(\mathcal{D}_n)$ , with respect to the generating set  $S$  of reflections in the faces of  $\mathcal{D}_n$ , equals

$$f_n(t) = \frac{(1+t)^3(1+t+\dots+t^{n-1})}{1-8t+8t^{n+1}-t^{n+2}}, \quad (4.1)$$

and similarly

$$f_\infty(t) = \frac{(1+t)^3}{(1-t)(1-8t)}. \quad (4.2)$$

Observe that the function (4.1) is anti-reciprocal, but the function (4.2) is not.

The computation of the growth rates  $\tau_n$ ,  $n \geq 0$ , for  $G(\mathcal{D}_n)$  and of the growth rate  $\tau_\infty$  for  $G(\mathcal{D}_\infty)$  gives

$$\tau_0 \approx 7.87298 < \tau_1 \approx 7.98453 < \dots < \tau_\infty = 8.$$

Thus, the Salem numbers numbers  $\tau_n$ ,  $n \geq 0$ , tend from below to  $\tau_\infty$ , which is a Pisot number.

Consider a finite-volume polytope  $\mathcal{P} \subset \mathbb{H}^n$  and a compact face  $F \in \Omega_{n-2}(\mathcal{P})$  with dihedral angle  $\alpha_F$ . We always suppose that  $\mathcal{P}$  is not degenerate (i.e. not contained in

a hyperplane). Suppose that there is a sequence of polytopes  $\mathcal{P}(k) \subset \mathbb{H}^n$  having the same combinatorial type and the same dihedral angles as  $\mathcal{P} = \mathcal{P}(1)$  apart from  $\alpha_F$  whose counterpart  $\alpha_F(k)$  tends to 0 as  $k \nearrow \infty$ . Suppose that the limiting polytope  $\mathcal{P}_\infty$  exists and has the same number of facets as  $\mathcal{P}$ . This means the facet  $F$ , which is topologically a co-dimension two ball, is contracted to a point, which is a vertex at infinity  $v_\infty \in \partial\mathbb{H}^n$  of  $\mathcal{P}_\infty$ . We call this process *contraction of the face  $F$  to an ideal vertex*.

REMARK. In the case  $n = 2$ , an ideal vertex of a Coxeter polygon  $\mathcal{P}_\infty \subset \mathbb{H}^2$  comes from “contraction of a compact vertex” [22]. This means a vertex  $F \in \Omega_0(\mathcal{P})$  of some hyperbolic Coxeter polygon  $\mathcal{P}$  is pulled towards a point at infinity.

In the above deformation process, the existence of the polytopes  $\mathcal{P}(k)$  in hyperbolic space is of fundamental importance. Let us consider the three-dimensional case. Since the angles of hyperbolic finite-volume Coxeter polyhedra are non-obtuse, Andreev’s theorem (Theorem 9) may be used in order to conclude about their existence and combinatorial structure.

## 4.1.2 Coxeter groups acting on hyperbolic three-space

### 4.1.2.1 Deformation of finite volume Coxeter polyhedra

Let  $\mathcal{P} \subset \mathbb{H}^3$  be a Coxeter polyhedron of finite volume with at least five faces. Suppose that  $k_1, k_2, n, l_1, l_2 \geq 2$  are integers. An edge  $e \in \Omega_1(\mathcal{P})$  is a *ridge of type*  $\langle k_1, k_2, n, l_1, l_2 \rangle$  if  $e$  is compact and has trivalent vertices  $v, w$  such that the dihedral angles at the incident edges are arranged counter-clockwise as follows: the dihedral angles along the edges incident to  $v$  are  $\frac{\pi}{k_1}, \frac{\pi}{k_2}$  and  $\frac{\pi}{n}$ , the dihedral angle along the edges incident to  $w$  are  $\frac{\pi}{l_1}, \frac{\pi}{l_2}$  and  $\frac{\pi}{n}$ . In addition, the faces sharing  $e$  are at least quadrilaterals (see Fig. 4.2).

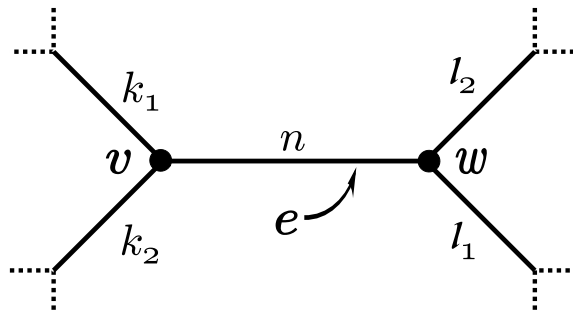


Figure 4.2: A ridge of type  $\langle k_1, k_2, n, l_1, l_2 \rangle$

NOTE. All the figures Fig. 4.4-4.10 are drawn according to the following pattern: only significant combinatorial elements are highlighted (certain vertices, edges and faces), and the remaining ones are not specified and overall coloured grey. In each figure, the polyhedron is represented by its projection onto one of its supporting planes, and its dihedral angles of the form  $\pi/m$  are labelled with  $m$ .

**Proposition 6** *Let  $\mathcal{P} \subset \mathbb{H}^3$  be a Coxeter polyhedron of finite volume with  $|\Omega_2(\mathcal{P})| \geq 5$ . If  $\mathcal{P}$  has a ridge  $e \in \Omega_1(\mathcal{P})$  of type  $\langle 2, 2, n, 2, 2 \rangle$ ,  $n \geq 2$ , then  $e$  can be contracted to a four-valent ideal vertex.*

PROOF. Denote by  $\mathcal{P}(m)$  a polyhedron having the same combinatorial type and the same dihedral angles as  $\mathcal{P}$ , except for the angle  $\alpha_m = \frac{\pi}{m}$  along  $e$ . We show that  $\mathcal{P}(m)$  exists for all  $m \geq n$ . Both vertices  $v, w$  of  $e \in \Omega_1(\mathcal{P}(m))$  are points in  $\mathbb{H}^3$ , since the sum of dihedral angles at each of them equals  $\pi + \frac{\pi}{m}$  for  $m \geq n \geq 2$ . Thus, condition  $\mathbf{m}_1$  of Andreev's theorem holds. Condition  $\mathbf{m}_0$  is obviously satisfied, as well as conditions  $\mathbf{m}_2$ - $\mathbf{m}_4$ , since  $\alpha_m \leq \alpha_n$ .

During the same deformation, the planes intersecting at  $e$  become tangent to a point  $v_\infty \in \partial\mathbb{H}^3$  at infinity. The point  $v_\infty$  is a four-valent ideal vertex with right angles along the incident edges. Denote the resulting polyhedron by  $\mathcal{P}_\infty$ .

Since the contraction process deforms only one edge to a point, no new 3- or 4-circuits do appear in  $\mathcal{P}_\infty$ . Hence, for the existence of  $\mathcal{P}_\infty \subset \mathbb{H}^3$  only condition  $\mathbf{m}_5$  of Andreev's theorem remains to be verified. Suppose that condition  $\mathbf{m}_5$  is violated and distinguish the following two cases for the polyhedron  $\mathcal{P}$  leading to  $\mathcal{P}_\infty$  under contraction of the edge  $e$ .

1.  *$\mathcal{P}$  is a triangular prism.* There are two choices of the edge  $e \in \Omega_1(\mathcal{P})$ , that undergoes contraction to  $v \in \Omega_\infty(\mathcal{P}_\infty)$ , as shown in Fig. 4.3 on the left and on the right. Since  $\mathcal{P}_\infty$  is a Coxeter polyhedron, the violation of  $\mathbf{m}_5$  implies that the dihedral angles along the edges  $e_1$  and  $e_2$  have to equal  $\pi/2$ . But then, either condition  $\mathbf{m}_2$  or  $\mathbf{m}_4$  is violated, depending on the position of the edge  $e$ .

2. *Otherwise*, the two possible positions of the edge  $e$  are in Fig. 4.4 and Fig. 4.5. The dihedral angles along the top and bottom edges are right, since  $\mathbf{m}_5$  is violated after contraction.

2.1 *Consider* the polyhedron  $\mathcal{P}$  in Fig. 4.4 on the right. Since  $\mathcal{P}$  is not a triangular prism, we may suppose (without loss of generality) that the faces  $I, II, III, IV$  in the picture are separated by at least one more face lying in the left grey region. But then, the faces  $I, II, III$  and  $IV$  of  $\mathcal{P}$  form a 4-circuit violating condition  $\mathbf{m}_3$  of Andreev's theorem.

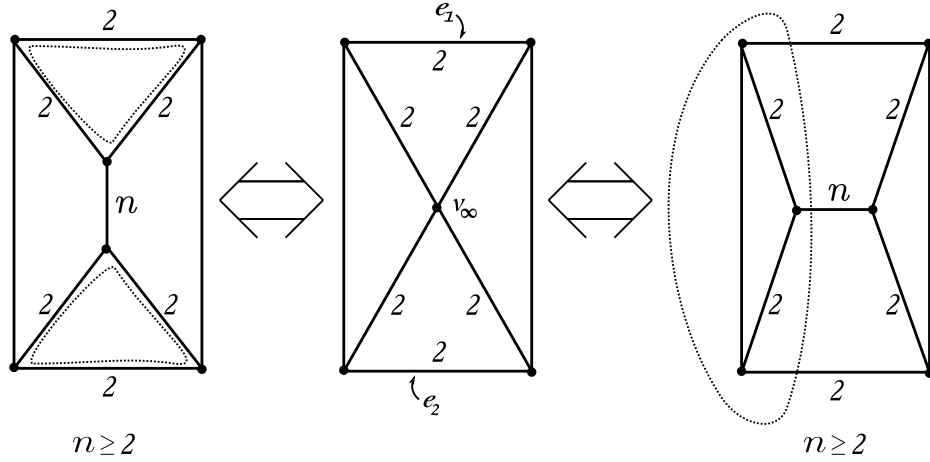


Figure 4.3: Two possible positions of the contracted edge  $e$ . The forbidden 3-circuit is dotted and forbidden prism bases are encircled by dotted lines

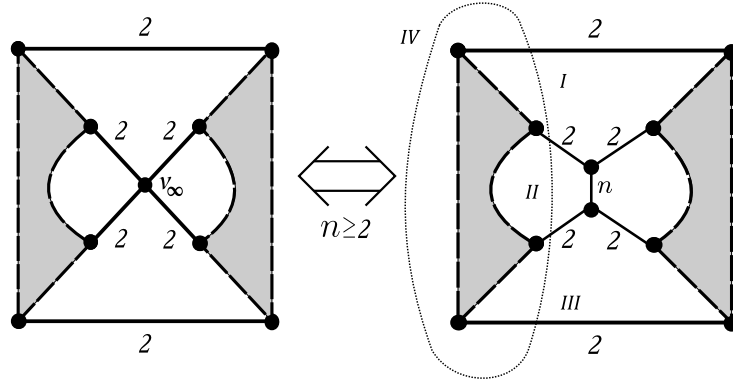


Figure 4.4: The first possible position of the contracted edge  $e$ . The forbidden 4-circuit is dotted. Face  $IV$  is at the back of the picture

2.2 Consider the polyhedron  $\mathcal{P}$  on the right in Fig. 4.5. As before, we may suppose that the faces  $I$ ,  $II$ ,  $III$  form a 3-circuit. This circuit violates condition  $\mathbf{m}_2$  of Andreev's theorem for  $\mathcal{P}$ .

Thus, the non-existence of  $\mathcal{P}_\infty$  implies the non-existence of  $\mathcal{P}$ , and one arrives at a contradiction. Q.E.D.

NOTE. Proposition 6 describes the unique way of ridge contraction. Indeed, there is only one infinite family of distinct spherical Coxeter groups representing  $Stab(v)$ , where  $v$  is a vertex of the ridge  $e$ , and this one is  $\Delta_{2,2,n}$ ,  $n \geq 2$ . One may compare the above limiting process for hyperbolic Coxeter polyhedra with the limiting process for orientable hyperbolic 3-orbifolds from [17].

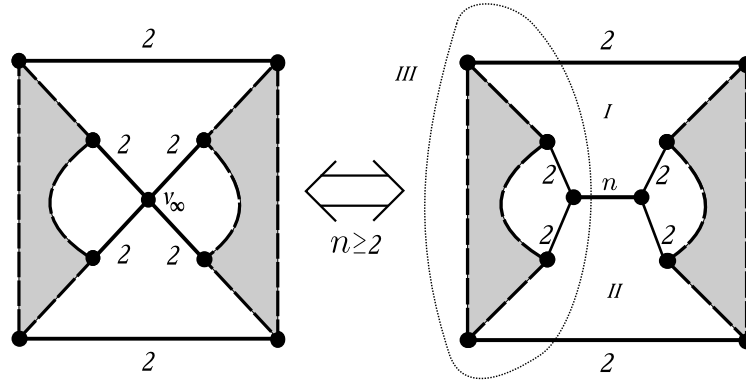


Figure 4.5: The second possible position of the contracted edge  $e$ . The forbidden 3-circuit is dotted. Face  $III$  is at the back of the picture

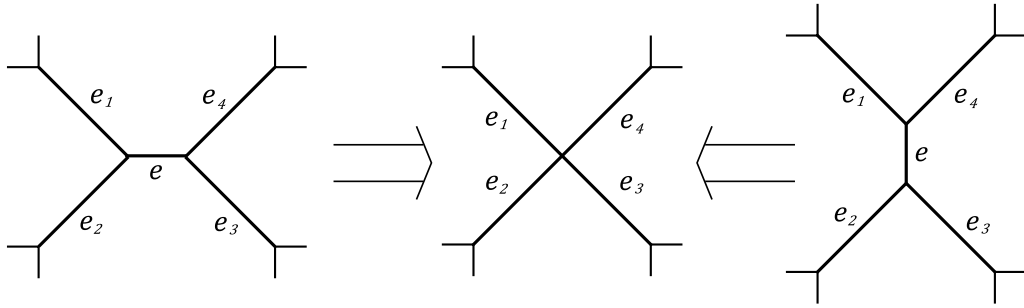


Figure 4.6: Two possible ridges resulting in a four-valent vertex under contraction

**Proposition 7** *Let  $\mathcal{P} \subset \mathbb{H}^3$  be a Coxeter polyhedron of finite volume with at least one four-valent ideal vertex  $v_\infty$ . Then there exists a sequence of finite-volume Coxeter polyhedra  $\mathcal{P}(n) \subset \mathbb{H}^3$  having the same combinatorial type and dihedral angles as  $\mathcal{P}$  except for a ridge of type  $\langle 2, 2, n, 2, 2 \rangle$ , with  $n$  sufficiently large, giving rise to the vertex  $v_\infty$  under contraction.*

PROOF. Consider the four-valent ideal vertex  $v_\infty$  of  $\mathcal{P}$  and replace  $v_\infty$  by an edge  $e$  in one of the two ways as shown in Fig. 4.6 while keeping the remaining combinatorial elements of  $\mathcal{P}$  unchanged. Let the dihedral angle along  $e$  be equal to  $\frac{\pi}{n}$ , with  $n \in \mathbb{N}$  sufficiently large. We denote this new polyhedron by  $\mathcal{P}(n)$ . The geometrical meaning of the “edge contraction” - “edge insertion” process is illustrated in Fig. 4.7. We have to verify the existence of  $\mathcal{P}(n)$  in  $\mathbb{H}^3$ .

Conditions  $\mathbf{m}_0$  and  $\mathbf{m}_1$  of Andreev’s theorem are obviously satisfied for  $\mathcal{P}(n)$ . Condition  $\mathbf{m}_5$  is also satisfied since  $n$  can be taken large enough.

Suppose that one of the remaining conditions of Andreev’s theorem is violated. The inserted edge  $e$  of  $\mathcal{P}(n)$  might appear in a new 3- or 4-circuit not present in  $\mathcal{P}$

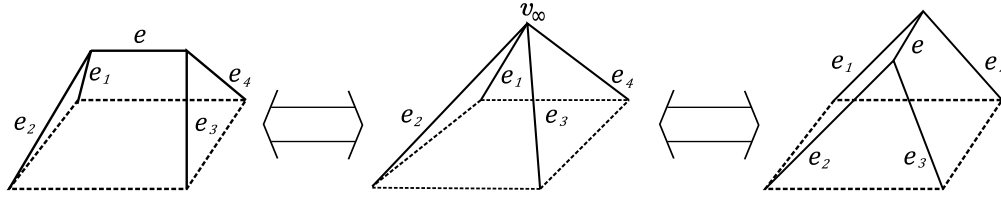


Figure 4.7: Pushing together and pulling apart the supporting planes of polyhedron’s faces results in an “edge contraction”-“edge insertion” process

so that several cases are possible.

1.  $\mathcal{P}(n)$  is a triangular prism. The polyhedron  $\mathcal{P}(n)$  violating condition  $\mathbf{m}_2$  of Andreev’s theorem is illustrated in Fig. 4.3 on the right. Since  $\mathcal{P}(n)$  is Coxeter, the 3-circuit depicted by the dashed line comprises the three edges in the middle, with dihedral angles  $\frac{\pi}{n}$ ,  $\frac{\pi}{2}$  and  $\frac{\pi}{2}$  along them. Contracting the edge  $e$  back to  $v_\infty$ , we observe that condition  $\mathbf{m}_5$  for the polyhedron  $\mathcal{P}$  does not hold.

Since there are no 4-circuits, the only condition of Andreev’s theorem for  $\mathcal{P}(n)$ , which might be yet violated, is  $\mathbf{m}_4$ . This case is depicted in Fig. 4.3 on the left. A similar argument as above leads to a contradiction.

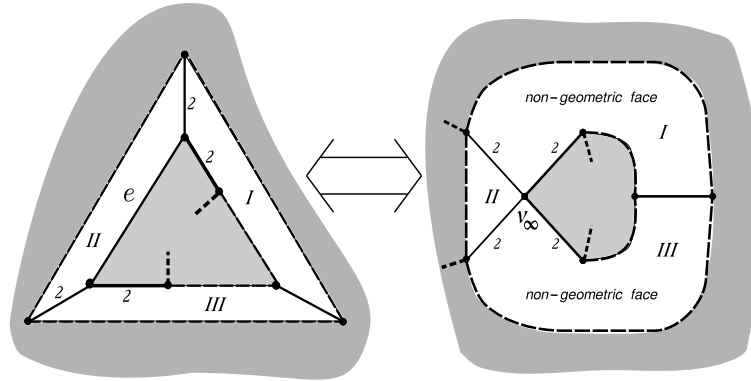


Figure 4.8: Forbidden 3-circuit: the first case

2. Otherwise, we consider the remaining unwanted cases, when either condition  $\mathbf{m}_2$  or condition  $\mathbf{m}_3$  is violated.

2.1 *Case of a 3-circuit.* In Fig. 4.8 and Fig. 4.9, we illustrate two ways to obtain a 3-circuit in  $\mathcal{P}(n)$  for all  $n$  sufficiently large, which violates condition  $\mathbf{m}_2$  of Andreev’s theorem. The faces of the 3-circuit are indicated by  $I$ ,  $II$  and  $III$ . In Fig. 4.8, the edge  $e$  is “parallel” to the circuit, meaning that  $e$  belongs to precisely one of the faces  $I$ ,  $II$  or  $III$ . In Fig. 4.9, the edge  $e$  is “transversal” to the circuit, meaning that  $e$  is the intersection of precisely two of the faces  $I$ ,  $II$  or  $III$ . Contracting  $e$  back to  $v_\infty$



leads to an obstruction for the given polyhedron  $\mathcal{P}$  to exist, as illustrated in Fig. 4.8 and Fig. 4.9 on the right. The polyhedron  $\mathcal{P}$  in Fig. 4.8 has two non-geometric faces, namely  $I$  and  $III$ , having in common precisely one edge and the vertex  $v_\infty$  disjoint from it. The polyhedron  $\mathcal{P}$  in Fig. 4.9 violates condition  $\mathbf{m}_5$  of Andreev's theorem because of the triple, that consists of the faces  $I$ ,  $II$  and  $III$  (in Fig. 4.9 on the right, the face  $III$  is at the back of the picture).

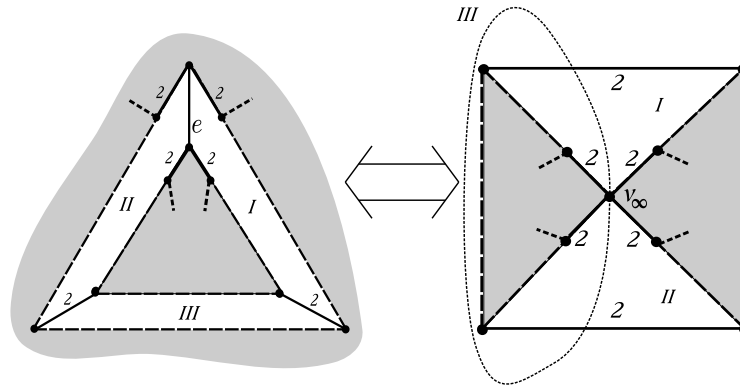


Figure 4.9: Forbidden 3-circuit: the second case. The forbidden circuit going through the ideal vertex is dotted. Face  $III$  is at the back of the picture

2.2 *Case of a 4-circuit.* First, observe that the sum of dihedral angles along the edges involved in a 4-circuit transversal to the edge  $e$  does not exceed  $\frac{3\pi}{2} + \frac{\pi}{n}$ , and therefore is less than  $2\pi$  for all  $n > 2$ . This means condition  $\mathbf{m}_3$  of Andreev's theorem is always satisfied for  $n$  sufficiently large.

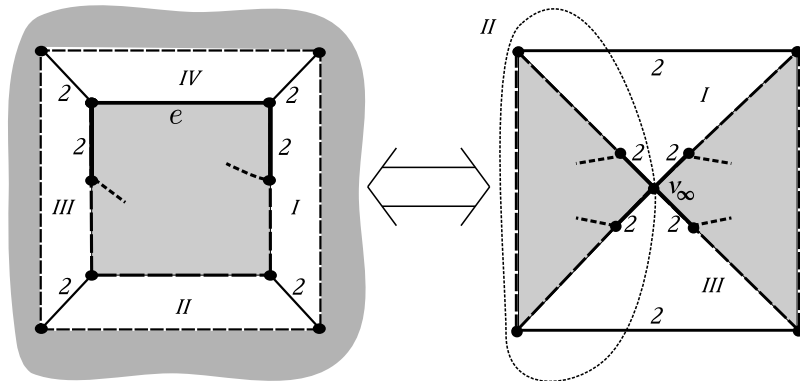


Figure 4.10: Forbidden 4-circuit. The forbidden circuit going through the ideal vertex is dotted. Face  $II$  is at the back of the picture

Finally, a 4-circuit parallel to the edge  $e$  in  $\mathcal{P}(n)$  is illustrated in Fig. 4.10. The faces in this 4-circuit are indicated by  $I$ ,  $II$ ,  $III$ ,  $IV$ . Suppose that the 4-circuit

violates condition  $\mathfrak{m}_3$ . Contracting  $e$  back to  $v_\infty$  (see Fig. 4.10 on the right) leads to a violation of  $\mathfrak{m}_5$  for  $\mathcal{P}$  because of the circuit, that consists of the faces  $I$ ,  $II$  and  $III$  (in Fig. 4.10 on the right, the face  $II$  is at the back of the picture). Q.E.D.

NOTE. The statements of Proposition 6 and Proposition 7 are essentially given in [59, p. 238] without proof. In the higher-dimensional case, no codimension two face contraction is possible. Indeed, the contraction process produces a finite-volume polytope  $\mathcal{P}_\infty \subset \mathbb{H}^n$ ,  $n \geq 4$ , whose volume is a limit point for the set of volumes of  $\mathcal{P}(k) \subset \mathbb{H}^n$  as  $k \rightarrow \infty$ . But, by the theorem of H.-C. Wang [59, Theorem 3.1], the set of volumes of Coxeter polytopes in  $\mathbb{H}^n$  is discrete if  $n \geq 4$ .

### 4.1.3 Limiting growth rates of Coxeter groups acting on $\mathbb{H}^3$

The result of this section is inspired by W. Floyd's work [22] on planar hyperbolic Coxeter groups. We consider a sequence of compact polyhedra  $\mathcal{P}(n) \subset \mathbb{H}^3$  with a ridge of type  $\langle 2, 2, n, 2, 2 \rangle$  converging, as  $n \rightarrow \infty$ , to a polyhedron  $\mathcal{P}_\infty$  with a single four-valent ideal vertex. According to [42], all the growth rates of the corresponding reflection groups  $G(\mathcal{P}(n))$  are Salem numbers. Our aim is to show that the limiting growth rate is a Pisot number.

The following definition will help us to make the technical proofs more transparent when studying the analytic behaviour of growth functions. For a given Coxeter group  $G$  with generating set  $S$  and growth function  $f(t) := f_{(G,S)}(t)$ , we set  $F(t) = F_{(G,S)}(t) := \frac{1}{f(t-1)}$ .

**Proposition 8** *Let  $\mathcal{P}_\infty \subset \mathbb{H}^3$  be a finite-volume Coxeter polyhedron with at least one four-valent ideal vertex obtained from a sequence of finite-volume Coxeter polyhedra  $\mathcal{P}(n)$  by contraction of a ridge of type  $\langle 2, 2, n, 2, 2 \rangle$  as  $n \rightarrow \infty$ . Denote by  $f_n(t)$  and  $f_\infty(t)$  the growth functions of  $G(\mathcal{P}(n))$  and  $G(\mathcal{P}_\infty)$ , respectively. Then*

$$\frac{1}{f_n(t)} - \frac{1}{f_\infty(t)} = \frac{t^n}{1-t^n} \left( \frac{1-t}{1+t} \right)^2.$$

Moreover, the growth rate  $\tau_n$  of  $G(\mathcal{P}(n))$  converges to the growth rate  $\tau_\infty$  of  $G(\mathcal{P}_\infty)$  from below.

PROOF. We calculate the difference of  $F_n(t)$  and  $F_\infty(t)$  by means of equation (2.9). In fact, this difference is caused only by the stabilisers of the ridge  $e \in \Omega_1(\mathcal{P}(n))$  and of its vertices  $v_i \in \Omega_0(\mathcal{P}(n))$ ,  $i = 1, 2$ . Let  $[k] := 1 + \dots + t^{k-1}$ . Here  $Stab(e) \simeq D_n$ , the dihedral group of order  $2n$ , and  $Stab(v_i) \simeq \Delta_{2,2,n}$ . The corresponding growth

functions are given by  $f_e(t) = [2][n]$  and  $f_{v_i}(t) = [2]^2[n]$ ,  $i = 1, 2$  (see Tables 3.3 and 3.4). Thus

$$F_n(t) - F_\infty(t) = \frac{1}{f_e(t)} - \frac{1}{f_{v_1}(t)} - \frac{1}{f_{v_2}(t)} = \frac{1}{t^n - 1} \left( \frac{t-1}{t+1} \right)^2. \quad (4.3)$$

Next, perform the substitution  $t \rightarrow t^{-1}$  on (4.3) and use the relation between  $F_n(t)$ ,  $F_\infty(t)$  and their counterparts  $f_n(t)$  and  $f_\infty(t)$  according to the definition above. As a result, we obtain the desired formula, which yields  $\frac{1}{f_n(t)} - \frac{1}{f_\infty(t)} > 0$  for  $t \in (0, 1)$ .

Consider the growth rates  $\tau_n$  and  $\tau_\infty$  of  $G(\mathcal{P}(n))$  and  $G(\mathcal{P}_\infty)$ . The least positive pole of  $f_n(t)$  is the least positive zero of  $\frac{1}{f_n(t)}$ , and  $f_n(0) = 1$ . Similar statements hold for  $f_\infty(t)$ . Hence, by the inequality above and by the definition of growth rate, we obtain  $\tau_n^{-1} > \tau_\infty^{-1}$ , or  $\tau_n < \tau_\infty$ , as claimed.

Finally, the convergence  $\tau_n \rightarrow \tau_\infty$  as  $n \rightarrow \infty$  follows from the convergence  $\frac{1}{f_n(t)} - \frac{1}{f_\infty(t)} \rightarrow 0$  on  $(0, 1)$ , due to the first part of the proof. Q.E.D.

NOTE. Given the assumptions of Proposition 8, the volume of  $\mathcal{P}(n)$  is less than that of  $\mathcal{P}_\infty$  by Schläfli's volume differential formula [40]. Thus, growth rate and volume are both increasing under contraction of a ridge.

Consider two Coxeter polyhedra  $\mathcal{P}_1$  and  $\mathcal{P}_2$  in  $\mathbb{H}^3$  having the same combinatorial type and dihedral angles except for the respective ridges  $H_1 = \langle k_1, k_2, n_1, l_1, l_2 \rangle$  and  $H_2 = \langle k_1, k_2, n_2, l_1, l_2 \rangle$ . We say that  $H_1 \prec H_2$  if and only if  $n_1 < n_2$ .

The following proposition extends Proposition 8 to a more general context.

**Proposition 9** *Let  $\mathcal{P}_1$  and  $\mathcal{P}_2$  be two compact hyperbolic Coxeter polyhedra having the same combinatorial type and dihedral angles except for an edge of ridge type  $H_1$  and  $H_2$ , respectively. If  $H_1 \prec H_2$ , then the growth rate of  $G(\mathcal{P}_1)$  is less than the growth rate of  $G(\mathcal{P}_2)$ .*

PROOF. Denote by  $f_1(t)$  and  $f_2(t)$  the growth functions of  $G(\mathcal{P}_1)$  and  $G(\mathcal{P}_2)$ , respectively. As before, we will show that  $\frac{1}{f_1(t)} - \frac{1}{f_2(t)} \geq 0$  on  $(0, 1)$ . Without loss of generality, we may suppose the ridges  $H_i$  to be of type  $\langle k_1, k_2, n_i, l_1, l_2 \rangle$ ,  $i = 1, 2$ , up to a permutation of the sets  $\{k_1, k_2\}$ ,  $\{l_1, l_2\}$  and  $\{\{k_1, k_2\}, \{l_1, l_2\}\}$ . By means of Table 3.3 showing all the finite triangle reflection groups, all admissible ridge pairs can be determined. We collected them in Tables 1–2 in Appendix 4.4. The rest of the proof, starting with the computation of  $\frac{1}{f_1(t)} - \frac{1}{f_2(t)}$  in accordance with Theorem 20, equations (3.6) and (3.7), follows by analogy to Proposition 8. Q.E.D.

From now on  $\mathcal{P}(n)$  always denotes a sequence of compact polyhedra in  $\mathbb{H}^3$  having a ridge of type  $\langle 2, 2, n, 2, 2 \rangle$ , with  $n$  sufficiently large, that converges to a polyhedron

$\mathcal{P}_\infty$  with a single four-valent ideal vertex. The corresponding growth functions for the groups  $G(\mathcal{P}_n)$  and  $G(\mathcal{P}_\infty)$  are denoted by  $f_n(t)$  and  $f_\infty(t)$ . As above, we will work with the functions  $F_n(t)$  and  $F_\infty(t)$ . By Theorem 21, both  $f_n(t)$  and  $F_n(t)$  are anti-reciprocal rational functions.

The next result describes *the virgin form* (see Section 3.3.3, equations (3.9)-(3.10)) of the denominator of  $F_\infty(t)$ .

**Proposition 10** *Let  $\mathcal{P}_\infty \subset \mathbb{H}^3$  be a polyhedron of finite volume with a single four-valent ideal vertex. Then the function  $F_\infty(t)$  related to the Coxeter group  $G(\mathcal{P}_\infty)$  is given by*

$$F_\infty(t) = \frac{t(t-1)P_\infty(t)}{Q_\infty(t)},$$

where  $Q_\infty(t)$  is a product of cyclotomic polynomials,  $\deg Q_\infty(t) - \deg P_\infty(t) = 2$ , and  $P_\infty(0) \neq 0$ ,  $P_\infty(1) < 0$ .

PROOF. The denominator of  $F_\infty(t)$  in its virgin form is a product of cyclotomic polynomials  $\Phi_k(t)$  with  $k \geq 2$ . By means of the equality  $F_\infty(1) = \chi(G(\mathcal{P}_\infty)) = 0$  (Theorem 22), the numerator of  $F_\infty(t)$  is divisible by  $t-1$ . Moreover, by [10, Corollary 5.4.5], the growth function  $f_\infty(t)$  for  $G(\mathcal{P}_\infty)$  has a simple pole at infinity. This means  $F_\infty(t)$  has a simple zero at  $t = 0$ , so that the numerator of  $F_\infty(t)$  has the form  $t(t-1)P_\infty(t)$ , where  $P_\infty(t)$  is a polynomial such that  $P_\infty(0) \neq 0$ . The desired equality  $\deg Q_\infty(t) - \deg P_\infty(t) = 2$  follows from  $f_\infty(0) = 1$ .

The main part of the proof is to show that  $P_\infty(1) < 0$ . By the above,  $\frac{dF_\infty}{dt}(1) = \frac{P_\infty(1)}{Q_\infty(1)}$  whose denominator is a product of cyclotomic polynomials  $\Phi_k(t)$  with  $k \geq 2$  evaluated at  $t = 1$ . Hence  $Q_\infty(1) > 0$ , and it suffices to prove that  $\frac{dF_\infty}{dt}(1) < 0$ .

Consider a sequence of combinatorially isomorphic compact polyhedra  $\mathcal{P}(n)$  in  $\mathbb{H}^3$  having a ridge of type  $\langle 2, 2, n, 2, 2 \rangle$  and converging to  $\mathcal{P}_\infty$ . By Proposition 8,

$$\frac{dF_n}{dt}(1) - \frac{dF_\infty}{dt}(1) = \frac{1}{4n}.$$

In order to show  $\frac{dF_\infty}{dt}(1) < 0$ , it is enough to prove that  $\frac{dF_n}{dt}(1) < 0$  for  $n$  large enough. To this end, we consider the following identity which is a consequence of Theorem 20, equations (3.6)-(3.7):

$$\frac{dF_n}{dt}(1) = \frac{1}{2} + \sum_{v \in \Omega_0(\mathcal{P}(n))} \frac{dg_v}{dt}(1).$$

In Table 3, we list all possible values  $\frac{dg_v}{dt}(1)$  depending on the subgroup  $Stab(v)$  of  $G(\mathcal{P}(n))$ . It follows that  $\frac{dg_v}{dt}(1) \leq -\frac{1}{16}$  for every  $v \in \Omega_0(\mathcal{P}(n))$ . Provided  $|\Omega_0(\mathcal{P}(n))| \geq 10$ , we obtain the estimate  $\frac{dF_n}{dt}(1) \leq -\frac{1}{8}$ .

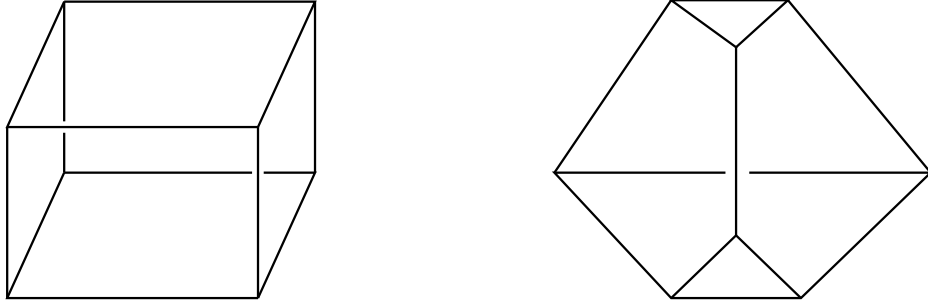


Figure 4.11: Simple polyhedra with eight vertices

Consider the remaining cases  $5 \leq |\Omega_0(\mathcal{P}(n))| < 10$ . By the simplicity of the polyhedron  $\mathcal{P}(n)$ , we have that  $2|\Omega_1(\mathcal{P}(n))| = 3|\Omega_0(\mathcal{P}(n))|$ . Therefore  $|\Omega_0(\mathcal{P}(n))|$  is an even number. Hence, the only cases consist of  $|\Omega_0(\mathcal{P}(n))| = 8$ , meaning that  $\mathcal{P}(n)$  is either a combinatorial cube or a doubly truncated tetrahedron (see Fig. 4.11), and  $|\Omega_0(\mathcal{P}(n))| = 6$ , meaning that  $\mathcal{P}(n)$  is a combinatorial triangular prism. In the former case, not all the vertices of  $\mathcal{P}(n)$  have their stabilizers isomorphic to  $\Delta_{2,2,2}$ , since  $\mathcal{P}(n)$  is a non-Euclidean cube or a non-Euclidean tetrahedron with two ultra-ideal vertices. Then Table 3 (see Appendix 4.4) provides the desired inequality  $\frac{dF_n}{dt}(1) < 0$ . The latter case requires a more detailed consideration. We use the list of hyperbolic Coxeter triangular prisms given by [32, 58]. These prisms have one base orthogonal to all adjacent faces. More general Coxeter prisms arise by gluing the given ones along their orthogonal bases, if the respective planar angles coincide.

Among all triangular Coxeter prisms, we depict in Fig. 34-36 (see Appendix 4.4) only ones having a ridge of type  $\langle 2, 2, n, 2, 2 \rangle$ . A routine computation of their growth functions allows to conclude  $\frac{dF_n}{dt}(1) < 0$ . Q.E.D.

**Proposition 11** *Let  $\mathcal{P}(n) \subset \mathbb{H}^3$  be a compact Coxeter polyhedron with a ridge of type  $\langle 2, 2, n, 2, 2 \rangle$  for  $n$  sufficiently large. Then the function  $F_n(t)$  related to the group  $G(\mathcal{P}(n))$  is given by*

$$F_n(t) = \frac{(t-1)P(t)}{(t^n-1)Q_\infty(t)},$$

where  $Q_\infty(t)$  is the denominator polynomial associated with the deformed polyhedron  $\mathcal{P}_\infty$  with a unique four-valent ideal vertex from Proposition 10, and  $P(t)$  is a product of cyclotomic polynomials and a Salem polynomial. In addition,  $P(1) = 0$ .

PROOF. Denote by  $Fin_n := \{f_\omega(t) \mid \omega \in \Omega_*(\mathcal{P}(n)) \text{ such that } G(\omega) \text{ is finite}\}$ , and by  $Fin_\infty := \{f_\omega(t) \mid \omega \in \Omega_*(\mathcal{P}_\infty) \text{ such that } G(\omega) \text{ is finite}\}$  where  $*$   $\in \{0, 1, 2\}$ . Let  $F_n(t) = \frac{P(t)}{Q(t)}$  be given in its virgin form, that means  $Q(t)$  is the least common multiple

of all polynomials in  $Fin_n$ . For the corresponding function  $F_\infty(t)$ , Theorem 13 implies that  $Q_\infty(t)$  is the least common multiple of all polynomials in  $Fin_\infty$ .

Denote by  $e$  the edge of  $\mathcal{P}(n)$  undergoing contraction, and let  $v_1, v_2$  be its vertices. Then the growth function of  $Stab(e) \cong D_n$  is  $f_e(t) = [2][n]$ , and the growth function of  $Stab(v_i) \cong \Delta_{2,2,n}$  is  $f_{v_i}(t) = [2]^2[n]$ ,  $i = 1, 2$ . The sets  $Fin_n$  and  $Fin_\infty$  differ only by the elements  $f_e(t), f_{v_1}(t), f_{v_2}(t)$ . Furthermore, both sets contain the polynomial  $[2]^2$ , since the polyhedra  $\mathcal{P}(n)$  and  $\mathcal{P}_\infty$  have pairs of edges with right angles along them and stabilizer  $D_2$ . The comparison of the least common multiples for polynomials in  $Fin_n$  and in  $Fin_\infty$  shows that  $Q(t) = Q_\infty(t) \cdot [n]$ , as claimed.

The assertion  $P(1) = 0$  follows from the fact that  $F_n(1) = 0$  while  $\lim_{t \rightarrow 1} \frac{t^n - 1}{t - 1} = n$ . Finally, the polynomial  $P(t)$  is a product of cyclotomic polynomials and a Salem polynomial by [42]. Q.E.D.

**Theorem 23** *Let  $\mathcal{P}(n) \subset \mathbb{H}^3$  be a compact Coxeter polyhedron with a ridge  $e$  of type  $\langle 2, 2, n, 2, 2 \rangle$  for sufficiently large  $n$ . Denote by  $\mathcal{P}_\infty$  the polyhedron arising by contraction of the ridge  $e$ . Let  $\tau_n$  and  $\tau_\infty$  be the growth rates of  $G(\mathcal{P}(n))$  and  $G(\mathcal{P}_\infty)$ , respectively. Then  $\tau_n < \tau_\infty$  for all  $n$ , and  $\tau_n \rightarrow \tau_\infty$  as  $n \rightarrow \infty$ . Furthermore,  $\tau_\infty$  is a Pisot number.*

PROOF. The first assertion follows easily from Proposition 8. We prove that  $\tau_\infty$  is a Pisot number by using some number-theoretical properties of growth rates. Consider the growth functions  $f_n(t)$  and  $f_\infty(t)$  of  $G(\mathcal{P}(n))$  and  $G(\mathcal{P}_\infty)$ , respectively, together with associated functions  $F_n(t) = \frac{1}{f_n(t-1)}$  and  $F_\infty(t) = \frac{1}{f_\infty(t-1)}$ . Then the growth rates  $\tau_n$  and  $\tau_\infty$  are the least positive zeros in the interval  $(1, +\infty)$  of the functions  $F_n(t)$  and  $F_\infty(t)$ .

By using Propositions 8, 10 and 11 in order to represent the numerator and denominator polynomials of  $F_n(t)$  and  $F_\infty(t)$ , one easily derives the equation

$$\frac{(t-1)P(t)}{(t^n-1)Q_\infty(t)} - \frac{t(t-1)P_\infty(t)}{Q_\infty(t)} = \frac{1}{t^n-1} \left( \frac{t-1}{t+1} \right)^2. \quad (4.4)$$

For the polynomial  $P(t)$ , we prove that

$$P(t) = t^{n+1}P_\infty(t) - \tilde{P}_\infty(t) \quad (4.5)$$

is a solution to (4.4), where  $\tilde{P}_\infty(t)$  denotes the reciprocal polynomial of  $P_\infty(t)$ , that is,  $\tilde{P}_\infty(t) = t^{\deg P_\infty(t)} P_\infty(t^{-1})$ . Since  $Q_\infty(t)$  is a product of cyclotomic polynomials  $\Phi_k(t)$  with  $k \geq 2$ , one has  $Q_\infty(t) = \tilde{Q}_\infty(t) = t^{\deg Q_\infty(t)} Q_\infty(t^{-1})$ .

Now, replace  $P(t)$  in (4.4) by its expression from (4.5) and simplify each term. This yields

$$\frac{t(t-1)P_\infty(t)}{Q_\infty(t)} - \frac{(t-1)\tilde{P}_\infty(t)}{Q_\infty(t)} = \left(\frac{t-1}{t+1}\right)^2.$$

By replacing the reciprocal polynomials and by using the fact of Proposition 10, saying that  $\deg Q_\infty(t) - \deg P_\infty(t) = 2$ , we obtain

$$\frac{t(t-1)P_\infty(t)}{Q_\infty(t)} + \frac{t^{-1}(t^{-1}-1)P_\infty(t^{-1})}{Q_\infty(t^{-1})} = \left(\frac{t-1}{t+1}\right)^2. \quad (4.6)$$

The identity for  $F_\infty(t)$  as described by Proposition 10 transforms the equation (4.6) into  $F_\infty(t) + F_\infty(t^{-1}) = \left(\frac{t-1}{t+1}\right)^2$ . Then Proposition 8 provides the equivalent identity  $F_n(t) + F_n(t^{-1}) = 0$ , which is true by the anti-reciprocity of  $F_n(t)$  (see Theorem 21).

As a consequence, the relation  $P(t) = t^{n+1}P_\infty(t) - \tilde{P}_\infty(t)$  holds for  $n$  large enough. Since we already know that  $P(t)$  is a product of cyclotomic polynomials and a Salem polynomial, Lemma 1 implies that  $P_\infty(t)$  is a product of cyclotomic polynomials and a Pisot polynomial. Hence, the growth rate  $\tau_\infty$  is a Pisot number. Q.E.D.

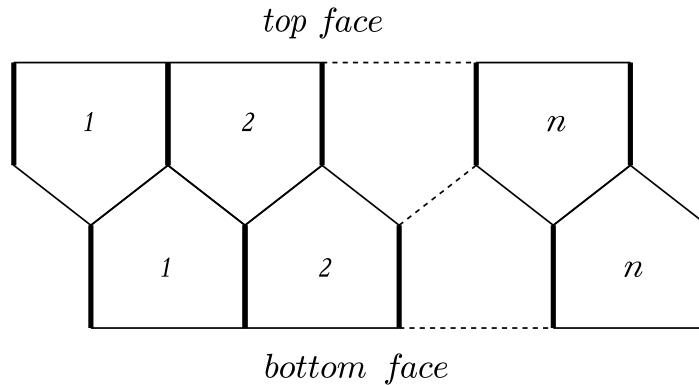


Figure 4.12: Löbell polyhedron  $\mathcal{L}_n$ ,  $n \geq 5$  with one of its perfect matchings marked with thickened edges. Left- and right-hand side edges are identified. All the dihedral angles are right

## 4.1.4 Examples

### 4.1.4.1 Deforming Löbell polyhedra

The family of Löbell polyhedra  $\mathcal{L}_n$ ,  $n \geq 5$  is described in Section 1.2.7.1. Contracting an edge of  $\mathcal{L}_5$ , a combinatorial dodecahedron, one obtains the smallest 3-dimensional right-angled polyhedron with a single ideal four-valent vertex. Contracting all the vertical edges of  $\mathcal{L}_n$  as shown in Fig. 4.12 one obtains an ideal right-angled anti-prism

$\mathcal{A}_n$ ,  $n \geq 5$ . Note, that contracted edges form a perfect matching of  $\mathcal{L}_n$  considered as a three-valent graph. The analogous ideal right-angled polyhedra  $\mathcal{A}_4$  and  $\mathcal{A}_3$  also exist. Observe that  $\mathcal{A}_3$  is a combinatorial octahedron. The growth rate of  $\mathcal{A}_n$ ,  $n \geq 3$ , belongs to the  $(2n)$ -th derived set of Salem numbers by Propositions 7 and 8.

#### 4.1.4.2 Deforming a Lambert cube

Contracting essential edges of a Lambert cube, one obtains a right-angled polyhedron  $\mathcal{R}$ . This polyhedron could also be obtained from the Lanner tetrahedron  $(3, 4, 4)$  by means of construction described in [43]. The polyhedron  $\mathcal{R}$  is known to have the minimal number of faces among all the right-angled three-dimensional hyperbolic polyhedra of finite volume [19].

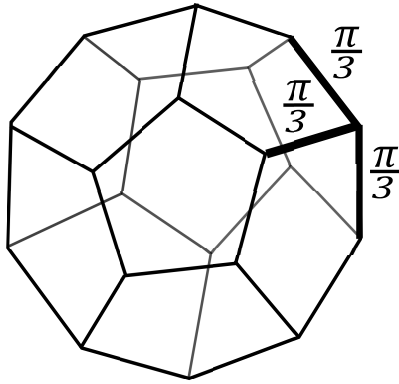


Figure 4.13: The dodecahedron  $\mathcal{D}$  with one ideal three-valent vertex. All the unspecified dihedral angles are right

#### 4.1.4.3 Finite volume Coxeter polyhedra with an ideal three-valent vertex

Consider the dodecahedron  $\mathcal{D}$  in Fig. 4.13. It has all but three right dihedral angles. The remaining ones, along the edges incident to a single ideal three-valent vertex, equal  $\frac{\pi}{3}$ . The growth function of the corresponding Coxeter group is given by

$$f(t) = \frac{(1+t)^3(1+t+t^2)}{9t^4 - 2t^2 - 8t + 1} =: \frac{Q(t)}{(t-1)P(t)},$$

where the polynomial  $P(t)$  has integer coefficients. Its reciprocal  $\tilde{P}(t)$  is the minimal polynomial of the corresponding growth rate  $\tau$ . More precisely,  $\tilde{P}(t) = 9 + 9t + 7t^2 - t^3$  with roots  $\tau \approx 8.2269405$  and  $\varsigma_1 = \overline{\varsigma_2} \approx -0.6134703 + 0.8471252i$ . Since  $\varsigma_1\varsigma_2 \approx 1.0939668 > 1$ , the growth rate  $\tau$  of the group  $G(\mathcal{D})$  is neither a Salem number, nor a Pisot number.



## 4.2 A note about Wang's theorem

Let  $\Gamma$  be a discrete group acting on  $\mathbb{H}^n$  by isometries. Then the quotient space  $\mathcal{O} := \mathbb{H}^n / \Gamma$  is a hyperbolic  $n$ -dimensional orbifold. The covolume of the group  $\Gamma$  is the volume of  $\mathcal{O}$  or, equivalently, the volume of a fundamental domain for the action of  $\Gamma$ .

Let us recall the following theorem by H.-C. Wang about the covolumes of discrete groups acting on  $\mathbb{H}^n$ .

**Theorem 24 (Theorem 3.1, [59])** *The set  $\text{Vol}_n$  of volumes of all hyperbolic  $n$ -dimensional orbifolds is discrete if  $n \geq 4$ .*

Let  $\mathcal{P}(k)$ ,  $k = 0, 1, 2, \dots$ , be an infinite sequence of finite-volume Coxeter polytopes in  $\mathbb{H}^n$ . Consider each  $\mathcal{P}(k)$  as a polytope in the Beltrami-Klein model  $\mathbb{B}^n$  of the hyperbolic space and denote this particular realisation by  $\widetilde{\mathcal{P}}(k)$ . Note that one can consider  $\widetilde{\mathcal{P}}(k)$  as a Euclidean polytope embedded in a unit ball  $\mathbb{B}^n$ . We say that the sequence  $\mathcal{P}(k)$  converges to a polytope  $\mathcal{P}_\infty \subset \mathbb{H}^n$  as  $k \rightarrow \infty$  if and only if the sequence  $\widetilde{\mathcal{P}}(k)$  converges to  $\widetilde{\mathcal{P}}_\infty$  as a sequence of convex bodies in  $\mathbb{E}^n$ , see [2, p. 256].

Consider Wang's theorem as stated in Theorem 24. Let  $\mathcal{P}(k)$ ,  $k = 1, 2, \dots$  be a sequence of Coxeter polytopes undergoing a co-dimension two face contraction, and thus tending to a certain finite-volume polytope  $\mathcal{P}_\infty$ . Let  $\Gamma_k := G(\mathcal{P}(k))$  be the reflection groups associated with the polytopes  $\mathcal{P}(k)$ . By the Schläfli formula, all  $\mathcal{P}(k)$  have different volumes [40] and  $\text{Vol } \mathcal{P}(k)$  increases with  $k \nearrow \infty$ . This gives rise to the sequence  $\mathcal{O}_k := \mathbb{H}^n / \Gamma_k$  of hyperbolic orbifolds such that the set  $\mathcal{V} := \{\text{Vol } \mathcal{O}_k | k = 1, 2, \dots\}$  has a limiting point, which is  $\text{Vol } \mathcal{P}_\infty$ . Clearly,  $\mathcal{V} \subset \text{Vol}_n$ . This contradicts Wang's theorem (Theorem 24). Thus, no face contraction is possible in dimension  $n \geq 4$ .

In the following, we shall prove an analogue to Wang's theorem (Theorem 24) in the particular case of *Coxeter orbifolds*, that means quotients of  $\mathbb{H}^n$  by a discrete reflection subgroup.

**Theorem 25** *There exists no infinite sequence  $\mathcal{P}(k) \subset \mathbb{H}^n$ ,  $k = 0, 1, 2, \dots$ , of pairwise non-isometric Coxeter polytopes of finite volume having the same combinatorial type, which tends to a non-degenerate non-compact finite-volume Coxeter polytope  $\mathcal{P}_\infty \subset \mathbb{H}^n$ , if  $n \geq 4$ .*

PROOF. First, we describe the four-dimensional picture. Let  $\mathcal{P}(k) \subset \mathbb{H}^4$  be an infinite sequence of Coxeter polytopes converging to a non-degenerate polytope  $\mathcal{P}_\infty$

as  $k \rightarrow \infty$ . Since the sequence  $\mathcal{P}(k)$  consists of non-isometric polytopes, there exist several faces  $F_1, \dots, F_m \in \Omega_2(\mathcal{P}(k))$ , such that the corresponding dihedral angles  $\alpha(F_1) = \pi/n_1, \dots, \alpha(F_m) = \pi/n_m$  tend to zero. This means that each face  $F_i$ ,  $i = 1, \dots, m$ , will be contracted to a point  $v_i \in \partial\overline{\mathbb{H}^4}$ . Indeed, for each  $F_i$  there exist two facets  $P_i, P'_i \in \Omega_3(\mathcal{P}(k))$  intersecting at  $F_i$  with dihedral angle  $\alpha(F_i)$ . While  $\alpha(F_i) \searrow 0$  the supporting hyperplanes of  $P_i$  and  $P'_i$  become tangent at a point  $v_i \in \partial\overline{\mathbb{H}^4}$ , since  $\mathcal{P}_\infty$  is of finite volume.

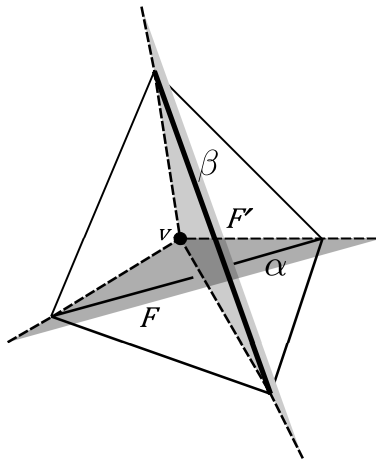


Figure 4.14: Vertex figure for a vertex of a compact face subject to contraction

Consider  $F$  – one of the faces above – say  $F := F_1$ . We claim that  $F$  is compact and each vertex  $v \in \Omega_0(F)$  has a tetrahedral vertex figure  $L$ , as shown in Fig. 4.14. Suppose on the contrary, that there exists an ideal vertex  $v_\infty \in \Omega_0(\mathcal{P}(k))$  of  $F$ . Consider the vertex figure  $L$  of  $v_\infty$ . Then  $L \subset \mathbb{E}^3$  is a Euclidean Coxeter polyhedron with one of its dihedral angles decreasing down to zero. But this is impossible due to the finiteness of the number of such polyhedra, see [29, Chapter 2.5]. Hence  $L$  is a spherical Coxeter tetrahedron, and one of its dihedral angles satisfies  $\alpha(F) \searrow 0$ . This implies  $G(L) \cong D_p \times D_q$ , for certain  $p, q \geq 2$ , by [29, Chapter 2.4]. We denote by  $\alpha := \alpha(F) = \pi/p$  the dihedral angle corresponding to the face  $F$ . Let  $F' \in \Omega_2(\mathcal{P}(k))$  be the face, such that  $v = F \cap F' \in \Omega_0(F)$ . Denote by  $\beta := \alpha(F') = \pi/q$  the corresponding dihedral angle of  $L$  at  $F'$ . The remaining dihedral angles of  $L$  are right. The edge lengths of  $L$  are  $\ell_\alpha = \beta$ ,  $\ell_\beta = \alpha$  and  $\pi/2$  for the remaining edges by means of spherical geometry formulas [59, Chapter 4.2]. We have  $\alpha \rightarrow 0$  and  $\ell_\alpha \rightarrow 0$ , since  $F$  is contracted to a point. Thus  $\beta \rightarrow 0$  and  $\ell_\beta \rightarrow 0$ , that means the face  $F'$  has to be contracted together with  $F$ . Moreover, if a face  $F' \in \Omega_2(\mathcal{P}(k))$  shares not only a vertex with  $F$ , but an edge  $e \in \Omega_1(\mathcal{P}(k))$ , then  $F'$  can not be contracted.

Supposing the contrary, we consider the vertex figure  $L$  of a vertex on  $e$ . Then  $L$  is a spherical Coxeter tetrahedron with more than two arbitrarily small dihedral angles. We arrive at a contradiction with the classification of spherical Coxeter polytopes, see [29, Chapter 2.4].

Let  $\mathcal{F}^*$  be the set of all two-dimensional faces that undergo contraction, together with their lower-dimensional subfaces, that is, adjacent edges and vertices. As described above, every two faces in  $\mathcal{F}^*$  share at most one vertex. Let  $\mathcal{G}$  be a graph having a vertex for each face in  $\mathcal{F}^*$  and an edge connecting two vertices if the corresponding faces intersect each other. Each vertex of  $\mathcal{G}$  has valency greater than or equal to three, since every two-dimensional face of  $\mathcal{P}(k)$  is at least triangular and each vertex  $v$  shared by two faces in  $\mathcal{F}^*$  has its vertex figure  $L$  as in Fig. 4.14. Hence,  $\mathcal{G}$  can not be a tree, since  $\mathcal{G}$  is finite. Let  $\mathcal{T}$  be a maximal sub-tree of  $\mathcal{G}$ . Then  $\mathcal{G} \setminus \mathcal{T} \neq \emptyset$ . Consider the fundamental group  $\pi_1(\mathcal{G})$ . By [38, Theorem 6.2], this is a free group, its rank is the number of edges in  $\mathcal{G} \setminus \mathcal{T}$ , and, moreover,

$$\chi(\mathcal{G}) = 1 - \text{rank } \pi_1(\mathcal{G}) \leq 0, \quad (4.7)$$

since  $\mathcal{G} \setminus \mathcal{T} \neq \emptyset$  implies  $\text{rank } \pi_1(\mathcal{G}) \geq 1$ .

Let  $f_i^*$ ,  $i = 0, 1, 2$ , be the number of vertices, edges and two-dimensional faces in  $\mathcal{F}^*$ . For the Euler characteristic of  $\mathcal{F}^*$ , we have  $\chi(\mathcal{F}^*) = \sum_{i=0}^2 (-1)^i f_i^*$ . Since the graph  $\mathcal{G}$  is homotopy equivalent to  $\mathcal{F}^*$ ,  $\chi(\mathcal{G}) = \chi(\mathcal{F}^*)^*$ . Let  $f_0^\infty \geq 1$  be the number of new ideal vertices that appear in  $\mathcal{P}_\infty$ . We have  $|\Omega_0(\mathcal{P}_\infty)| = |\Omega_0(\mathcal{P}(k))| - f_0^* + f_0^\infty$  and  $|\Omega_i(\mathcal{P}_\infty)| = |\Omega_i(\mathcal{P}(k))| - f_i^*$ ,  $i = 1, 2$ . By definition of face contraction,  $|\Omega_3(\mathcal{P}_\infty)| = |\Omega_3(\mathcal{P}(k))|$ . Then

$$\begin{aligned} \chi(\mathcal{P}_\infty) &= \sum_{i=0}^3 (-1)^i |\Omega_i(\mathcal{P}_\infty)| = \sum_{i=0}^3 (-1)^i |\Omega_i(\mathcal{P}(k))| - \sum_{i=0}^2 (-1)^i f_i^* + f_0^\infty = \\ &= \chi(\mathcal{P}(k)) - \chi(\mathcal{G}) + f_0^\infty. \end{aligned}$$

Since  $\mathcal{P}_\infty$  is non-degenerate,  $\chi(\mathcal{P}_\infty) = \chi(\mathcal{P}(k))$ . Finally, we obtain

$$\chi(\mathcal{G}) = f_0^\infty \geq 1. \quad (4.8)$$

But this new inequality (4.8) contradicts (4.7). Hence there is no sequence of Coxeter polytopes  $\mathcal{P}(k) \subset \mathbb{H}^4$  having all the same combinatorial type which converges to a non-degenerate polytope  $\mathcal{P}_\infty$ .

To generalise this theorem to the case of higher dimensions  $n \geq 5$ , we consider an  $(n-2)$ -dimensional face  $F \in \Omega_{n-2}(\mathcal{P}(k))$ , a vertex  $v \in \Omega_0(F)$  and its vertex figure  $L$ .

\* If the graph  $\mathcal{G}$  is not connected, we set  $\chi(\mathcal{G}) = \sum_{i=1}^m \chi(\mathcal{G}_i)$ , when  $\mathcal{G} = \bigsqcup_{i=1}^m \mathcal{G}_i$ .

By an argument similar to that of the four-dimensional case,  $L$  is a spherical Coxeter  $n$ -simplex such that  $G(L) \cong D_{n_1} \times \cdots \times D_{n_k}$  if  $n$  is even, or  $G(L) \cong D_{n_1} \times \cdots \times D_{n_k} \times A_1$  if  $n$  is odd, with  $k = \lfloor n/2 \rfloor$ ,  $n_i \geq 2$  integers. Then we consider two faces  $F, F' \in \Omega_{n-2}(\mathcal{P}(k))$ , with  $F$  subject to contraction, sharing the vertex  $v$  and intersecting each other at a codimension four face only. This codimension four face gives rise to a spherical Coxeter tetrahedron as in Fig. 4.14, and the proof proceeds by analogy. Q.E.D.

### 4.3 The optimality of the hyperbolic 24-cell

In this section, we consider the 24-cell  $\mathcal{C}$ , that is a four-dimensional regular ideal hyperbolic polytope with Schläfli symbol  $\{3, 4, 3\}$  (see [11, Chapter 13.5]) and with all dihedral angles right. The polytope  $\mathcal{C}$  has 24 octahedral facets, 96 triangular faces, 96 edges and 24 cubical vertex figures. It could be obtained by means of the Wythoff construction [11, Section 11.6] performed with the simplex  $\odot \text{---} \bullet \overset{4}{\text{---}} \bullet \text{---} \bullet \overset{4}{\text{---}} \bullet$ . We show that the 24-cell has minimal volume and minimal facet number among all ideal right-angled polytopes in  $\mathbb{H}^4$ . In the sequel, we reproduce mainly the content of the work [37].

#### 4.3.1 Hyperbolic right-angled polytopes

Let  $\mathcal{P}$  be a polytope in the hyperbolic  $n$ -dimensional space  $\mathbb{H}^n$ . Let  $f_k$  denote the number  $\text{card } \Omega_k(\mathcal{P})$  of  $k$ -dimensional faces and let  $\mathbf{f}(\mathcal{P}) = (f_0, \dots, f_{n-1})$  be the *face vector* of the polytope  $\mathcal{P}$ .

Call  $\mathcal{P} \subset \mathbb{H}^n$  a *regular* hyperbolic polytope if it is combinatorially isomorphic to a regular  $n$ -dimensional Euclidean polytope and all the dihedral angles of  $\mathcal{P}$  in its co-dimension two faces are equal. Recall that there are infinitely many regular polygons. Dimension three provides five Platonic solids. There exist six regular four-dimensional polytopes. Starting from dimension five, there are only three combinatorial types of convex regular polytopes (see [11, Table I]).

A polytope is *right-angled* if all the dihedral angles equal  $\pi/2$ . Notice that the only regular four-dimensional polytope, realisable as an ideal right-angled hyperbolic one, is the 24-cell. Considered as a regular polytope, it has the Schläfli symbol  $\{3, 4, 3\}$ , octahedral facets  $\{3, 4\}$  and cubical vertex figures  $\{4, 3\}$ . We denote it by  $\mathcal{C}$  and call it *the hyperbolic 24-cell*.

Recall that a polytope  $\mathcal{P} \subset \mathbb{H}^n$  is *simple* if each vertex belongs to  $n$  facets only, and  $\mathcal{P}$  is called *simple at edges* if each edge belongs to  $n - 1$  facets only. Every vertex

figure of a compact acute-angled hyperbolic polytope is a combinatorial simplex of co-dimension one [59, p. 108, Theorem 1.8]. Every vertex figure of an ideal right-angled hyperbolic polytope is a combinatorial cube of co-dimension one [15, Proposition 1]. Thus, a compact acute-angled hyperbolic polytope is simple and an ideal right-angled hyperbolic polytope is simple at edges.

Let us consider the following two problems in the class of four-dimensional ideal right-angled hyperbolic polytopes.

**I:** Find a polytope of minimal volume,

**II:** Find a polytope of minimal facet number.

Since Coxeter's work [11], the 24-cell is known for its nice combinatorial and geometric Euclidean structure. We shall demonstrate that the 24-cell solves both problem **I** on minimal volume and problem **II** on minimal facet number. Question **I** is closely related to the volume spectrum of four-dimensional hyperbolic manifolds [45], question **II** is new and is both of combinatorial and geometric nature. Furthermore, using the results of [35, 41] (Theorem 19), we obtain a new dimension bound for ideal right-angled hyperbolic polytopes. The case of right-angled hyperbolic polytopes with both proper and ideal vertices was considered before in [15, 43].

### 4.3.2 The 24-cell and volume minimality

**Lemma 2 (Combinatorial identities)** *Let  $\mathcal{P} \subset \mathbb{H}^4$  be an ideal right-angled polytope with face vector  $\mathbf{f}(\mathcal{P}) = (f_0, f_1, f_2, f_3)$ . Then the following combinatorial identities hold.*

$$f_0 - f_1 + f_2 - f_3 = 0, \tag{4.9}$$

$$f_1 = 4 f_0, \tag{4.10}$$

$$12 f_0 = \sum_{F \in \Omega_2(\mathcal{P})} f_0(F). \tag{4.11}$$

**PROOF.** We list the proofs of (4.9)-(4.11) below in the respective order.

(4.9) This is Euler's identity. Since  $\mathcal{P}$  is a convex four-dimensional polytope, its surface  $\partial\mathcal{P}$  is homeomorphic to  $\mathbb{S}^3$ . Hence, for the Euler characteristic of  $\partial\mathcal{P}$ , we have  $f_0 - f_1 + f_2 - f_3 =: \chi(\partial\mathcal{P}) = \chi(\mathbb{S}^3) = 0$ .

(4.10) Let  $v \in \Omega_0(\mathcal{P})$  be a vertex. Each vertex figure  $\mathcal{P}_v$  of  $\mathcal{P}$  is a cube. The vertices of  $\mathcal{P}_v$  correspond to the edges of  $\mathcal{P}$  emanating from a given vertex  $v \in \Omega_0(\mathcal{P})$ . This

means that eight edges are adjacent at  $v$ . On the other hand, each edge has two vertices. Thus, we obtain  $2f_1 = 8f_0$  and (4.10) follows.

(4.11) The edges of the vertex figure  $\mathcal{P}_v$ , a cube, correspond to the two-dimensional faces of  $\mathcal{P}$  meeting  $v$ . Thus, twelve two-dimensional faces meet at each vertex. Hence, if we sum up the number of vertices  $f_0(F)$  over all the two-dimensional faces  $F \in \Omega_2(\mathcal{P})$ , we count each vertex of  $\mathcal{P}$  twelve times. Then the desired formula follows and the lemma is proven. Q.E.D.

**Lemma 3 (Volume formula)** *Let  $\mathcal{P} \subset \mathbb{H}^4$  be an ideal right-angled polytope with face vector  $\mathbf{f}(\mathcal{P}) = (f_0, f_1, f_2, f_3)$ . Then its volume equals*

$$\text{Vol } \mathcal{P} = \frac{f_0 - f_3 + 4}{3} \pi^2.$$

PROOF. We shall compute the growth function  $f(t)$  of  $G(\mathcal{P})$ . By Theorems 13 and 21 we obtain

$$\frac{1}{f(t)} = 1 - \frac{f_3}{[2]} + \frac{f_2}{[2]^2} - \frac{f_1}{[2]^3}, \quad (4.12)$$

where the denominators come from the fact that the vertex figure of each vertex is a Euclidean cube (both combinatorially and geometrically, see Section 3.2.1), Table 3.4 and Proposition 1. Thus, every finite rank  $k$ ,  $k = 1, 2, 3$ , subgroup of  $G(\mathcal{P})$  that contributes to formula (4.12) is a direct product of  $k$  copies of  $A_1$ . These are stabilisers of  $(4 - k)$ -faces of  $\mathcal{P}$ , respectively. A vertex stabiliser is an infinite Coxeter group generated by reflections in the faces of a three-dimensional cube (see Table 3.2). Hence, all the vertex stabilisers of  $\mathcal{P}$  do not contribute to formula (4.12).

Now we apply relations (4.9)-(4.10) together with  $\text{Vol } \mathbb{S}^4 = 8\pi^2/3$  and compute the volume of  $\mathcal{P}$  by Theorem 22:

$$\text{Vol } \mathcal{P} = \frac{1}{2} \frac{\text{Vol } \mathbb{S}^4}{f(1)} = \frac{f_0 - f_3 + 4}{3} \pi^2.$$

Q.E.D.

The hyperbolic 24-cell  $\mathcal{C}$  has  $f_0 = f_3 = 24$ ,  $f_1 = f_2 = 96$ , see [11, Table I, (ii)]. Hence, by the lemma above, its volume equals  $4\pi^2/3$ .

**Theorem 26 (Minimal volume)** *A four-dimensional ideal right-angled hyperbolic polytope of minimal volume is  $\mathcal{C}$ , up to an isometry.*

PROOF. Let us consider an ideal right-angled hyperbolic polytope  $\mathcal{P} \subset \mathbb{H}^4$ . Let  $f_2(k)$  denote the number of its two-dimensional  $k$ -gonal faces,  $k \geq 3$ , which are ideal hyperbolic polygons. Then

$$f_2 = f_2(3) + \cdots + f_2(N),$$

where  $N = \max_{F \in \Omega_2(\mathcal{P})} f_0(F) \geq 3$ . By Lemma 2, formula (4.11), we obtain

$$12 f_0 = \sum_{F \in \Omega_2(\mathcal{P})} f_0(F) = 3 f_2(3) + \cdots + N f_2(N).$$

By using Lemma 2, formulas (4.9)-(4.10), one subsequently computes

$$f_0 - f_3 = 4f_0 - f_2 = \frac{1}{3} \sum_{k=4}^N (k-3)f_2(k) \geq 0. \quad (4.13)$$

Then, by Lemma 3,

$$\text{Vol } \mathcal{P} \geq \frac{4}{3} \pi^2 = \text{Vol } \mathcal{C}.$$

If  $\text{Vol } \mathcal{P}$  equals the volume of  $\mathcal{C}$ , one immediately has  $f_2(k) = 0$  for all  $k \geq 4$  by (4.13). This means that all the two-dimensional faces of  $\mathcal{P}$  are triangles. Consider a facet  $P \in \Omega_3(\mathcal{P})$ . Observe that  $P \subset \mathbb{H}^3$  is an ideal right-angled polyhedron which has only triangular faces. Then  $P$  is a combinatorial octahedron and it is isometric to the right-angled hyperbolic octahedron by Andreev's theorem (Theorems 8 and 9). Hence, all the facets of  $\mathcal{P}$  are ideal right-angled octahedra. So the polytope  $\mathcal{P}$  is combinatorially isomorphic to a regular four-dimensional Euclidean polytope with octahedral facets only, that is, the 24-cell by [11, Table I, (ii)]. Thus  $\mathcal{P}$  is isometric to  $\mathcal{C}$  by Andreev's theorem (Theorem 8). Q.E.D.

### 4.3.3 The 24-cell and facet number minimality

**Theorem 27 (Minimal facet number)** *The facet number of a four-dimensional ideal right-angled hyperbolic polytope  $\mathcal{P}$  satisfies  $f_3(\mathcal{P}) \geq f_3(\mathcal{C}) = 24$ . Any four-dimensional ideal right-angled hyperbolic polytope  $\mathcal{P}$  with  $f_3(\mathcal{P}) = 24$  is isometric to the hyperbolic 24-cell  $\mathcal{C}$ .*

The proof will be based on Proposition 12 and Lemma 4 below. Their proofs will be given in Section 4.3.3.3.

#### 4.3.3.1 Three-dimensional ideal right-angled hyperbolic polyhedra with few faces

Let  $\mathcal{A}_k \subset \mathbb{H}^3$ ,  $k \geq 3$ , be an ideal right-angled antiprism depicted in Fig. 4.15. In the figure, the leftmost and the rightmost edges are identified, so that the surface of the polyhedron is partitioned into top and bottom  $k$ -gonal faces and  $2k$  triangular faces in the annulus between them. Such an antiprism exists for every  $k \geq 3$  and it is unique up to an isometry due to Andreev's theorem (Theorems 8 and 9).

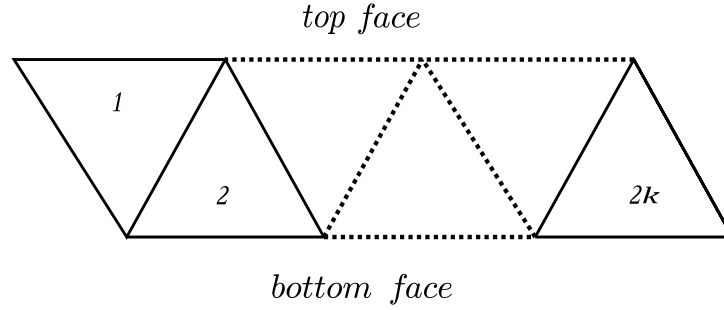


Figure 4.15: Antiprism  $\mathcal{A}_k$ ,  $k \geq 3$ .

Antiprisms  $\mathcal{A}_k$  will later play the rôle of possible facets for a four-dimensional ideal right-angled hyperbolic polytope in the proof of Theorem 27.

**Proposition 12 (Antiprism’s optimality)** *A three-dimensional ideal right-angled hyperbolic polyhedron of minimal face number, which has at least one  $k$ -gonal face,  $k \geq 3$ , is isometric to the antiprism  $\mathcal{A}_k$  with  $f_2(\mathcal{A}_k) = 2k + 2$ .*

PROOF. Let  $\mathcal{P} \subset \mathbb{H}^3$  be an ideal right-angled polyhedron. Let  $F \in \Omega_2(\mathcal{P})$  be a  $k$ -gonal face,  $k \geq 3$ . For each edge  $e \in \Omega_1(F)$  there is exactly one further face adjacent to  $F$  along  $e$ . For each vertex  $v$ , being four-valent by Andreev’s theorem (Theorem 9), there exists a face intersecting  $F$  at  $v$  only. Moreover, all the faces mentioned above are different from each other, so that we have  $f_2(\mathcal{P}) \geq 2k + 1$ . Observe that these faces can not constitute yet a polyhedron. Indeed, consider  $F$  as a “bottom” face of  $\mathcal{P}$ . Then the new faces we have added make a surface wrapping around the interior of  $\mathcal{P}$  along the edges of  $F$ . Since all vertices are four-valent, at least one additional “top” face is required to close up the polyhedron. Hence  $f_2(\mathcal{P}) \geq 2k + 2$ . The antiprism  $\mathcal{A}_k$  satisfies

$$f_2(\mathcal{A}_k) = 2k + 2 \tag{4.14}$$

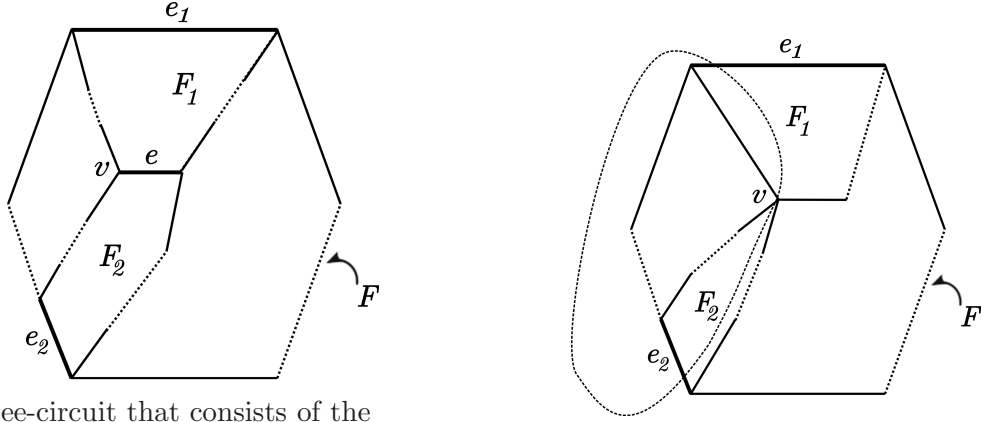
and so has minimal face number.

It remains to show that a polyhedron  $\mathcal{P}$  with  $f_2(\mathcal{P}) = f_2(\mathcal{A}_k)$  is in fact isometric to  $\mathcal{A}_k$ . Since  $\mathcal{P}$  has four-valent vertices,  $2f_1(\mathcal{P}) = 4f_0(\mathcal{P})$ . From this equality and Euler’s identity  $f_0(\mathcal{P}) - f_1(\mathcal{P}) + f_2(\mathcal{P}) = 2$  we obtain that

$$f_2(\mathcal{P}) = f_0(\mathcal{P}) + 2. \tag{4.15}$$

Consider the faces adjacent to the  $k$ -gon  $F$  along its edges. We shall prove that no pair of them can have a common vertex  $v \notin \Omega_0(F)$ . By supposing the contrary, let us denote two such faces  $F_i$ ,  $i = 1, 2$ , and let them intersect at  $v$ . Observe that  $F_i$ ,





(a) Three-circuit that consists of the faces  $F$ ,  $F_1$  and  $F_2$

(b) Circuit that is indicated by the dashed line

Figure 4.16: Circuits deprecated by Andreev's theorem

$i = 1, 2$ , are adjacent to  $F$  along two disjoint edges  $e_1$  and  $e_2$ . In fact, if  $e_1$  intersects  $e_2$  in a vertex  $u \in \Omega_0(F)$ , then since  $\mathcal{P}$  has convex faces we obtain two geodesic segments joining  $v$  to  $u$ . One of them belongs to  $F_1$  and the other belongs to  $F_2$ . This is impossible, unless the considered segments are represented by a common edge  $e$  of  $F_i$ ,  $i = 1, 2$ , adjacent to both  $v$  and  $u$ . But then the vertex  $u$  has only three adjacent edges:  $e_1$ ,  $e_2$  and  $e$ . This is a contradiction to  $u$  having valency four. Now if  $F_1$  and  $F_2$  share an edge  $e$  such that  $v \in \Omega_0(e)$ , then condition  $(\mathbf{m}_2)$  of Andreev's theorem (Theorem 9) does not hold as depicted in Fig. 4.16a. If  $F_1$  and  $F_2$  share only the vertex  $v$ , then condition  $(\mathbf{m}_5)$  of Andreev's theorem (Theorem 9) is not satisfied as depicted in Fig. 4.16b.

Suppose that a face  $F'$  adjacent to the  $k$ -gon  $F \in \Omega_2(\mathcal{P})$  along an edge is not triangular. Then  $F'$  has  $f_0(F')$  vertices, and two among them are already counted in  $f_0(F)$ . Hence we have at least

$$\sum_{\substack{F' \text{ adjacent to} \\ F \text{ along an edge}}} (f_0(F') - 2) \geq (k - 1) + 2 = k + 1$$

additional vertices, since  $f_0(F') \geq 3$  for each  $F'$  among  $k$  faces adjacent to  $F$  and at least one such face  $F'$  has  $f_0(F') \geq 4$ . Thus  $f_0(\mathcal{P}) \geq 2k + 1$ , and by (4.15) the estimate  $f_2(\mathcal{P}) \geq 2k + 3$  follows. Equality (4.14) implies  $f_2(\mathcal{P}) > f_2(\mathcal{A}_k)$  and we arrive at a contradiction. Hence all the faces adjacent to  $F$  along its edges are triangular.

Consider the faces of  $\mathcal{P}$  adjacent to the  $k$ -gon  $F \in \Omega_2(\mathcal{P})$  only at its vertices. Suppose that one of them, say  $F'$ , is not triangular. Then we have

$$\sum_{\substack{F' \text{ adjacent to} \\ F \text{ at a vertex}}} f_1(F') \geq 3(k - 1) + 4 = 3k + 1$$

additional edges. But then  $f_1(\mathcal{P}) \geq 4k + 1$  and we arrive at a contradiction. Indeed, in this case  $f_1(\mathcal{P}) > f_1(\mathcal{A}_k) = 4k$ .

Hence we have a  $k$ -gonal face  $F$ ,  $k \geq 3$ , together with  $2k$  triangular side faces adjacent to it along the edges and at the vertices. By adding another one  $k$ -gonal face we close up the polyhedron  $\mathcal{P}$ , while its vertex number remains unchanged. Observe that there is no other way to finish this construction without increasing the vertex number.

Thus, an ideal right-angled polyhedron  $\mathcal{P} \subset \mathbb{H}^3$  having minimal face number, which contains at least one  $k$ -gon, is combinatorially isomorphic to  $\mathcal{A}_k$ . By Theorems 8-9 the polyhedron  $\mathcal{P}$  is isometric to  $\mathcal{A}_k$ . Q.E.D.

NOTE (TO PROPOSITION 12). The classification of *polygonal maps* on the two-dimensional sphere given in [14] provides another argument to show the uniqueness of antiprism stated above. Namely, [14, Theorem 1] says that  $\mathcal{P}$  has in fact not less than two  $k$ -gonal faces. Hence  $f_2(\mathcal{P}) = 2k + 2$  if and only if  $\mathcal{P}$  has exactly two  $k$ -gonal faces and  $2k$  triangular faces. Polygonal maps of this kind are classified by [14, Theorem 2]. Among them only the map isomorphic to the one-skeleton of  $\mathcal{A}_k$  satisfies Steiniz's theorem [63, Chapter 4]. Thus, the polyhedron  $\mathcal{P}$  is combinatorially isomorphic to  $\mathcal{A}_k$ .\*

#### 4.3.3.2 Combinatorial constraints on facet adjacency

Let  $F_1, \dots, F_m$  be an ordered sequence of facets of a given hyperbolic polytope  $\mathcal{P} \subset \mathbb{H}^4$  such that each facet is adjacent only to the previous and the following ones either through a co-dimension two face or through an ideal vertex, while the last facet  $F_m$  is adjacent only to the first facet  $F_1$  (through a co-dimension two face or through an ideal vertex, as before) and no three of them share a lower-dimensional face. Call the sequence  $F_1, \dots, F_m$  a  $(k, \ell)$  circuit,  $k + \ell = m$ , if it comprises  $k$  co-dimension two faces and  $\ell$  ideal vertices shared by the facets. We complete the analysis carried out in [43] in the following way.

**Lemma 4 (Adjacency constraints)** *Let  $\mathcal{P} \subset \mathbb{H}^4$  be an ideal right-angled polytope. Then  $\mathcal{P}$  contains no  $(3, 0)$ ,  $(4, 0)$  and  $(2, 1)$  circuits.*

PROOF. By [43, Proposition 4.1] there are no  $(3, 0)$  and  $(2, 1)$  circuits. Suppose on the contrary that there exists a  $(4, 0)$  circuit formed by the facets  $F_k \in \Omega_3(\mathcal{P})$ ,  $k = 1, 2, 3, 4$ . Let  $e_k$ ,  $k = 1, 2, 3, 4$ , denote the outer unit vector normal to the support

---

\* the author is grateful to Michel Deza for indicating the very recent paper [14].

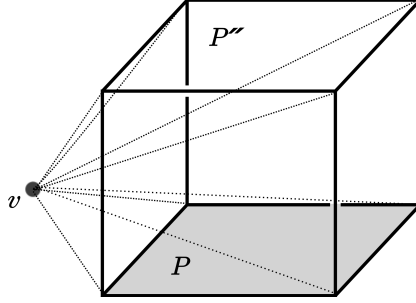


Figure 4.17: The vertex figure  $\mathcal{P}_v$

hyperplane of  $F_k$ . Consider the Gram matrix of these vectors w.r.t. the Lorentzian form  $\langle \cdot, \cdot \rangle_{4,1}$ :

$$G = (\langle e_i, e_j \rangle)_{i,j=1}^4 = \begin{pmatrix} 1 & 0 & -\cosh \rho_{13} & 0 \\ 0 & 1 & 0 & -\cosh \rho_{24} \\ -\cosh \rho_{13} & 0 & 1 & 0 \\ 0 & -\cosh \rho_{24} & 0 & 1 \end{pmatrix},$$

where  $\rho_{ij} > 0$  is the length of the common perpendicular between two disjoint support hyperplanes for  $F_i$  and  $F_j$  respectively. The eigenvalues of  $G$  are  $\{1 \pm \cosh \rho_{13}, 1 \pm \cosh \rho_{24}\}$ , that means two of them are strictly negative and two are strictly positive. Thus, we arrive at a contradiction with the signature of a Lorentzian form. Q.E.D.

#### 4.3.3.3 Proof of Theorem 27

Let  $\mathcal{P} \subset \mathbb{H}^4$  be an ideal right-angled polytope. Let  $P \in \Omega_3(\mathcal{P})$  be a facet. For every two-face  $F \in \Omega_2(P)$  there exists a corresponding facet  $P' \in \Omega_3(\mathcal{P})$ ,  $P' \neq P$ , such that  $P$  and  $P'$  share the face  $F$ . Since each vertex figure of  $\mathcal{P}$  is a cube, there exists an opposite facet  $P'' \in \Omega_3(\mathcal{P})$  for every vertex  $v \in \Omega_0(P)$ . The vertex figure is depicted in Fig. 4.17, where the grey bottom face of the cube corresponds to  $P$  and the top face corresponds to  $P''$ . These new facets  $P'$  and  $P''$  together with  $P$  are pairwise different. In order to show this we use the following convexity argument.

CONVEXITY ARGUMENT. First, observe that no facet of a convex polytope can meet another one at two different two-faces. Now suppose that  $P' \in \Omega_3(\mathcal{P})$  is a facet adjacent to  $P$  at a face  $F \in \Omega_2(P)$  and a single vertex  $v \in \Omega_0(P)$  not in  $F$ . The facets  $P$  and  $P'$  have non-intersecting interiors, but the geodesic going through a given point of  $F$  to  $v$  belongs to both of them by the convexity of  $\mathcal{P}$ . So we arrive at a contradiction.

The same contradiction arises if we suppose that there is a facet  $P' \in \Omega_3(\mathcal{P})$  adjacent to  $P$  at two distinct vertices  $v, v' \in \Omega_0(P)$ . In this case we consider the geodesic in  $P$  going through  $v$  to  $v'$ .

By the convexity argument above, the facet number of  $\mathcal{P}$  has the lower bound

$$f_3(\mathcal{P}) \geq f_2(P) + f_0(P) + 1,$$

or, by means of equality (4.15),

$$f_3(\mathcal{P}) \geq 2f_2(P) - 1. \quad (4.16)$$

Observe that the hyperbolic 24-cell  $\mathcal{C}$  has only triangle two-faces. Suppose that  $\mathcal{P}$  has at least one  $k$ -gonal face  $F \in \Omega_2(\mathcal{P})$  with  $k \geq 4$ . We shall show that the estimate  $f_3(\mathcal{P}) \geq 25$  holds, by considering several cases as follows.

A) Suppose that  $\mathcal{P}$  has a  $k$ -gonal two-dimensional face with  $k \geq 6$ . Then, by (4.16) and Proposition 12, we have

$$f_3(\mathcal{P}) \geq 2f_2(\mathcal{A}_k) - 1 = 2(2k + 2) - 1 \geq 27.$$

Thus  $\mathcal{P}$  can not be isometric to  $\mathcal{C}$ .

B) Suppose that  $\mathcal{P}$  has a pentagonal two-dimensional face  $F$  contained in a facet  $P \in \Omega_3(\mathcal{P})$ . Suppose  $P$  is not isometric to  $\mathcal{A}_5$ . This assumption implies  $f_2(P) > 12$ . Then (4.16) grants  $f_3(\mathcal{P}) \geq 25$ .

C) Suppose that all the facets of  $\mathcal{P}$  containing a pentagonal two-face are isometric to  $\mathcal{A}_5$ . Let  $P_0$  be one of them. Then it has two neighbouring facets  $P_k$ ,  $k = 1, 2$  both isometric to  $\mathcal{A}_5$ . Now we count the facets adjacent to  $P_k$ ,  $k = 0, 1, 2$  in Fig. 4.18, where  $P_0$  is coloured grey. Observe that two-faces in Fig. 4.18 sharing an edge are marked with the same number and belong to a common facet, since  $\mathcal{P}$  is simple at edges. However, the two-faces marked with different numbers, correspond to different adjacent facets. Suppose on the contrary that there are two faces  $F \in \Omega_2(P_i)$ ,  $F' \in \Omega_2(P_j)$ ,  $i, j \in \{0, 1, 2\}$ , marked with distinct numbers and a facet  $P' \in \Omega_3(\mathcal{P})$  such that  $P'$  is adjacent to  $P_i$  at  $F$  and to  $P_j$  at  $F'$  and consider the following cases.

- C.1) If  $i = j$ , we arrive at a contradiction by the convexity argument above.
- C.2) If  $i = 0$ ,  $j \in \{1, 2\}$ , then there exists a unique geodesic joining a point  $p$  of  $F$  to a point  $p'$  of  $F'$ . Observe in Fig. 4.18, that the point  $p'$  may be chosen so that  $p' \in F' \cap P_0$ . Then the geodesic between  $p$  and  $p'$  intersects both the interior of  $P'$  and the interior of  $P_0$ . Again, we use the convexity argument and arrive at a contradiction.

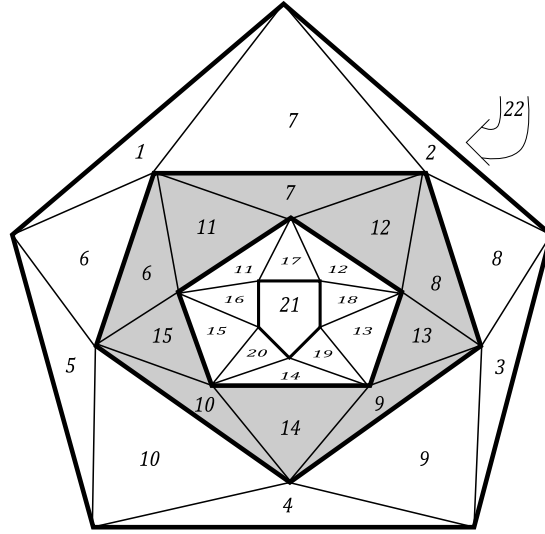


Figure 4.18: Three facets of  $\mathcal{P}$  isometric to  $\mathcal{A}_5$  and their neighbours

C.3) Let  $i = 1$ ,  $j = 2$ . Then if there exist a face  $\tilde{F} \in \Omega_2(P_0)$ ,  $\tilde{F} \cap F \neq \emptyset$ , and a face  $\tilde{F}' \in \Omega_2(P_0)$ ,  $\tilde{F}' \cap F' \neq \emptyset$ , we reduce our argument to case C.1 by considering a geodesic segment joining a point of  $\tilde{F} \cap F$  to a point of  $\tilde{F}' \cap F'$ .

The only case when no such two faces  $\tilde{F}$  and  $\tilde{F}'$  exist is if  $F$  has number 21 and  $F'$  has number 22 in Fig. 4.18. Then the  $(4, 0)$ -circuit  $P_0P_1P'P_2$  appears, in contrary to Lemma 4.

Thus, one has 22 new facets adjacent to  $P_k$ ,  $k = 0, 1, 2$ . Together with  $P_k$  themselves,  $k = 0, 1, 2$ , they provide  $f_3(\mathcal{P}) \geq 25$ .

D) By now, cases A, B and C imply that if an ideal right-angled hyperbolic polytope  $\mathcal{P} \subset \mathbb{H}^4$  has at least one  $k$ -gonal face with  $k \geq 5$ , then  $f_3(\mathcal{P}) \geq 25$ . Suppose that  $\Omega_2(\mathcal{P})$  contains only triangles and quadrilaterals.

By Andreev's theorem (Theorem 9), each facet  $P \in \Omega_3(\mathcal{P})$  has only four-valent vertices. By assumption,  $P$  has only triangular and quadrilateral faces. Combinatorial polyhedra of this type are introduced in [13] as *octahedrites* and the list of those possessing up to 17 vertices is given. Note that in view of (4.16) we may consider octahedrites that have not more than twelve faces or, by equality (4.15) from Proposition 12, ten vertices. In Fig. 4.19, 4.20 we depict only those realisable as ideal right-angled hyperbolic polyhedra with eight, nine and ten vertices.

The ideal right-angled octahedron has six vertices and completes the list. By considering each of the polyhedra in Fig. 4.19 and Fig. 4.20 as a possible facet  $P \in \Omega_3(\mathcal{P})$ , we shall derive the estimate  $f_3(\mathcal{P}) \geq 25$ .

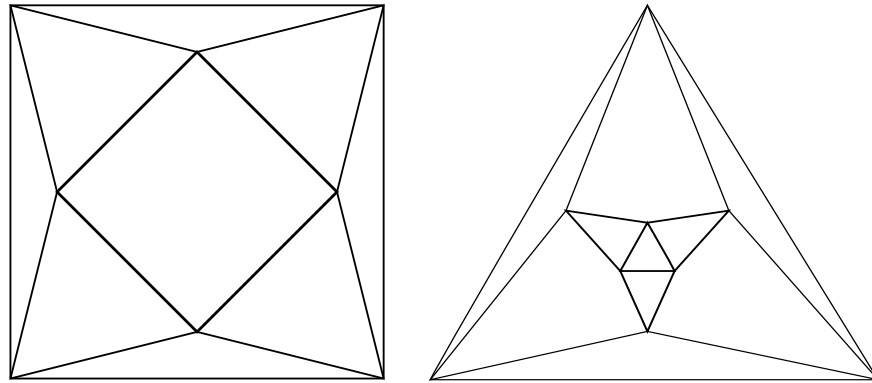


Figure 4.19: Hyperbolic octahedrites with 8 (left) and 9 (right) vertices

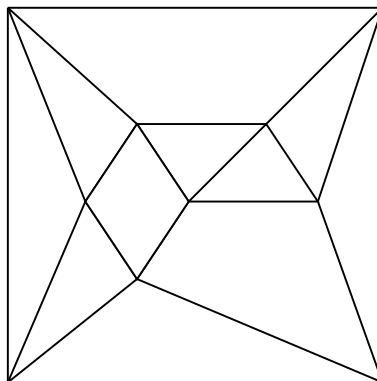


Figure 4.20: Hyperbolic octahedrite with 10 vertices

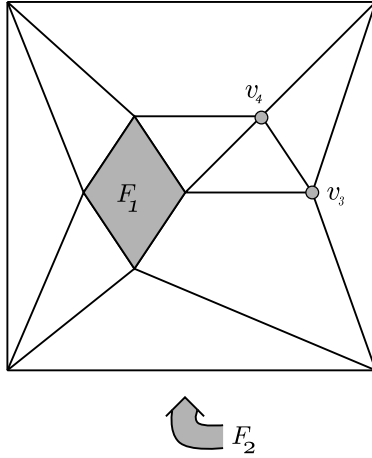


Figure 4.21: Hyperbolic octahedrite with 10 vertices as a facet of  $\mathcal{P}$  and its neighbours

D.1) Let  $P_0 \in \Omega_3(\mathcal{P})$  be the hyperbolic octahedrite with ten vertices depicted in Fig. 4.21. Consider the facets of  $\mathcal{P}$  adjacent to  $P_0$  at its faces. One has  $f_2(P_0) = 12$ , and hence  $f_3(\mathcal{P}) \geq 12$ . Consider the faces coloured grey in Fig. 4.21: the front face is called  $F_1$  and the back face, called  $F_2$ , is indicated by the grey arrow.

The facets  $P_1, P_2 \in \Omega_3(\mathcal{P})$  adjacent to  $P_0$  at  $F_1$  and  $F_2$ , respectively, contain quadrilaterals among their faces. By Proposition 12, it follows that  $f_2(P_i) \geq f_2(\mathcal{A}_4) = 10$ ,  $i = 1, 2$ . We shall count all new facets  $P'$  brought by face adjacency to  $P_i$ ,  $i = 1, 2$ .

Observe that no  $P'$ , which does not share an edge with  $P_0$ , can be adjacent simultaneously to  $P_i$  and  $P_j$ ,  $i, j \in \{1, 2\}$ , at two-faces, since otherwise the  $(4, 0)$  circuit  $P_1P_0P_2P'$  appears in contrary to Lemma 4.

Each facet  $P'$  that shares an edge with  $F_k$ ,  $k = 1, 2$ , is already counted as adjacent to  $P_0$ . The facets  $P_1$  and  $P_2$  are already counted as well, by the same reason. Then the total number of new facets coming together with  $P_1$  and  $P_2$  is at least  $\sum_{i=1}^2 f_2(P_i) - \sum_{i=1}^2 f_1(F_i) - 2 \geq 2 \cdot 10 - 2 \cdot 4 - 2 = 10$ . This implies the estimate  $f_3(\mathcal{P}) \geq 12 + 10 = 22$ .

Consider the facets  $P_i$ ,  $i = 3, 4$ , adjacent to  $P_0$  only at the corresponding circumscribed grey vertices  $v_i$ ,  $i = 3, 4$ , in Fig. 4.21. Then consider the case if  $P'$  is adjacent to  $P_j$ ,  $j \in \{1, 2\}$  at a two-face  $F' \in \Omega_2(P_j)$ . If there exist a face  $\widetilde{F}' \in \Omega_2(P_0)$  such that  $F' \cap \widetilde{F}' \neq \emptyset$ , then choose a point  $p \in F' \cap \widetilde{F}'$  and use the convexity argument again for the geodesic going through  $p$  to  $v_i$ . If  $F' \cap \widetilde{F}' = \emptyset$ , then the  $(2, 1)$  circuit  $P_0P_1P'$  appears in contrary to Lemma 4. Adding up two new facets gives  $f_3(\mathcal{P}) \geq 24$ . Finally, we count  $P_0$  itself and arrive at the estimate  $f_3(\mathcal{P}) \geq 25$ .

D.2) Let  $P_0 \in \Omega_3(\mathcal{P})$  be the hyperbolic octahedrite with nine vertices and eleven faces depicted on the right in Fig. 4.19. Consider the facets adjacent to  $P_0$  at its

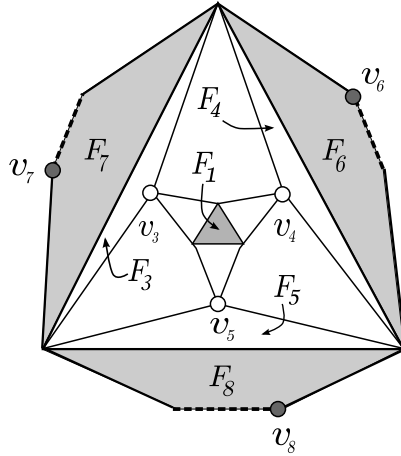


Figure 4.22: Hyperbolic octahedrite with 9 vertices as a facet of  $\mathcal{P}$  and its neighbours (omitted edges are dotted)

two-dimensional faces. By counting them, we have  $f_3(\mathcal{P}) \geq f_2(P_0) = 11$ .

Consider the facet  $P_1$  adjacent to the triangle face  $F_1$  of  $P_0$  coloured grey in the center of Fig. 4.22. By Proposition 12, we have  $f_2(P_1) \geq f_2(\mathcal{A}_3) = 8$ . By excluding already counted facets adjacent to  $P_0$  like in case D.1, the facet  $P_1$  brings new  $f_2(P_1) - f_1(F_1) - 1 \geq 8 - 3 - 1 = 4$  ones by face adjacency. Then  $f_3(\mathcal{P}) \geq 15$ . The visible part of the facet  $P_2$  adjacent to  $P_0$  at its back face  $F_2$  is coloured grey in Fig. 4.22. Again, we have  $f_2(P_2) \geq f_2(\mathcal{A}_3) = 8$ . By counting new facets adjacent to  $P_2$  at faces, it brings another  $f_2(P_2) - f_1(F_2) - 1 \geq 8 - 3 - 1 = 4$  new ones. Hence  $f_3(\mathcal{P}) \geq 19$ .

The facets  $\widehat{P}_k$ ,  $k = 3, 4, 5$ , adjacent to  $P_0$  only at the circumscribed hollow vertices  $v_k$ ,  $k = 3, 4, 5$ , in Fig. 4.22 are different from the already counted ones either by the convexity argument or by Lemma 4, which forbids  $(2, 1)$  circuits, c.f. the argument of case D.1. Thus  $f_3(\mathcal{P}) \geq 22$ .

Let  $\widehat{P}_k$ ,  $k = 6, 7, 8$ , be the facets of  $\mathcal{P}$  adjacent to  $P_2$  only at the respective circumscribed grey vertices  $v_k$ ,  $k = 6, 7, 8$  in Fig. 4.22. Let the faces of  $P_1$  and  $P_2$ , that contain a single circumscribed hollow or grey vertex, be  $F_k$ ,  $k = 3, \dots, 8$ . Finally, let  $P(k)$ ,  $k = 6, 7, 8$ , denote the facets adjacent to  $P_2$  at  $F_k$ ,  $k = 6, 7, 8$ , respectively.

By the convexity argument or by Lemma 4, similar to D.1, the facets  $\widehat{P}_i$ ,  $i = 6, 7, 8$  can not coincide with the already counted ones, except for  $\widehat{P}_j$ ,  $j = 3, 4, 5$  and the facets adjacent only to  $P_1$ .

First consider the case when a facet from  $\widehat{P}_i$ ,  $i \in \{6, 7, 8\}$ , coincides with  $\widehat{P}_j$ ,  $j \in \{3, 4, 5\}$ . Then



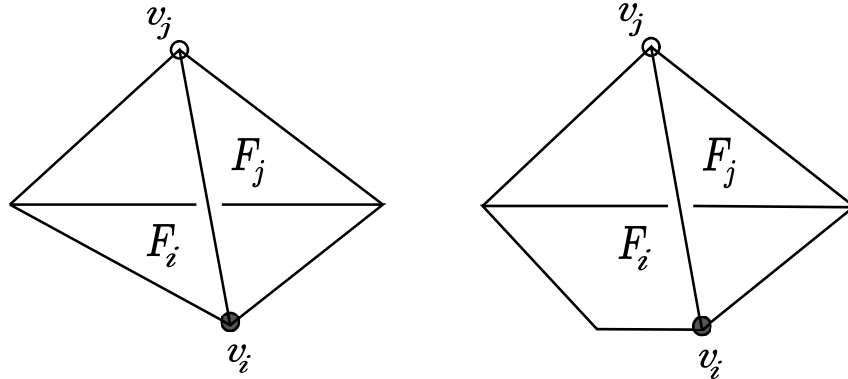


Figure 4.23: Sub-graphs  $\tau$  (on the left) and  $\sigma$  (on the right)

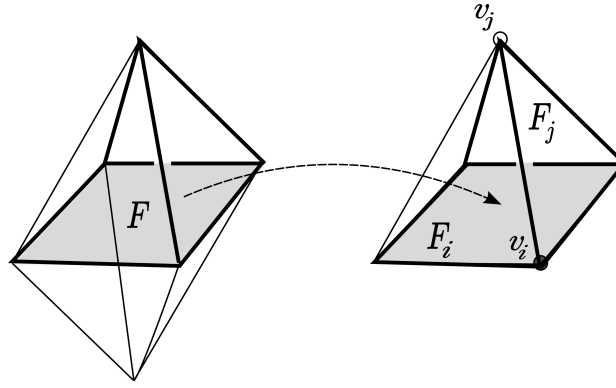


Figure 4.24: Sub-graph  $\sigma$  in an octahedron (on the left) and in the facet  $P(i)$  (on the right)

- 1) either  $\widehat{P}_i = \widehat{P}_j$  is such that  $(i, j) \neq (7, 3), (6, 4)$  and  $(8, 5)$ , so the  $(2, 1)$  circuit  $\widehat{P}_j P(i) P_0$  appears;
- 2) or  $\widehat{P}_i = \widehat{P}_j$  has  $(i, j) = (7, 3), (6, 4)$ , or  $(8, 5)$ , and contains therefore a part of the geodesic going from  $v_i$  to  $v_j$  by convexity. Since the edge shared by  $F_i$  and  $F_j$  belongs to three facets  $P_0, P_2$  and  $P(i)$ , then  $P(i)$  is adjacent to  $P_0$  at  $F_j$  and to  $P_2$  at  $F_i$ . Hence  $P(i)$  contains the vertices  $v_i, v_j$  and the geodesic segment between them as well. Since  $P(i)$  and  $\widehat{P}_i$  have non-intersecting interiors, the two following cases are only possible.

**2.1)** The geodesic segment  $v_i v_j$  belongs to a triangle face of  $P(i)$ : then  $v_i v_j$  is an edge. Observe that the face  $F_j$  of  $P(i)$  is always a triangle, as in Fig. 4.22, while the face  $F_i$  is either a triangle or a quadrilateral. Then the edges of  $F_i, F_j$  and the edge  $v_i v_j$  constitute a sub-graph in the one-skeleton of  $P(i)$ . The possible sub-graphs  $\tau$  and  $\sigma$  depending on the vertex number of  $F_i$  are depicted in Fig. 4.23. The graph  $\tau$  is the

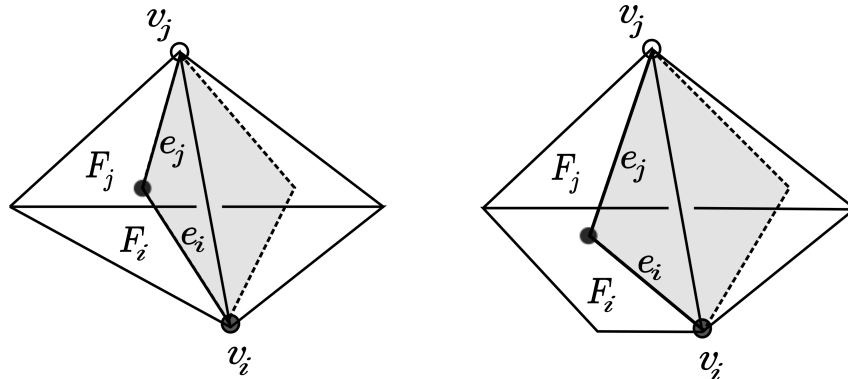


Figure 4.25: The segment  $v_i v_j$  belongs to a quadrilateral face

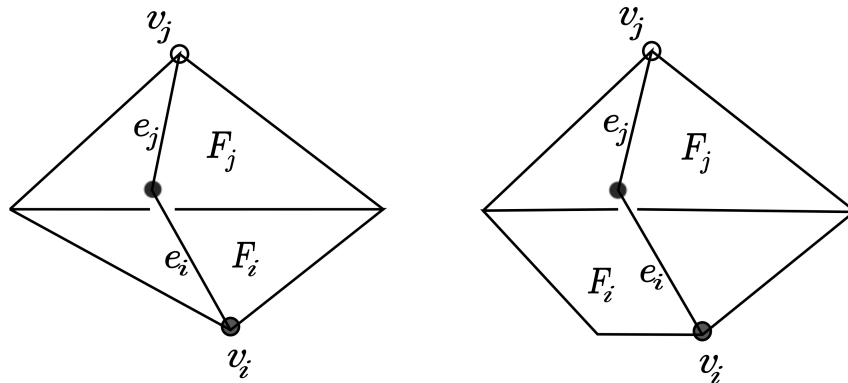


Figure 4.26: Sub-graphs  $\nu$  (on the left) and  $\omega$  (on the right)

one-skeleton of a tetrahedron. The graph  $\sigma$  is the one-skeleton of a square pyramid without one vertical edge. By assumption, the facet  $P(i)$  is an octahedrite with not more than ten vertices. Such octahedrites are depicted in Fig. 4.19-4.20, and none of them contains in its one-skeleton a sub-graph combinatorially isomorphic to  $\tau$  or  $\sigma$ .

The case when  $P(i)$  is an octahedron still remains. Clearly, its one-skeleton does not contain a sub-graph combinatorially isomorphic to  $\tau$ . However, it contains a sub-graph isomorphic to  $\sigma$ . The only possible sub-graph embedding of  $\sigma$  into the one-skeleton of an octahedron, up to a symmetry, is given in Fig. 4.24 on the left. But then the face  $F_i$  of  $P_2$  correspond to the interior domain  $F$  in  $P(i)$  coloured grey in Fig. 4.24 on the right. Thus, we arrive at a contradiction with the convexity of facets.

**2.2)** The geodesic segment  $v_i v_j$  belongs to a quadrilateral face of  $P(i)$ . The general picture of this case is given in Fig. 4.25. Again two sub-graphs  $\nu$  and  $\omega$  arise, as depicted in Fig. 4.26. Such sub-graphs appear at most for the octahedrites as given

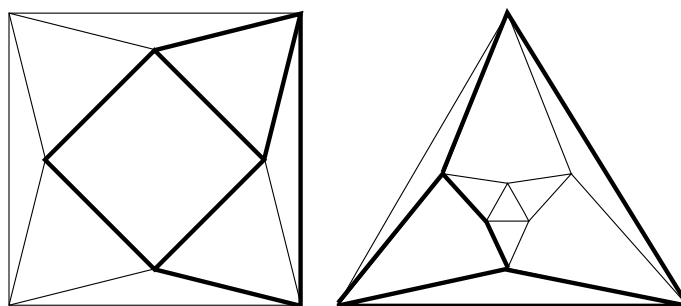
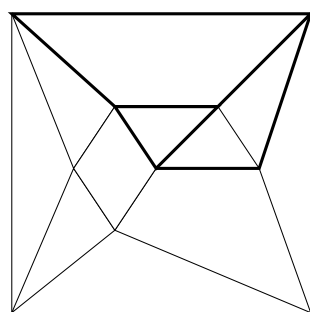
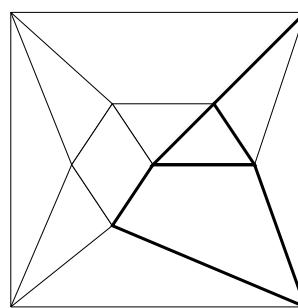


Figure 4.27: Embeddings of the graph  $\nu$  into octahedrite facets with 8 (left) and 9 (right) vertices

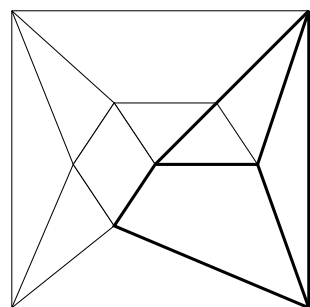


(a) Embedding 1

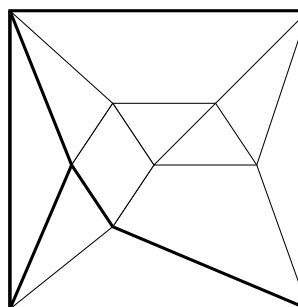


(b) Embedding 2

Figure 4.28: Embeddings of the graph  $\omega$  into the octahedrite facet with 10 vertices



(a) Embedding 3



(b) Embedding 4

Figure 4.29: Embeddings of the graph  $\omega$  into the octahedrite facet with 10 vertices

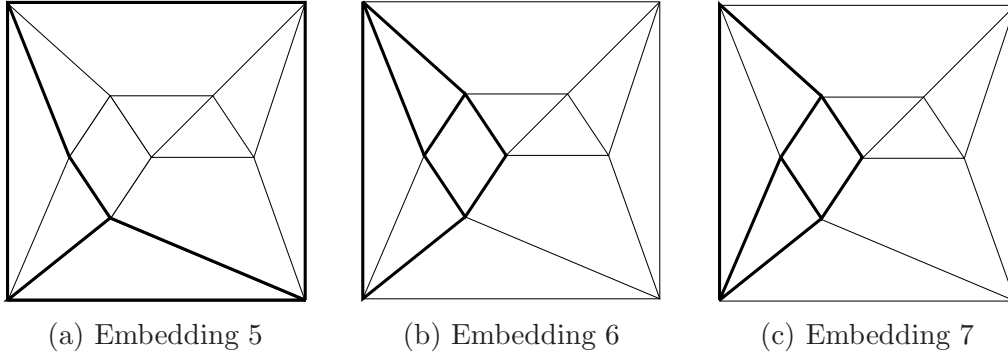


Figure 4.30: Embeddings of the graph  $\omega$  into the octahedrite facet with 10 vertices

in Fig. 4.19-4.20. Observe, that none of them contains in its one-skeleton a sub-graph isomorphic to  $\nu$ .

All possible embeddings of  $\omega$  into the one-skeleton of each considered octahedrite are given, up to a symmetry, in Fig. 4.27, 4.28a-4.30c. Since the edges  $e$  and  $e'$  belong to a single face as in Fig. 4.25, we arrive at a contradiction, since there is no embedding of  $\omega$  with this property.

Finally, consider the case when a facet from  $\widehat{P}_i$ ,  $i \in \{6, 7, 8\}$ , coincides with a facet  $P'$  adjacent only to  $P_1$  at a two-face. Then the  $(4, 0)$  circuit  $P_0P_1P'P(i)$  arises, in contrary to Lemma 4.

So the facets  $\widehat{P}_k$ ,  $k = 6, 7, 8$ , are different from the already counted ones. Adding them up, we obtain  $f_3(\mathcal{P}) \geq 22 + 3 = 25$ .

D.3) Let  $P_0 \in \Omega_3(\mathcal{P})$  be the hyperbolic octahedrite with eight vertices depicted on the left in Fig. 4.19. Observe that this polyhedron is combinatorially isomorphic to  $\mathcal{A}_4$ , and hence isometric to it by Andreev's theorem (Theorem 8). Moreover, we suppose that all facets of  $\mathcal{P}$  are isometric to  $\mathcal{A}_4$ , since other possible facet types are already considered in D.1 and D.2.

Consider the facets  $P_k$ ,  $k = 1, 2$ , adjacent to the front and the back quadrilateral faces of  $P_0$ . The facets  $P_i$ ,  $i = 0, 1, 2$ , are depicted together in Fig. 4.31, where  $P_0$  is coloured grey. We count the facets adjacent to  $P_i$ ,  $i = 1, 2, 3$ , at faces in Fig. 4.31. Observe that different numbers on the faces shown in Fig. 4.31 correspond to distinct facets of  $\mathcal{P}$  adjacent to them. The counting arguments are completely analogous to those of C. Hence, we obtain the estimate  $f_3(\mathcal{P}) \geq 18$ . By taking into account the facets  $P_i$ ,  $i = 1, 2, 3$ , themselves, it becomes  $f_3(\mathcal{P}) \geq 21$ .

Consider the facets  $\widehat{P}_i$ ,  $i = 1, 2, 3, 4$ , adjacent to  $P_2$  only at its circumscribed vertices  $v_i$ ,  $i = 1, 2, 3, 4$  in Fig. 4.31. By analogy with the proof in D.2, the  $\widehat{P}_i$ 's are

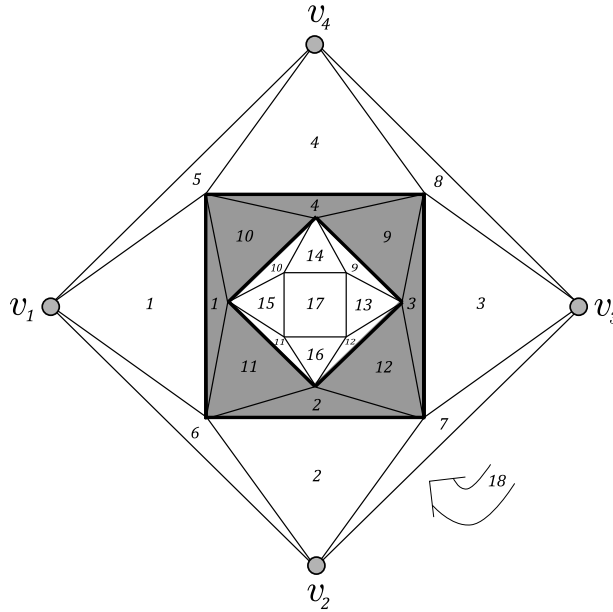


Figure 4.31: Hyperbolic octahedrite with 8 vertices as a facet of  $\mathcal{P}$  and its neighbours

different from the already counted ones. Thus, we add four new facets and obtain  $f_3(\mathcal{P}) \geq 25$ .

Hence, a polytope  $\mathcal{P}$  with  $f_3(\mathcal{P}) = 24$  has only octahedral facets and, by the argument from Theorem 26, is isometric to the hyperbolic 24-cell.  $\square$

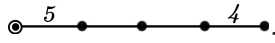
#### 4.3.3.4 A dimension bound for ideal right-angled hyperbolic polytopes

Let us note that Nikulin's inequality previously stated as Theorem 19 could be generalised to the case of finite-volume hyperbolic polytopes. Namely, Nikulin's inequality relies on the fact that the given polytope is *simple*. It has been shown by A. Khovanskiĭ [35], that the condition of being *simple at edges* already suffices.

**Corollary (of Theorem 27)** *There are no ideal right-angled hyperbolic polytopes in  $\mathbb{H}^n$ , if  $n \geq 7$ .*

PROOF. Suppose that  $\mathcal{P} \subset \mathbb{H}^n$  is an ideal right-angled hyperbolic polytope,  $n \geq 4$ . Since we have  $f_4^3(\mathcal{P}) \geq 24$  by Theorem 27, then the Nikulin-Khovanskiĭ inequality (Theorem 19) implies  $n \leq 5$  for  $n$  odd and  $n \leq 6$  for  $n$  even. Q.E.D.

## 4.4 Towards the optimality of the hyperbolic 120-cell

In this section, we consider the 120-cell  $\mathcal{Z}$ , that is a four-dimensional regular compact hyperbolic polytope with Schläfli symbol  $\{5, 3, 3\}$  (see [11, Chapter 7.8]) and all dihedral angles right. The polytope  $\mathcal{Z}$  has 120 octahedral facets, 720 pentagonal faces, 1200 edges and 600 tetrahedral vertex figures. It could be obtained by means of the Wythoff construction [11, Section 11.6] performed with the simplex . In the following, we shall refer to  $\mathcal{Z}$  as to *the hyperbolic 120-cell*. Like in Section 4.3, one may ask the following questions regarding the class of all compact right-angled polytopes in  $\mathbb{H}^4$ :

**I:** Does the hyperbolic 120-cell have minimal volume ?

**II:** Does the hyperbolic 120-cell have minimal facet number ?

Below we present some partial results concerning the combinatorial and geometric properties of compact right-angled polytopes in  $\mathbb{H}^4$ . One fact is that the inequality  $f_3(\mathcal{P}) > f_3(\mathcal{Z}) = 120$  implies  $\text{Vol } \mathcal{P} > \text{Vol } \mathcal{Z} = 34/3 \pi^2$  (see Corollary below). Thus, Question **II** is the most interesting one. Let us recall, that first it was posed by È.B. Vinberg and L. Potyagaïlo in [43].

**Lemma 5 (Combinatorial identities)** *Let  $\mathcal{P} \subset \mathbb{H}^4$  be a compact polytope with face vector  $\mathbf{f}(\mathcal{P}) = (f_0, f_1, f_2, f_3)$ . Then the following combinatorial identities hold.*

$$f_0 - f_1 + f_2 - f_3 = 0, \quad (4.17)$$

$$f_1 = 2 f_0, \quad (4.18)$$

$$4 f_0 = \sum_{P \in \Omega_3(\mathcal{P})} f_0(P). \quad (4.19)$$

**PROOF.** We list the proofs of (4.17)-(4.19) below in the respective order.

(4.17) This is Euler's identity, the same as in Lemma 2.

(4.18) Let  $v$  be a vertex of  $\mathcal{P}$ . Each vertex figure  $\mathcal{P}_v$  of  $\mathcal{P}$  is a tetrahedron, since  $\mathcal{P}$  is a compact non-obtuse polytope. The vertices of  $\mathcal{P}_v$  correspond to the edges emanating from  $v$ . Thus, there are four edges adjacent at each vertex  $v \in \Omega_0(\mathcal{P})$ . On the other hand, each edge has two vertices. Thus  $4 f_0 = 2 f_1$  and (4.18) follows.

(4.19) The faces of the vertex figure  $\mathcal{P}_v$ , which is a tetrahedron, correspond to the facets of  $\mathcal{P}$  sharing  $v$ . Thus, four facets meet at each vertex. Hence if we sum up the number of vertices  $f_0(P)$  over all the facets  $P \in \Omega_3(\mathcal{P})$ , we count each vertex of  $\mathcal{P}$  four times. Then formula (4.19) follows and the lemma is proven. Q.E.D.

**Lemma 6 (Proposition 3.5(d), [34])** *Let  $\mathcal{P} \subset \mathbb{H}^4$  be a compact right-angled polytope. Then its volume equals*

$$\text{Vol } \mathcal{P} = \frac{f_0 - 4f_3 + 16}{12} \pi^2. \quad (4.20)$$

The above lemma leads to the following corollary.

**Corollary (of Lemma 6)** *Let  $\mathcal{P} \subset \mathbb{H}^4$  be a compact right-angled polytope. Then the inequality  $f_3(\mathcal{P}) > f_3(\mathcal{L}) = 120$  implies  $\text{Vol } \mathcal{P} > \text{Vol } \mathcal{L} = 34/3 \pi^2$ .*

PROOF. By [30], one knows that the minimal number of faces (as well as edges and vertices) for a compact right-angled polyhedron in  $\mathbb{H}^3$  belongs to the right-angled hyperbolic dodecahedron  $\mathcal{D}$  (or, equivalently, the Löbell polyhedron  $\mathcal{L}_5$ ). Since each facet of a (compact) right-angled polytope  $\mathcal{P} \subset \mathbb{H}^4$  is a (compact) right-angled polyhedron  $P \subset \mathbb{H}^3$ , as explained in Section 4.3.1, we have  $f_0(P) \geq f_0(\mathcal{D}) = 20$  for each  $P \in \Omega_3(\mathcal{P})$ . Thus, by formula (4.19),

$$4f_0 = \sum_{P \in \Omega_3(\mathcal{P})} f_0(P) \geq 20f_3,$$

i.e.  $f_0 \geq 5f_3$ , and hence, if  $f_3 > 120$ , the above inequality implies  $f_0 - 4f_3 \geq f_3 > 120$  and, by Lemma 6, it turns out that  $\text{Vol } \mathcal{P} > \text{Vol } \mathcal{L} = 34/3 \pi^2$ . Q.E.D.

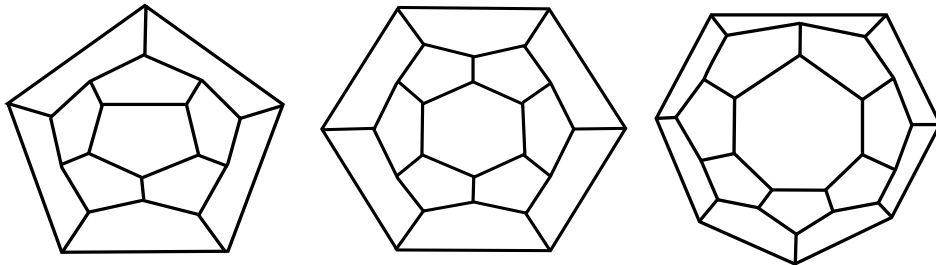


Figure 4.32: The polyhedra  $R_5$ ,  $R_6$  and  $R_7$  (from left to right)

In the work [30], the ordering of the compact right-angled polyhedra in  $\mathbb{H}^3$  with respect to their volumes has come into view. In [50, 57] the list of the first eleven compact right-angled polyhedra with respect to their volume is given.

From [4], we know that, in general, the volume in this family of polyhedra increases with the number of their faces (edges, vertices). The first six polyhedra described in [50, 57] are depicted in Fig. 4.32-4.33. The table of their volumes is given (see Table 4 in Appendix 4.4).

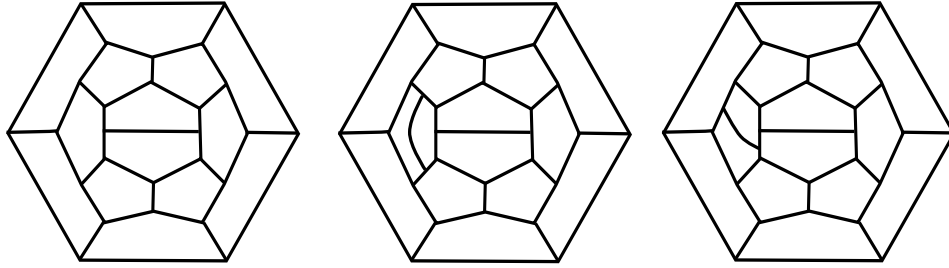


Figure 4.33: The polyhedra  $R6_1^1$ ,  $R6_1^2$  and  $R6_2^2$  (from left to right)

In the following, let us define a set  $\text{Small}$  of *small polyhedra* as being the set containing the compact right-angled polyhedra  $R5$ ,  $R6$ ,  $R6_1^1$ ,  $R7$ ,  $R6_1^2$  and  $R6_2^2$  and possibly further ones.\*

QUESTION 1. Let  $\mathcal{P} \subset \mathbb{H}^4$  be a compact right-angled polytope with face vector  $\mathbf{f}(\mathcal{P}) = (f_0, f_1, f_2, f_3)$ , such that for each  $P \in \Omega_3(\mathcal{P})$  we have  $P \notin \text{Small}$ . Then  $f_3(\mathcal{P}) > f_3(\mathcal{Z}) = 120$  and  $f_0(\mathcal{P}) > f_0(\mathcal{Z}) = 600$ .

At the end of this work, we suggest the following conjecture.

QUESTION 2. Let  $\mathcal{P} \subset \mathbb{H}^4$  be a compact right-angled polytope, which has a facet that is not a right-angled dodecahedron. Then  $f_3(\mathcal{P}) > f_3(\mathcal{Z})$  and  $f_0(\mathcal{P}) > f_0(\mathcal{Z})$ .

We remark that the components of the face vector  $\mathbf{f}(\mathcal{P})$  are independent.

---

\* using the notation of [57]. In our notation  $R5$ ,  $R6$ ,  $R7$  are the Löbell polyhedra  $\mathcal{L}_5$ ,  $\mathcal{L}_6$ ,  $\mathcal{L}_7$ , respectively.



# Appendix A

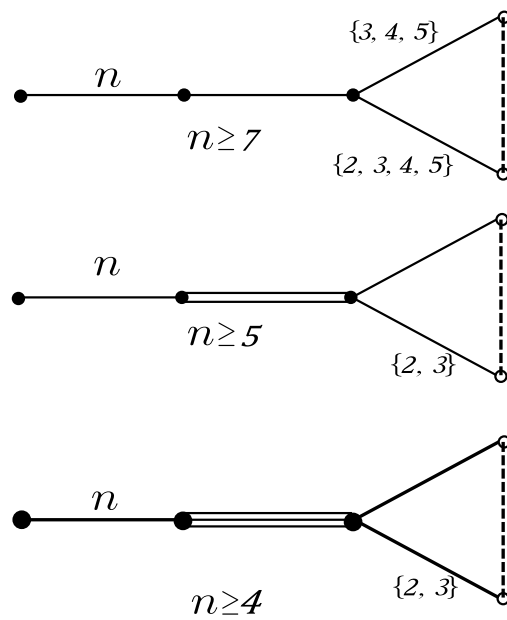


Figure 34: Prisms that admit contraction of an edge: the first picture

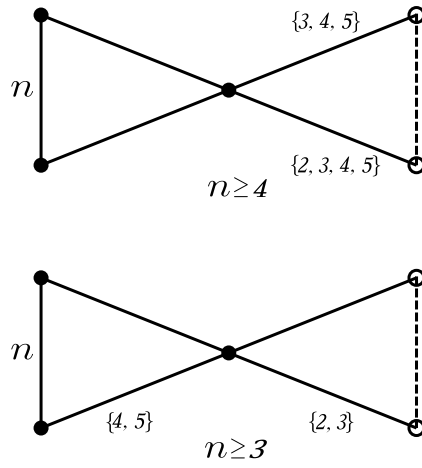


Figure 35: Prisms that admit contraction of an edge: the second picture

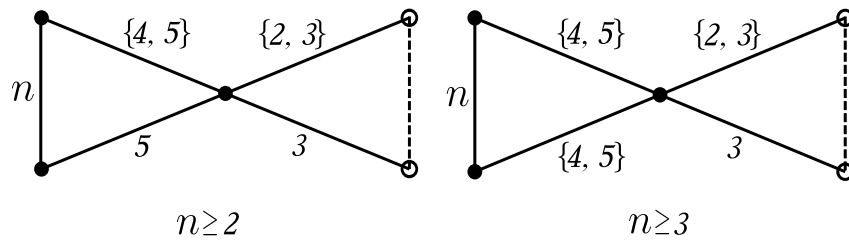


Figure 36: Prisms that admit contraction of an edge: the third picture

Type of $H_1$	Type of $H_2$	$\frac{1}{f_1(t)} - \frac{1}{f_2(t)} =$
$\langle 2, 2, n, 2, 2 \rangle,$ $n \geq 2$	$\langle 2, 2, n + 1, 2, 2 \rangle,$ $n \geq 2$	$\frac{t^n(1-t)^3}{(1-t^n)(1-t^{n+1})(1+t)^2},$ $n \geq 2$
$\langle 2, 2, 2, 2, 3 \rangle$	$\langle 2, 2, 3, 2, 3 \rangle$	$\frac{t^2(1-t)}{(1+t)^3(1+t^2)}$
$\langle 2, 2, 3, 2, 3 \rangle$	$\langle 2, 2, 4, 2, 3 \rangle$	$\frac{t^3(1-t)}{(1+t)^3(1-t+t^2)(1+t+t^2)}$
$\langle 2, 2, 4, 2, 3 \rangle$	$\langle 2, 2, 5, 2, 3 \rangle$	$\frac{t^4(1-t)(1-t+t^2)(1+t+t^2)}{(1+t)^3(1+t^2)(1-t+t^2-t^3+t^4)(1+t+t^2+t^3+t^4)}$
$\langle 2, 2, 2, 2, 4 \rangle$	$\langle 2, 2, 3, 2, 4 \rangle$	$\frac{t^2(1-t)(1+t^2)}{(1+t)^3(1-t+t^2)(1+t+t^2)}$
$\langle 2, 2, 2, 2, 5 \rangle$	$\langle 2, 2, 3, 2, 5 \rangle$	$\frac{t^2(1-t)(1+2t^2+t^3+2t^4+t^5+2t^6+t^7+2t^8+t^{10})}{(1+t)^3(1+2t^2+3t^4+3t^6+3t^8+2t^{10}+t^{12})}$
$\langle 2, 3, 2, 2, 3 \rangle$	$\langle 2, 3, 3, 2, 3 \rangle$	$\frac{t^2(1-t)}{(1+t)(1+t^2)(1+t+t^2)}$
$\langle 2, 3, 3, 2, 3 \rangle$	$\langle 2, 3, 4, 2, 3 \rangle$	$\frac{t^3(1-t)}{(1+t)^3(1+t^2)(1-t+t^2)}$
$\langle 2, 3, 4, 2, 3 \rangle$	$\langle 2, 3, 5, 2, 3 \rangle$	$\frac{t^4(1-t)}{(1+t)^3(1+t^2)(1-t+t^2-t^3+t^4)}$
$\langle 2, 3, 2, 2, 4 \rangle$	$\langle 2, 3, 3, 2, 4 \rangle$	$\frac{t^2(1-t)(1+t+t^2+t^3+t^4)}{(1+t)^3(1+t^2)(1-t+t^2)(1+t+t^2)}$

Table 1: Table for Proposition 9

Type of $H_1$	Type of $H_2$	$\frac{1}{f_1(t)} - \frac{1}{f_2(t)} =$
$\langle 2, 3, 2, 2, 5 \rangle$	$\langle 2, 3, 3, 2, 5 \rangle$	$\frac{t^2(1-t)(1+t^2)(1+t^3+t^6)}{(1+t)^3(1+3t^2+5t^4+6t^6+6t^8+5t^{10}+3t^{12}+t^{14})}$
$\langle 2, 4, 2, 2, 4 \rangle$	$\langle 2, 4, 3, 2, 4 \rangle$	$\frac{t^2(1-t)}{(1+t)^3(1-t+t^2)}$
$\langle 2, 4, 2, 2, 5 \rangle$	$\langle 2, 4, 3, 2, 5 \rangle$	$\frac{t^2(1-t)(1+t^2)(1+t^3+t^6)}{(1+t)^3(1-t+t^2)(1-t+t^2-t^3+t^4)(1+t+t^2+t^3+t^4)}$
$\langle 2, 5, 2, 2, 5 \rangle$	$\langle 2, 5, 3, 2, 5 \rangle$	$\frac{(1-t)t^2(1+t^2+2t^3-t^4+2t^5+t^6+t^8)}{(1+t)^3(1-t+t^2)(1-t+t^2-t^3+t^4)(1+t+t^2+t^3+t^4)}$

Table 2: Table for Proposition 9 (continuation)

Vertex group $Stab(v)$	Its Coxeter exponents			Quantity $\frac{dg_v}{dt}(1)$
	$m_1$	$m_2$	$m_3$	
$\Delta_{2,2,n}, n \geq 2$	1	1	$n - 1$	$-\frac{1}{8} \left(1 - \frac{1}{n}\right)$
$\Delta_{2,3,3}$	1	2	3	$-\frac{1}{8}$
$\Delta_{2,3,4}$	1	3	5	$-\frac{5}{32}$
$\Delta_{2,3,5}$	1	5	9	$-\frac{3}{16}$

Table 3: Table for Proposition 10. The column on the right follows from Theorem 20, formulas (3.6)-(3.7)

Polyhedron	Volume	Polyhedron	Volume
$R5$	4.3062	$R7$	7.5632
$R6$	6.0230	$R6_1^2$	7.8699
$R6_1^1$	6.9670	$R6_2^2$	8.0002

Table 4: Volumes of small polyhedra from Section 4.4

# References

- [1] D. ALLCOCK, “Infinitely many hyperbolic Coxeter groups through dimension 19”, *Geom. Topol.* **10** (2006), 737-758.
- [2] E.M. ANDREEV, “On convex polyhedra in Lobačevskii space”, *Math. USSR Sb.* **10** (1970), no. 3, 413-440.
- [3] E.M. ANDREEV, “On convex polyhedra of finite volume in Lobačevskii space”, *Math. USSR Sb.* **12** (1970), no. 2, 255-259.
- [4] C.K. ATKINSON, “Volume estimates for equiangular hyperbolic Coxeter polyhedra”, *Alg. Geom. Topol.* **9** (2009), 1225-1254.
- [5] R. BENEDETTI, C. PETRONIO, “Lectures on Hyperbolic Geometry”. Berlin, Heidelberg: Springer-Verlag, 1992. (Universitext Series)
- [6] N. BOURBAKI, “Lie groups and Lie algebras. Chapters 4-6”. Berlin, Heidelberg: Springer-Verlag, 2008. (Elements of Mathematics)
- [7] J.W. CANNON, “The growth of the closed surface groups and compact hyperbolic groups” (unpublished).
- [8] J.W. CANNON, P. WAGREICH, “Growth functions of surface groups”, *Math. Ann.* **293** (1992), 239-257.
- [9] R. CHARNEY, M.W. DAVIS, “Reciprocity of growth functions of Coxeter groups”, *Geom. Dedicata* **39** (1991), 373-378.
- [10] M. CHAPOVALOV, D. LEITES, R. STEKOLSCHIK, “The Poincaré series of the hyperbolic Coxeter groups with finite volume of fundamental domains”, *J. Non-linear Math. Phys.* **17** (2010), 169-215.
- [11] H.S.M. COXETER, “Regular Polytopes”, 3rd ed. New York: Dover, 1973.

- [12] M.W. DAVIS, “The geometry and topology of Coxeter groups”, Princeton: Princeton University Press, 2008. (LMS Monograph Series **32**)
- [13] M. DEZA, M. SHTOGRIN, “Octahedrites”, *Symmetry Cult. Sci.* **11** (2000), no. 1-4, 27-64.
- [14] M. DEZA, M.D. SIKIRIĆ AND M. SHTOGRIN, “Fullerene-like spheres with faces of negative curvature”, arXiv:1112.3320.
- [15] G. DUFOUR, “Notes on right-angled Coxeter polyhedra in hyperbolic spaces”, *Geom. Dedicata* **147** (2010), no. 1, 277-282.
- [16] W.D. DUNBAR, J.H. HUBBARD, R.K.W. ROEDER, “Andreev’s Theorem on Hyperbolic Polyhedra”, *Ann. Inst. Fourier* **57** (2007), no. 3, 825-882.
- [17] W.D. DUNBAR, G.R. MEYERHOFF, “Volumes of hyperbolic 3-orbifolds”, *Indiana Univ. Math. J.* **43** (1994), 611-637.
- [18] D. EPSTEIN, A. IANO-FLETCHER, U. ZWICK, “Growth functions and automatic groups”, *Experiment. Math.* **5** (1996), 297-315.
- [19] B. EVERITT, J.G. RATCLIFFE, S.T. TSCHANTZ, “Right-angled Coxeter polytopes, hyperbolic 6-manifolds, and a problem of Siegel”, to appear in *Math. Ann.*
- [20] A. FELIKSON, P. TUMARKIN, “On hyperbolic Coxeter polytopes with mutually intersecting facets”, *J. Combin. Theory A* **115** (2008), 121-146.
- [21] A. FELIKSON, P. TUMARKIN, “Coxeter polytopes with a unique pair of non-intersecting facets”, *J. Combin. Theory A* **116** (2009), 875-902.
- [22] W.J. FLOYD, “Growth of planar Coxeter groups, P.V. numbers, and Salem numbers”, *Math. Ann.* **293** (1992), 475-483.
- [23] E. GHATE, E. HIRONAKA, “The arithmetic and geometry of Salem numbers”, *Bull. Amer. Math. Soc.* **38** (2001), 293-314.
- [24] R. GRIGORCHUK, P. DE LA HARPE, “On problems related to growth, entropy, and spectrum in group theory”, *J. Dynam. Control Systems* **3** (1997), no. 1, 51-89.
- [25] P. DE LA HARPE, “Topics in geometric group theory”. Chicago, London: The University of Chicago press, 2000. (Chicago Lect. in Math.)

- [26] P. DE LA HARPE, “Groupes de Coxeter infinis non affines”, *Exposition. Math.* **5** (1987), 91-96.
- [27] G.J. HECKMAN, “The volume of hyperbolic Coxeter polytopes of even dimension”, *Indag. Math., New Ser.* **6** (1995), no. 2, 189-196.
- [28] E. HIRONAKA, “The Lehmer Polynomial and Pretzel Links”, *Can. Math. Soc. Bulletin* **44** (2001), 440-451.
- [29] J.E. HUMPHREYS, “Reflection Groups and Coxeter Groups”, *Cambridge studies in advanced mathematics* **29**, 1990.
- [30] T. INOUE, “Organizing volumes of right-angled hyperbolic polyhedra”, *Alg. Geom. Topol.* **8** (2008), 1523-1565.
- [31] N. JOHNSON, R. KELLERHALS, J. RATCLIFFE, S. TSCHANTZ, “The size of a hyperbolic Coxeter simplex”, *Transformation Groups* **4** (1999), 329-353.
- [32] I.M. KAPLINSKAYA, “Discrete groups generated by reflections in the faces of simplicial prisms in Lobachevskian spaces”, *Math. Notes* **15** (1974), 88-91.
- [33] R. KELLERHALS, A. KOLPAKOV, “The minimal growth rate of cocompact Coxeter groups in hyperbolic 3-space”, *Institute Mittag-Leffler preprint series*, no. 24, spring 2012 program.
- [34] R. KELLERHALS, G. PERREN, “On the growth of cocompact hyperbolic Coxeter groups”, *Europ. J. Comb.* **32** (2011), 1299-1316.
- [35] A.G. KHOVANSKII, “Hyperplane sections of polyhedra, toroidal manifolds, and discrete groups in Lobachevskii space”, *Functional Analysis and Its Applications* **20** (1986), no. 1, 41-50.
- [36] A. KOLPAKOV, “Deformation of finite-volume hyperbolic Coxeter polyhedra, limiting growth rates and Pisot numbers”, *European J. Comb.* **33** (2012), no. 8, 1709-1724.
- [37] A. KOLPAKOV, “On the optimality of the ideal right-angled 24-cell”, *Algebr. Geom. Topol.* (2012), in print.
- [38] W. MASSEY, “Algebraic topology: an introduction”. Berlin, Heidelberg: Springer-Verlag, 1987. (Graduate texts in mathematics)

- [39] J. MILNOR “A note on curvature and fundamental group” in *Collected Papers. I. Geometry* (Publish or Perish, Houston, TX, 1994), pp. 55-61.
- [40] J. MILNOR “The Schläfli differential equality” in *Collected Papers. I. Geometry* (Publish or Perish, Houston, TX, 1994), pp. 281-295.
- [41] V.V. NIKULIN, “On the classification of arithmetic groups generated by reflections in Lobachevsky spaces”, *Mathematics of the USSR-Izvestiya* **18** (1982), no. 1, 99-123.
- [42] W. PARRY, “Growth series of Coxeter groups and Salem numbers”, *J. Algebra* **154** (1993), 406-415.
- [43] L. POTYAGAILO, È. VINBERG, “On right-angled reflection groups in hyperbolic spaces”, *Comment. Math. Helv.* **80** (2005), no. 1, 63-73.
- [44] M.N. PROKHOROV, “Absence of discrete reflection groups with non-compact fundamental polyhedron of finite volume in Lobachevsky space of large dimensions”, *Mathematics of the USSR-Izvestiya* **28** (1987), 401-411.
- [45] J.G. RATCLIFFE, “Foundations of hyperbolic manifolds”. New York: Springer-Verlag, 1994. (Graduate Texts in Math.; 149).
- [46] I. RIVIN, “A characterization of ideal polyhedra in hyperbolic 3-space”, *Ann. Math.* **143** (1996), no. 1, 51-70.
- [47] R.K.W. ROEDER, “Constructing hyperbolic polyhedra using Newton’s Method”, *Exper. Math.* **16** (2007), no. 4, 463-492.
- [48] R. SALEM, “Power series with integral coefficients”, *Duke Math. J.* **12** (1945), 153-172.
- [49] J.P. SERRE, “Cohomologie des groupes discrets”, *Ann. of Math. Stud.* **70** (1971), 77-169.
- [50] K. SHMEL’KOV, A. VESNIN, “The initial list of compact hyperbolic right-angled polyhedra”, preprint.
- [51] C. SIEGEL, “Some remarks on discontinuous groups”, *Ann. of Math.*, **46** (1945), 708-718.



- [52] L. SOLOMON, “The orders of the finite Chevalley groups”, *J. Algebra* **3** (1966), 376-393.
- [53] R. STEINBERG, “Endomorphisms of linear algebraic groups”, *Mem. Amer. Math. Soc.* **80** (1968).
- [54] E. SUÁREZ-PEIRÓ “Poliedros de Dirichlet de 3-variedades cónicas y sus deformaciones”, Thesis, Universitat Complutense de Madrid, 1998.
- [55] A.L. TALAMBUTSA “Attainability of the minimal exponential growth rate for free products of finite cyclic groups”, *Proc. Steklow Inst. Math.* **274** (2011), no. 1, 289-302.
- [56] A.YU. VESNIN, “Volumes of hyperbolic Löbell 3-manifolds”, *Math. Notes* **64** (1998), no. 1, 15-19.
- [57] A.YU. VESNIN, “Volumes and Normalized Volumes of Right-Angled Hyperbolic Polyhedra”, *Atti Semin. Mat. Fis. Univ. Modena* **57** (2010), 159-169.
- [58] È.B. VINBERG, “Hyperbolic reflection groups”, *Russian Math. Surv.*, **40** (1985), no. 1, 31-75.
- [59] È.B. VINBERG, “Geometry. II: Spaces of constant curvature”, *Encycl. Math. Sci.* **29**, 139-248 (1993).
- [60] P. WAGREICH, “The growth function of a discrete group” in *Groups Actions and Vector Fields. Proceedings, Vancouver 1981. (Lecture Notes in Math. 956)*, pp. 125-144.
- [61] J.S. WILSON, “On exponential growth and uniformly exponential growth for groups”, *Invent. Math.* **155** (2004), no. 2, 287-303.
- [62] T. ZEHRT, “The covolume of discrete subgroups of  $\text{Iso}(\mathbb{H}^{2m})$ ”, *Discrete Math.* **309** (2009), 2284-2291.
- [63] G. ZIEGLER, “Lectures on polytopes”, Berlin: Springer-Verlag, 1995.

## CURRICULUM VITÆ

### PERSONAL INFORMATION

- Born: 19 March 1987, Novosibirsk, USSR
- Citizenship: Citizen of Russia

### EDUCATION

- 2009 Ph.D. study at the University of Fribourg, Switzerland;
- 2008 Graduated from the Novosibirsk State University;
- 2004 – 2008 Undergraduate study at the Novosibirsk State University;
- 2002 – 2004 Specialised educational scientific centre at the Novosibirsk State University;
- 1994 – 2002 Secondary school, Novosibirsk.

### EMPLOYMENT

- 2009 Assistant at the University of Fribourg, Switzerland
- 2008 – 2009 Assistant at the Novosibirsk State University
- 2008 – 2009 Minor researcher at the Sobolev Institute of Mathematics of RAS, Novosibirsk

### ACADEMIC DISTINCTIONS

- 2010 – 2012 Doctoral studies at the University of Fribourg supported by the Swiss National Science Foundation project no. 200021-131967/1
- 2009 – 2010 Doctoral studies at the University of Fribourg supported by the Swiss National Science Foundation project no. 200020-113199/1
- 2009 Visit to ICTP, Trieste, Italy partially supported by the Russian Fund for Basic Research project no. 09-01-09225 and by the ICTP visitor program
- 2008 A.A. Lyapunov honour award for undergraduate scientific studies at the Novosibirsk State University
- 2007 A.A. Lyapunov honour award for undergraduate scientific studies at the Novosibirsk State University

## PAPERS & PRE-PRINTS

“The minimal growth rate of cocompact Coxeter groups in hyperbolic 3-space”,  
Institute Mittag-Leffler preprint series, No.24, spring 2012 (with R. Kellerhals)

“Examples of rigid and flexible Seifert fibred cone-manifolds”, arXiv:1004.2376

“On the optimality of the ideal right-angled 24-cell”, *Algebr. Geom. Topol.*,  
accepted

“Volume of a doubly truncated hyperbolic tetrahedron”, *Æquationes Mathematicæ*,  
accepted; arXiv:1203.1061 (with J. Murakami)

“Deformation of finite-volume hyperbolic Coxeter polyhedra, limiting growth  
rates and Pisot numbers”, *European J. Combinatorics*, 2012; arXiv:1105.6267

“Volume formula for a  $\mathbb{Z}_2$ -symmetric spherical tetrahedron through its edge  
lengths”, *Arkiv för Matematik*, 2011; arXiv:1007.3948 (with A. Mednykh and  
M. Pashkevich)

“Spherical structures on torus knots and links”, *Siberian Math. Journal*, 2009;  
arXiv:1008.0312 (with A. Mednykh)